(Front Cover)

Doctoral Thesis

Shibaura Institute of Technology

Dynamic Analysis of Transfemoral Prosthesis Function using Finite Element Method

March 2020

Mohd Syahmi Jamaludin

(Spline)

Doctoral Thesis
Shibaura Institute of Technology

Dynamic Analysis of Transfemoral Prosthesis
Function using Finite Element Method

March 2020
Mohd Syahmi Jamaludin

A DISSERTATION SUBMITTED TO THE GRADUATE SCHOOL OF ENGINEERING AND SCIENCE OF SHIBAURA INSTITUTE OF TECHNOLOGY

by

MOHD SYAHMI BIN JAMALUDIN

IN PARTIAL FULFILLMENT OF THE REQUIREMENTS FOR THE DEGREE OF

DOCTOR OF ENGINEERING

MARCH 2020

To my mother, for everything she has given to me.

To my wife and my two-little daughters, for their love and expectation.

I dedicate this thesis to my late father for his support and encouragement during his time in this world.

Acknowledgments

I owe a deep sense of gratitude to all kindnesses and supports for my studies. Like once said that no one succeeds all by themselves, the work would not have been completed without the help of many individuals.

Firstly, I would like to express my sincere gratitude to my advisor Prof. Akihiko Hanafusa for the continuous support of my Ph.D study and related research, for his patience, motivation, and immense knowledge. His guidance helped me in all the time of research and writing of this thesis. I could not have imagined having a better advisor and mentor for my Ph.D study.

Besides my advisor, I would like to thank the rest of my prosthetic and orthotics committee: Prof. Yamamoto Shinichirou, Prof. Yukio Agarie, Prof. Hiroshi Otsuka, and Prof. Kengo Ohnishi for their insightful comments and encouragement, but also for the hard question which incented me to widen my research from various perspectives.

I thank my fellow lab mates in for the stimulating discussions, for the sleepless nights we were working together before deadlines, and for all the fun we have had in the last three years. Also, I thank my friends in the Malaysian Community in Shibaura Institute of Technology (SIT) for their support and encouragement during my time in the university

I would like to thank to SIT for granted myself a scholarship through these 3 years of the study. With the financial support, I can complete this study with flying colour and able to focus during performing the whole research.

Last but not the least, I would like to thank my family: my mother and to my brothers and sister for supporting me spiritually throughout writing this thesis and my life in general. Moreover, those achievements of mine could not be attained without the presence of my wife, who has always been by my side and has given me strength to overcome the difficulties during these three years of hard working.

Saitama, March 2020

Mohd Syahmi Jamaludin

Abstract

Prosthetic socket is a device that use by an amputee to assist their daily routine activity. It is also used to help an amputee to overcome their lack of confident because of the disability and help to improve their quality of life (QoL) from post-traumatic accident. The demand of prosthetic device in recent years has increased and it was driven by increasing the number of amputees in around the world. The high demand of the device gives an opportunity to the fabricator to increase their prosthetic device fabrication. However, due to extensive time used during fabricating the socket and lack of expertise in the prosthesis and orthotic (PO) field, fabricator cannot achieve the demand. In conjunction of the matter, engineer and prosthesis has provide an assistive method to reduce the time consume during the socket fabrication. A pre-fabrication analysis by quantitative measurement was proposed to develop an evaluation system for improving the existing prosthetic device fabrication. In the study, utilization of finite element method (FEM) to conduct the quantitative evaluation of transfemoral prosthetic socket has been proposed. The study consists of analysis the accuracy of the Magnetic Resonant Imaging (MRI) based three-dimensional (3D) model used in the simulation, analysis of the geometrical deformation of the residuum during interaction with socket and analysis of the pressure distribution occurred inside the socket during various situation. The finding of the study suggests FEM can be classified as an alternative method to evaluate the pre-fabrication prosthetic device. FEM can help the engineer and prosthesis to design the prosthetic device according to subject comfortability without undergone the preliminary socket fitting session. Furthermore, with the pre-fabrication evaluation system, the intervention of prosthesis can be reduced together with the fabricating time. The study includes with seven chapter structured as follow:

Chapter 1: Introduction

This chapter provides an outline of the whole work. The background study will be elaborate in this chapter. The introduction of transfemoral prosthesis, finite element method and the relationship between proposed study with the real-world activity will be elaborated. The objective, scope of study, limitation of the study also will be clarified in this chapter.

Chapter 2: Literature and Technical Review

This chapter will explain the needed of the study and a relationship with the past study. This chapter will review a technical study of finite element analysis (FEA) that act as a fundamental of the overall study. This chapter also presents a

revision of the previous studies. Some prevailing results of studies are also introduced to clarify the novelty of the contributions in this work.

Chapter 3: Accuracy Evaluation of on 3D Reconstruction of Transfemoral Residuum Model

This chapter present an evaluation towards 3D reconstructed model of residuum. This chapter explain the important of the model accuracy towards providing an alternative method replacing the actual human experiment. The accuracy of the model will be evaluated based on the relationship between number of intersections point during constructing the model and the volumetric value of the model.

Chapter 4: Evaluation on Effect of Geometrical Changes of Prosthetic Socket Towards Transfemoral Residuum Model

This chapter present the evaluation on the effect of prosthetic socket changes towards residuum. The study focusing on evaluating two type of prosthetic socket. The geometrical shape of residuum and the socket consider to be differed to enhance the contact surface between both of it. The geometrical changes were observed during complete stage of donning simulation. The evaluation result is an important key toward improving an accuracy of the model design.

Chapter 5: Analysis of The Pressure Distribution Inside Prosthetic Socket in Various Situation.

This chapter presents a pressure distribution analysis occurred in prosthetic socket. The pressure measured in donning process simulation and gait cycle simulation. The 3D model created in the simulation were MRI based. The models were pre-determined with dynamic parameter that based on previous study. The result then compared with actual experiment data conducted from previous study. The result showed high correlation between simulation and experiment measurement.

Chapter 6: Evaluation System for Magnetic Resonance Imaging (MRI) Based Three-Dimensional (3D) Modelling of a Transfemoral Prosthetic Socket Using Finite Elements Method

This chapter present a process of developing an evaluation system of transfemoral prosthetic socket that was created using Magnetic resonant imaging (MRI) database. The evaluation is defined by the volume changes of residuum before and after inserted inside the prosthetic socket. the evaluation then will be compared with database from actual volumetric volume from the experiment.

Chapter 7: Conclusion and Future Work

This chapter conclusions the study about the transfemoral prosthesis function analysis using finite element method. The achievements and the limitation of this research was explained briefly. Furthermore, some solution to improve of this work was discussed.

Nomenclature

Roman Symbols

3D→Three Dimension

AD→Anterior Distal

AKA→Above Knee Amputation

AP→Anterior Proximal

CAD→ Computer Aid Design

CAT-CAM→ Contour Adducted Trochanteric Controlled Alignment Method

COP→ Centre of Pressure

FE→ Finite Element

FEA→ Finite Element Analysis

FEM→ Finite Element Method

GRF→ Ground Reaction Force

HFE→ High Frequency Events

IDF→ International Diabetes Federation

LD→ Lateral Distal

LP→ Lateral Proximal

MCCT→ Manual Compression Casting Technique

MD→ Medial Distal

MP→ Medial Proximal

MRI→ magnetic resonance image

NRCD→ National Disabled Persons Rehabilitation Centre

PD→Posterior Distal

PP→ Posterior Proximal

UCLA→ University of California Los Angeles

UK→ United of Kingdom

US→ United State

Contents

List of Figure

List of Tables

Chapter 1

Introduction

In this chapter, the introduction of transfemoral prosthetic device will be explained. The introduction involves a briefing of related component in the device, history of transfemoral prosthetic device, briefing of current situation of prosthetic device inside and outside Japan and Malaysia and statistical analysis of amputees in Japan in recent years. The issues or problem related to the prosthetic device will be explained briefly. In other section, the objective of the study will be explained together with the scope of the study.

1.1 Background Study

1.1.1 Overview of Amputation Issue

Amputation is not a new thing in this era. In fact, the amputation has been discovered for a long time ago. For instant, artificial limbs of some type, such as a forked stick, have been used since the beginning of mankind, but the earliest recorded use of a limb prosthesis is that of a Persian soldier who was reported by Herodotus to have escaped about 484 B.C. from stocks by cutting off one of his feet and replacing it with a wooden one [1]. The Amputee Coalition of America estimates that there are 185,000 new lower extremity amputations each year just within the United States [2] and an estimated population of 2 million American amputees [3]. It is projected that the amputee population will more than double by the year 2050 to 3.6 million.

According to the 2014 edition of the white paper for disabled people in Japan [4], among 3.66 million people, 29 per 1000 persons are with physical disabilities. The breakdown for the disabilities is 8.8% (0.315 million) for visual impairment, 10.1% (0.36 million) is for hearing and speech disorders, and 50.6 % (1.81 million) is for physical impairment. Internal disorders are said to be 30.5% (1.01 million). Physical disabled people were recorded has more than half of the total disabilities shown in Table 1.1. The data collected from a survey done by Ministry of Health, Labor and Welfare of Japan.

Table 1.1 Data of people with disability in Japan recorded at 2014.

		Total Number	In house	In facilities
People with Physical Impairment	Below 18 YO	98000	93000	5000
	Above 18 YO	3564000	3483000	81000
	TOTAL	3663000	3576000	87000
People with Intellectual disability	Below 18 YO	125000	117000	8000
	Above 18 YO	410000	290000	120000
	Unknown Age	12000	12000	0
	TOTAL	547000	419000	128000
		Total Number	In house	In facilities
People with mental disability	Below 20 YO	179000	176000	3000
	Above 20 YO	3011000	2692000	319000
	Unknown Age	11000	10000	1000
	TOTAL	3201000	2878000	323000

In Japan, the main causes of the amputation were peripheral vascular disorder and traumatic accident [5]. The amputation people are relying on assistive device to support their active daily living (ADL) activities. As recorded in Hyogo prefecture between 1968 to 1992, the incidence of amputation was 6.2/100,000 population per year, and trauma accounted for 70% of the causes of amputation. Although there were no changes in the total number of amputations during those 25 years, the percentage of amputations due to arteriosclerosis obliterans and diabetes mellitus was increasing [5]. Furthermore, a survey conducted in Okayama prefecture described 58.2% of lower limb amputations were caused by peripheral circulatory disorder in the area [6]. In most survey conducted within Japan, the residential areas and details of these subjects are unclear, only amputation due to peripheral vascular disorder has been surveyed, and the incidence of amputation is unclear due to lack of any community-based surveys [5-7]. An appropriate community-based survey in an area representing an average population of Japan is required to uncover the incidence and causes of amputation in Japan. Kita Kyushu City is a local city with a population of one million and is believed to reflect the average condition of Japan [8-9].

According to World Health Organization (WHO) [10], 0.5% of the population of a developing country have a disability that will require a prosthesis or orthosis and related rehabilitation services. This prediction suggests that around 160,000 of Malaysia's current population of 32 million [11] need prosthetic or orthotic devices. The population is projected to reach 38.5 million by 2040 [11], including approximately 200,000 individuals with a physical disability. The main causes of the amputation are due to diabetes mellitus disease where 17.5% increment of diabetes patient recorded in 2006 [12]. According to scientific study [13], diabetes mellitus is a key risk factor leading to lower limb amputation such that in 2005, the loss of a lower limb due to diabetes was estimated to occur every 30 seconds somewhere in the world [14]. In Malaysia, the National Limb Fitting Centre was created to provide a service regarding the prosthetic and orthotic throughout the nation. However, the centre acting as one centre stand alone and it its suggested to provide optimum access to prosthetic service by developing the centre at national, state and district level [10].

Even though the amputation in Malaysia is not critical compared with other ASEAN country, the government take a proactive action to emphasising the issue. It is estimated around Malaysian Ringgit (RM) 4000 to RM 15000 of price to own a prosthetic socket and it is expensive considering minimum average salary of Malaysian is RM 1100 [15]. The cost of prostheses is a major issue in Malaysia and Malaysia Ministry of Health with collaboration with welfare department and social security organisation has initiate `Tabung Bantuan Perubatan' (Medical Aid Fund) to help amputee owning the prosthetic device. The lack of structured prosthetic service management system leads to reimbursement issues which increase the waiting period for amputees to be fitted with a prosthesis. These constraints are likely to remain as major obstacles to improving the nation's prosthetic service unless there are substantial changes in government policies to achieve mutual concordance concerning prosthetic services [15].

In the most developed nations the annual incidence of foot ulceration, which precedes amputation in 85% of cases, is about 2%. In poorer, developing nations a lack of access to care places about half of all persons with diabetes at risk for foot ulceration, and diabetes-related amputations are very common [16]. Yet, the vast majority of amputations both in the US. and abroad are preventable.

1.1.2 Solution of The Amputation

The prosthetic device has been introduced as a solution for the amputation for the past decades. Historically, the provision of prosthetic services in Malaysia began in 1937 when the British established an orthopaedic appliance workshop in the National Leprosy Control Center in Sungai Buloh [17]. By definition, prosthetic device is an artificial substitute or replacement of a part of the body such as a tooth, eye, a facial bone, the palate, a hip, a knee or another joint, the leg, an arm, etc. A prosthesis is designed for functional or cosmetic reasons or both. Typical prostheses for joints are the hip, knee, elbow, ankle, and finger joints. Prosthetic implants can be parts of the joint such as a unilateral knee. Joint replacement and arthroplasty mean the same thing.

The amputation divided in two parts which are upper and lower limb amputation. Lower limb amputation categorized in number of different levels as shown in figure 1.1. The most common amputation occurred in United Kingdom was transtibial amputation [18]. Numbers of factors are necessary to decide the ideal prosthetic device according to the level of amputation such as healing potential, rehabilitation potential, prosthetic consideration and discharge arrangement [19].

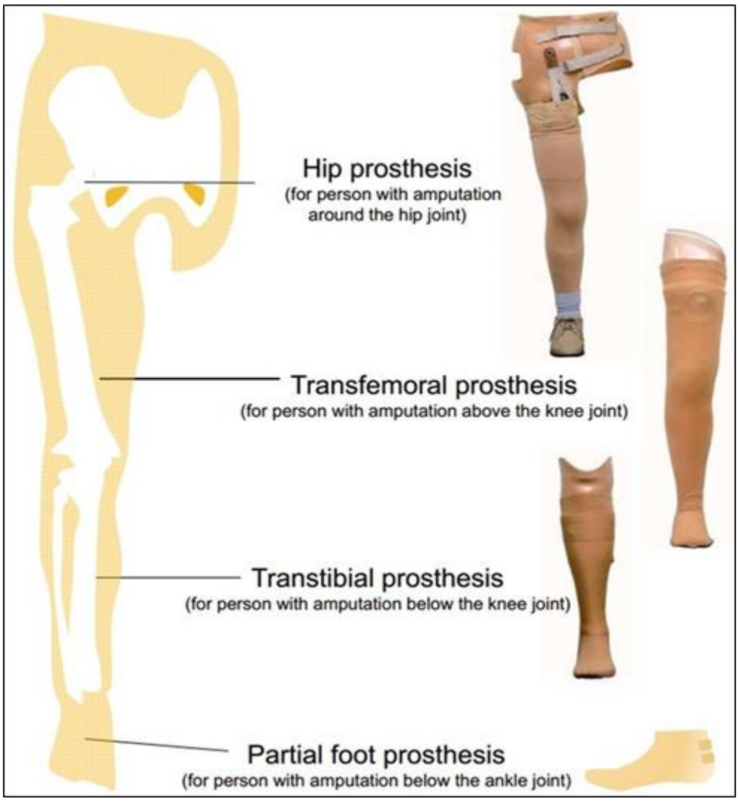

Figure 1.1 Level of Amputation (NRCD - Japan)

The study focusing on amputation above the knee joint which known as transfemoral prosthesis. Advances in technology, materials and prosthetics have had a considerable positive impact on the quality of life of individual with transfemoral amputation. In the past ambulation wearing a transfemoral prosthesis was laboured and often painful. Only the most physically fit individual attempted to run with their prostheses. Now socket designs better approximate anatomy of lower limb, suspension systems enhance and maintain intimate residuum contact within the socket and dynamic prosthetics feet and knee component offer improved, energy-efficient function. The result has been a significant improvement in quality of gait, allowing more people with transfemoral amputation to walk comfortably and naturally with their prosthesis. In addition, athletes with amputation can run in a natural "step-over-step" pattern with a higher degree of stability and comfort than previous possible. The future of people with transfemoral amputation is bright where a lot research has been conducted to improve in many aspects such as the aero dynamic of the socket, knee joint mechanism, prosthetic stability according to work scope and time consume to fabricate the prosthetic socket.

Figure 1.2 Athletes with transfemoral amputation run in natural pattern (Ottobock Ltd.)

1.2 Introduction to Transfemoral Prosthesis Device

Transfemoral prosthesis device was define as a device used by people with above knee amputation to assist their ADL activities especially their walking gait. The device also helps the amputee to regain their self-confident after their traumatic accident. With the device people with amputation can live like a normal people and merge in the committee on their neighbourhood. Most of the amputee has so much support from their family and the government in every country are determined to help this unfortunate group.

The major components of a lower extremity prosthesis are the socket (with or without a socket liner), a suspension system, interposed joint components (as needed), a shank (pylon), and a prosthetic foot. The prosthetic foot is typically a component that functions and looks like a foot but that may take other forms or functions for water or other sports activities. As shown in figure 1.3, there are three basic mechanism for lower limb prostheses device which are hip prosthesis, transfemoral prosthesis and transtibial prosthesis. Each of the device have a different component to adapt the walking mechanism handled by each amputee.

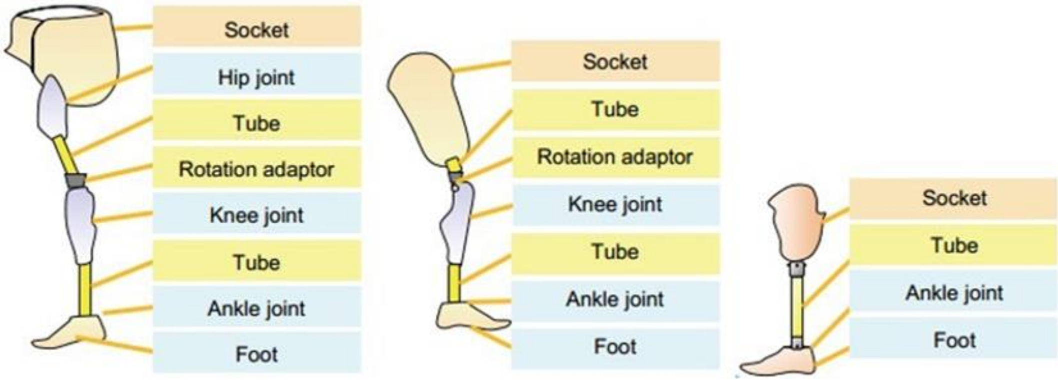

Figure 1.3 Main components of the lower limb prosthesis (NRCD Japan). Hip prosthesis (left); Transfemoral prosthesis (middle) and Transtibial prosthesis (right)

1.2.1 Prosthetic Device Management for Transfemoral Amputation

An amputation proximal to the anatomical knee joint is referred to as a transfemoral (above knee) amputation. The transfemoral residual limb varies in length, depending on how much of the femur has been retained. The shape of the residual limb is likely to be a tapered cylinder so that donning a prosthesis is less difficult. Suspension can be challenging, however, as a result of this cylindrical shape of the residuum. The fleshiness of the transfemoral residuum present an opportunity for suction suspention.as the length of the residuum decreases, socket suspension and control of the prosthetic knee become more problematic.

The successful prosthetic management of individual who have suffered an amputation above the knee involves providing a prosthesis that is comfortable in containing the residuum, stable during the stance phase of gait, smooth in transition to the swing phase of gait and acceptable in appearance [20]. In choosing component for an individual`s transfemoral prosthesis, the prosthetic team must consider the interrelationship among component`s weight, function, cosmesis, comfort and cost. Often the most functional or technologically sophisticated component are also the heaviest, most expensive, most likely to need maintenance and least cosmetic. Because of the great variation in physical characteristics, health, and preferred activities of individual with transfemoral amputation, no single material, component or transfemoral design is appropriate for all persons with amputation. The preferences and needs of each individual must be considered carefully in the context of weight, function, cosmesis, comfort and cost for the optimal prosthetic outcome.

1.2.2 Prosthetic Socket

The socket serves as the interface between the residuum and the prosthesis. The type of socket takes an important role in determining the comfortability of amputee during wearing the socket. There are several type of prosthetic socket used by the amputee for specific amputation and for transfemoral amputation, there are four type of prosthetic was commonly used by the amputee which are quadrilateral (quad) socket, ischial-ramal containment (IRC) socket, the Marlo Anatomical Socket (MAS), and subischial socket shown in figure 1.4 and figure 1.5 showed the cross section for each of the socket.

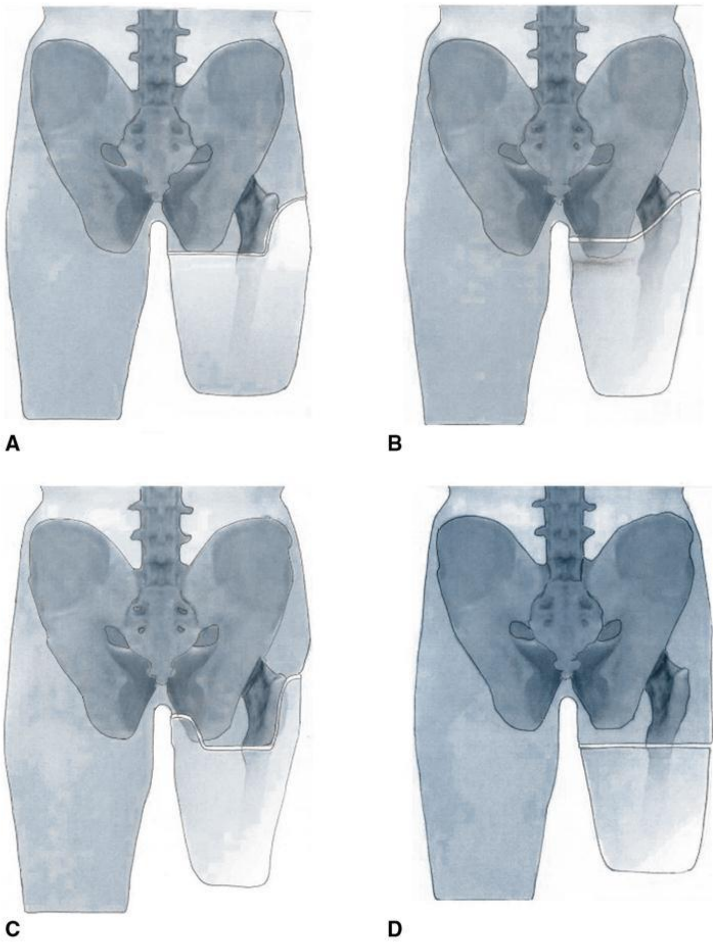

Figure 1.4 Comparison of the design of the quadrilateral (quad) socket (**A**), the ischial-ramal containment (IRC) socket (**B**), the Marlo Anatomical Socket (MAS) (**C**) and subischial socket (**D**)

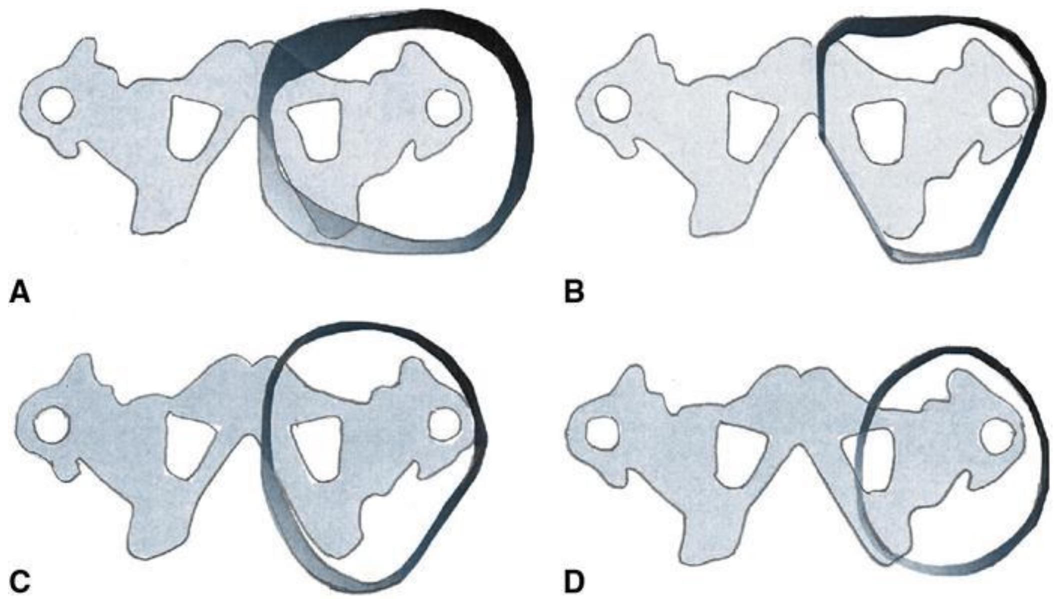

Figure 1.5 A cross section for (A) quad socket; (B) IRC socket; (C) MAS; (D) subischial socket

From the cross section, the different between each socket can be describe where for quad socket, it has a narrow anteroposterior dimension while for IRC socket and MAS, they have narrow mediolateral dimension and for subischial socket, it has a more oval shape which is consistent with the shape of the proximal. The degree to which the prosthetic socket design can influence the position of the transacted femur has been hotly disputed. Many researches have been conducted to understand the relation between alignment, socket design and femoral adduction. In [21], the researcher concluded that the prosthetic socket cannot provide enough lateral pressure to change the position of femur. However, there is also consensus that indicates that an intimately contoured socket in optimal alignment enhances an individual`s gait, decrease energy expenditure, increase socket comfort, and improves overall function [22].

In the study, an improved IRC socket has been introduced which is Manual Compression Casting Technique (MCCT) socket. The socket was inspired and created by Professor Yukio Agarie from Niigata University of Health and Welfare (NUHW). The improvement has been made by the adjusting the anterolateral and sagittal directions of the IRC socket. With the improvement, the proximal pressure of the socket can be improve thus improving the stability of the amputee stance. Figure 1.6 showed two different type of socket created by Professor Yukio Agarie where one is IRC socket (also known as IRC-UCLA) and another one is IRC-MCCT socket. Both sockets were used in whole of the study.

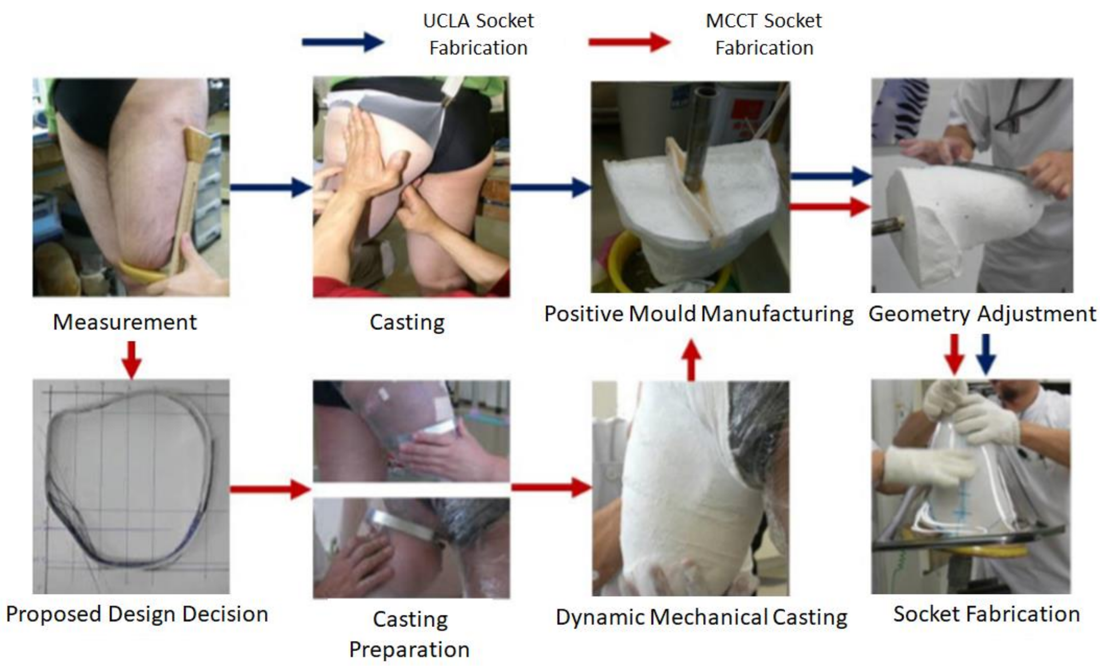

Figure 1.6 The process of IRC socket fabrication by Professor Yukio Agarie. The Blue arrow is process of IRC-UCLA socket fabrication and the red arrow is a process IRC-MCCT socket fabrication.

1.2.3 Transfemoral Suspension System

Keeping the prosthesis on in its optimal functional position is more challenging for individual with transfemoral amputation than with transtibial amputation. The suspension system uses to keep a prosthesis device from falling off the residuum. The system can be categorized into the following:

- Self-suspension of the socket - This makes use of the anatomic shape of the residual limb (Syme or knee disarticulation).

- Suction suspension - Methods of creating suction suspension include the use of an appropriate suction socket design, of a gel suspension liner.

- Suspension device or harness - Such equipment includes belts, cuffs, wedges, straps, and sleeves.

A traditional pull-in suction suspension uses negative air pressure, skin-to-socket contact and muscle tension to hold the socket onto the residuum. The socket's intimate fit creates a seal between the skin of the residual limb and the socket. When air is driven out of the end of the socket, a small negative pressure strong enough to suspend the socket on the residuum develops inside the socket. This form of suspension allows excellent proprioceptive feedback and is lightweight. One disadvantage of the suction socket is its inability to tolerate much weight or volume fluctuation up or down before it requires replacement.

Figure 1.7 Subject donning a suction socket using a pull sock. The air expulsion valve has been removed so that the donning sock can be pulled completely out of the socket.

1.2.4 Prosthetic Knee Units

The function of the human knee joint is difficult to replicate. The knee mechanism must provide support during the stance phase of ambulation, produce smooth control during the swing phase and maintain unrestricted motion for sitting and kneeling to achieve an optimal functionality. There are many types of knee mechanism available in the recent market. It depends on individual to choose the mechanism and also it depends on the activity's individual choose to do.

Prosthetic knee mechanisms have two primary function. First, to simulate normal gait, the prosthetic knee must smoothly flex and extend through the swing phase of gait. The speed or rate of shin advancement during swing is determined by the mechanical properties of the prosthetic knee unit. The prosthetic knee can have a single axis with a simple hinge and a single pivot point, or it may have a polycentric axis with multiple centres of rotation. Seconds, the prosthetic knee must remain stable as body weight rolls forward over the prosthetic foot during the stance phase of gait. The major categories of commonly used prosthetic knee units vary with respect to how, and to what degree, they accomplish these two tasks.

Prosthetic science is advancing the types of knees now available. The hydraulic- based Otto Bock C-Leg (Otto Bock Health Care, Minneapolis, Minnesota) provides several benefits over purely mechanical knee systems.

These microprocessor- controlled knees improve upon the timing of the hydraulic and pneumatic knees. The patient can ambulate at greater speeds with optimal, biomechanically correct symmetry while expending less energy. Most importantly, the user can safely walk step over step up and down stairs. The built-in battery lasts anywhere from 25-40 hours, which means that it can support a full day of activity. The recharge can be performed overnight or while traveling in a car (via a cigarette lighter adapter). The magnetorheological-fluid based Rheo Knee(Ossur, Reykjavic, Iceland; Ossur North America, Aliso Viejo, California) is capable of ”learning” how the patient walks.

Electronic sensors on the artificial joint measure the joint’s angle and the loads it is bearing, 1,000 times per second while a computer chip controls the viscosity of magnetic fluid inside the knee. Tiny metal particles suspended in the fluid form small chains when the magnetic field is turned on, causing the fluid to become thicker. That, in turn, affects the stiffness of the joint, which is modified constantly while the knee is in use, allowing for a smooth swing of the leg. However, the cost of technologically advanced knees is prohibitor for most amputees.

Figure 1.8 Straight (left) and bent (right) images of the hydraulic prosthetic knee joint are seen [23].

1.2.5 Prosthetic Foot

Individual with transfemoral amputation can use majority of the prosthetic feet and ankle option that are available. One of the important considerations in choosing a prosthetic foot is its influence on stability of the prosthetic knee during stance. A foot that can reach foot flat quickly is preferable because it enhance stance phase knee stability. Reaching foot flat quickly is especially important for individual who have a short residuum or weak hip extensors. Prosthetic foot are broadly classified as energy-returning feet or nonenergy-returning feet. Nonenergy-returning feet include the solid-ankle, cushioned-heel (SACH) foot and the single-axis foot. The SACH foot mimics ankle plantar flexion, which allows for a smooth gait. The prosthetic is a low-cost, low-maintenance foot for a sedentary patient who has had a BKA or an AKA. The rigid forefoot provides an anterior lever arm and proprioception. The single-axis foot adds passive plantar flexion and dorsiflexion, which increase stability during the stance phase. They are most commonly used for patients with a transfemoral amputation if knee stability is desired. Energy-returning feet are probably improperly named because, in fact, they do not return energy. They do, however, assist the body's natural biomechanics and allow for greater cadence or less oxygen consumption. The multi-axis foot and the dynamic-response foot are members of this family. The multi-axis foot adds inversion, eversion, and rotation to plantar flexion and dorsiflexion; it handles uneven terrain well and is a good choice for the individual with a minimal-to-moderate activity level.

For active individual, dynamic response feet and those with flexible keels may be advantages. The energy-storing capabilities of these prosthetic feet at push-off promote rapid advancement of the shin section during swing phase. This enhances the ability of the individual who is using a transfemoral prosthesis to walk at faster speeds. The dynamic-response foot is the top-of-the-line foot and is commonly used by young, active persons and by athletic individuals. The forefoot acts like a spring, compressing in the stance phase and rebounding at toe-off. Geriatric patients benefit from the light weight of these feet.

1.3 Common issue in transfemoral prosthesis industry

1.3.1 Increment of transfemoral amputation number.

In recent years, number of transfemoral amputation has rapidly increased. In Japan, 25% of increment of transfemoral amputation was estimated due to peripheral vascular disorder within 5 years. The increment has pushed the prosthetic industry to increase their prosthetic device quantity. However, the industry of prosthetic facing a human resource problem to meet the demand. Also, the quantity of rehabilitation workers included therapist, physiotherapist, prostheses specialize and rehabilitation engineer in the country were low compare to the quantity of the amputee. According to the 2013 edition survey published by the Ministry of Health, Labour and Welfare of Japan, the rehabilitation workers has a total of 214,133 people, but the number of prosthetics and orthotics is only 4,262. The number is considered to be a small quantity, and at the same time, the workload for prosthetic orthosis are large.

In a prosthetic device fabricator views especially prosthetic socket fabricator, the amputee quantity increment gave them an opportunity to expand their fabrication scale. Every amputee is most likely needing a prosthetic device to support their daily life activities. However, the allocated time to produce such device is long due to various of process of evaluation before it being fabricate. Figure 1.9 showed the conventional method to fabricate the prosthetic socket.

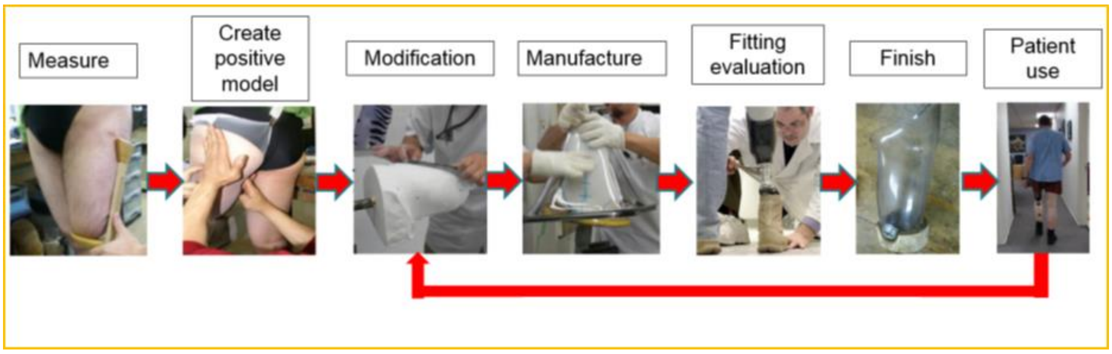

Figure 1.9 Conventional prosthetic socket fabrication

The human resource and socket fabrication issues are a primary matter that need to be solve. Many researches have been conducted to solve the matter. An alternative method to fabricate the prosthetic socket has be introduced by utilizing a three-dimensional (3D) printing method and the method still has many evaluations needs to be conducted before it can be use.

1.3.2 Evaluation of prosthetic socket in pre and post fabrication

Many patients experience serious discomfort wearing a conventional prosthesis because of pain, instability during walking, pressure sores, bad smell or skin irritation. In addition, sitting is uncomfortable and pelvic and lower back pain due to unstable gait is often seen in these patients. The main dis- advantage of the current prosthesis is the attachment of a rigid prosthesis socket to a soft and variable body. The socket must fit tightly for stability during walking but should also be comfortable for sitting [24]. The evaluation of prosthetic socket is important to understand patient needs and understand the suitability between the device and the patient. The evaluation is categorized into two part which is pre-fabrication evaluation and post-fabrication evaluation. For conventional fabrication process, the pre-fabrication evaluation is not included in the process. It is because the evaluation can not be conduct to the thing that yet be created. However, post-fabrication evaluation can be conducted to evaluate the suitability level between the patient and the socket. The evaluation consists of a level of comfortability, socket fitting with the residuum and the stability of the patient during wearing the socket.

In details, the post-evaluation divided by three prime evaluation which are

I. Socket Fitting Evaluation
II. Dynamic of Knee Joint Evaluation
III. Stability evaluation based on ground reaction force (GRF)

Socket fitting evaluation is conducted to measure the skin-to-socket contact. When a socket is not a snug fit, the resulting gap allows the residuum to move more than it should; and the result is often sores, blisters, and ongoing pain. Experienced prosthetic practitioners know that fitting well distributes the weight and pressure evenly over areas of the residual limb that can tolerate regular pressure. Evidence shows that a good fit can also help ease phantom pain. Sometimes prostheses that cause pain or discomfort are too tight. When the socket is too constrictive, it can inhibit circulation and cause swelling or friction that results in skin abrasions. Problems with how well prostheses fit can be related to fluctuations in body weight. If you gain or lose weight, it can have an impact on the fit of your prosthesis.

The dynamic knee joint evaluation is conducted to make patient walking gait nearly similar or similar with normal walking gait. Prosthetic knee designers have used components such as springs and dampers and optimized them with an aim of replicating ideal knee moment required for walking with able-bodied kinematics [25]. However, many challenges to design and choose a good knee joint prosthesis because it depends on individual patient features, finance ability and using purpose. The understand of knee joint operation and load appeared are important parameters for design and improve quality of knee joint. Nowadays, many studies continuing finds the solution for study the quality of knee joint by using advanced technologies.

The stability evaluation based on GRF is conducted to study the relationship between design of prosthetic device and the pressure beneath the prosthesis foot. GRF is a main parameter used in biomedical analysis to estimate the joint load and evaluate the quality of the prosthesis. The information of ground re- action forces and beneath pressure of foot prosthesis is conventionally achieved using dynamics method or the experimental method. However, these methods have some limitation for a prosthetist and designers to choose the best prosthesis solution for transfemoral patient.

1.3.3 Transfemoral Prosthesis Research Difficulty

Amputation at the transfemoral level can be very challenging for the amputee as well for the surgeon, the prosthetist, the physical therapist, and every member of the health care team. In the United States, this amputation level is most commonly known as an above-knee amputation, or AKA, whereas elsewhere it is referred to as a transfemoral amputation because the amputation occurs in the thigh, through the femur. The term transfemoral amputation is gaining favour in the United States because it more accurately describes the amputation level involved. Many of the same issues are faced by amputees with knee disarticulations. Except where noted, the information provided in this monograph applies to both transfemoral amputations and knee disarticulations.

Transfemoral amputations are performed less often than in the past because of new understandings of the importance of preserving the knee joint. As recently as 30 years ago, transfemoral amputations were performed frequently in patients with foot infections that required amputation. At that time, the impact of amputation level on rehabilitation and function was not fully understood. Also, the prevailing belief was that a thigh-level amputation was significantly more likely to heal than an amputation at the calf (called a transtibial amputation) or foot because amputations in the calf and foot had very poor healing rates. Thanks to better amputation surgical technique, vascular reconstruction, patient selection, and improved antibiotic treatment, amputations at the calf and foot now have an excellent chance of resulting in a well healed, functional limb.

Despite the current emphasis on performing amputations that preserve limb length, many transfemoral amputations are still required. Of the more than 1.2 million people in the United States living with limb loss, 18.5% are transfemoral amputees, according to the latest figures provided by the National Centre for Health Statistics. Dillingham and associates reported that 266,465 transfemoral amputations were performed in the United States between 1988 and 1996 (the most recent years available), an average of 29,607 annually.

Although transfemoral amputations are fairly common, adjusting to life after this surgery is not simple. The transfemoral amputee must deal with increased energy consumption for ambulation, balance, and stability; a more complicated prosthetic device; difficulty rising from sitting to standing; and, unlike amputation levels in the tibia and the foot, prosthetic discomfort while sitting. The cost of a transfemoral prosthesis is also significantly higher than for a transtibial prosthesis.

Learning to walk after a transfemoral amputation is many times harder than learning to walk after a transtibial amputation. The transfemoral amputee not only has to learn to use a prosthetic knee but also must learn to coordinate the interaction of the foot componentry with the prosthetic knee, which requires more mental energy. In addition, achieving a comfortable socket fit is more challenging. Skills such as coming to a stand, standing balance, ambulation, and negotiating hills, stairs, and uneven terrain are more difficult. The transfemoral amputee has more difficulty with balance and decreased proprioception and therefore has both a greater risk and greater fear of falling. For these reasons, the rehabilitation process is much more difficult for the transfemoral amputee than for the transtibial amputee. Physical therapy is more prolonged (usually at least twice as long as for the transtibial amputee), and a better understanding of prosthetic components is required on the part of the physical therapist.

For the transfemoral amputee to achieve the best possible outcome, it is necessary for the physical therapist to understand the prosthetic components and how they work. The physical therapist must also know how to train the patient to function in all mobility situations and must also be familiar with issues that are relevant specifically to amputees, such as phantom pain, residual limb skin issues, and the importance of the trained peer visitor.

Physical therapists generally receive little formal training specific to working with amputees, and once in practice, most physical therapists may see one amputee a year, if that. In addition, prostheses continually change as new components become available. For many therapists, keeping up with the constantly changing world of prosthetic components is the most challenging aspect of working with amputees, especially if the basic mechanics of the prostheses are not understood. The purpose of this monograph is to provide a resource of the basic medical and prosthetic issues involved in transfemoral amputation so that with this understanding, the physical therapist is better able to treat the transfemoral amputee in such a way that a positive experience results for both the amputee and the therapist.

1.4 Research Objectives

Motivated by the recent issue regarding the transfemoral prosthesis especially in number of human resource issue, time consume issue and lack of pre-fabrication evaluation issue, the research has purposed a convenient method by using finite element method (FEM) to evaluate the function of the socket, the knee joint, feet and collected the data for determine quality of transfemoral prosthesis operation for pre-fabrication analysis. The main objectives of the dissertation are as follow:

- Developing the three-dimensional (3D) model of residuum with precise parameter of actual residuum where the model consists of multi-material properties includes: skin, fat, muscle and bone.
- Designing a simulation mimicking an actual donning process to improve the evaluation fitting of transfemoral prosthesis socket in stance phase of gait.
- Developing an evaluation system for transfemoral prosthetic socket for the socket model created using Magnetic resonant imaging (MRI) data.

The utilization of finite element method (FEM) is a primary method to achieve the objectives. The research is expected to create an overall evaluation system for the transfemoral prosthetic device especially the socket and helping the prosthetist develop biologically realistic lower-limb assistive devices that improve amputee locomotion. Furthermore, the results of the study can aid the prosthesis designer in the design of the prosthesis parts and the structure of the artificial leg, and in material selection.

By achieving the objective, fat distribution inside the transfemoral residual limb can be analyse. The fat distribution pattern and composition can be confirmed by comparing the 3D model with MRI data collected from specific subjects. The overall analysis considers as a novelty of this research because its include analysis of fat distribution analysis, fat composition behaviour of residual limb before and after inserting into prosthetic socket, pressure distribution during inserting into socket and walking phase that so far not been done in the biomedical field.

1.5 Structure of the dissertation

This dissertation is composed of six chapters.

Chapter 1 provides an outline of the whole work. The background study will be elaborate in this chapter. The introduction of transfemoral prosthesis, finite element method and the relationship between proposed study with the real-world activity will be elaborated. The objective, scope of study, limitation of the study also will be clarified in this chapter.

Chapter 2 will explain the needed of the study and a relationship with the past study. This chapter will review a technical study of finite element analysis (FEA) that act as a fundamental of the overall study. This chapter also presents a revision of the previous studies. Some prevailing results of studies are also introduced to clarify the novelty of the contributions in this work.

Chapter 3 present an evaluation towards 3D reconstructed model of residuum. This chapter explain the important of the model accuracy towards providing an alternative method replacing the actual human experiment. The accuracy of the model will be evaluated based on the relationship between number of intersections point during constructing the model and the volumetric value of the model.

Chapter 4 present the evaluation on the effect of prosthetic socket changes towards residuum. The study focusing on evaluating two type of prosthetic socket. The geometrical shape of residuum and the socket consider to be differed to enhance the contact surface between both of it. The geometrical changes were observed during complete stage of donning simulation. The evaluation result is an important key toward improving an accuracy of the model design.

Chapter 5 chapter presents a pressure distribution analysis occurred in prosthetic socket. The pressure measured in donning process simulation and gait cycle simulation. The 3D model created in the simulation were MRI based. The models were pre-determined with dynamic parameter that based on previous study. The result then compared with actual experiment data conducted from previous study. The result showed high correlation between simulation and experiment measurement.

Chapter 6 will conclude the study about the transfemoral prosthesis function analysis using finite element method. The achievements and the limitation of this research was explained briefly. Furthermore, some solution to improve of this work was discussed.

Chapter 7 present the future work related to this study. An improvement of the research will be elaborate in order to increase the capabilities of the research output in the future. In this chapter, one of the novelty approaches has been introduced. The non-linear walking simulation of transfemoral prosthesis device was introduced and the parameter of the simulation was defined by using commercial video analysis software. The simulation can be used in the future to predict the ground reaction force of transfemoral prostheses during the walking and study the behaviour of pressure distribution during wearing the socket while working. From the future study, the advance and accurate prosthetic socket can be developed.

1.6 Scope of Study

In this research, several scopes of study are required to enhance the result of the research. The scope of study is divided by three main parts which are subjects, methodology and experiment procedures.

The research was conducted by utilize a three subject`s data. The quantity of the subject is small and not enough for a statistical analysis. However, there are several types of experiment was conducted using the same subject. The cumulative number of the experiment with the same subject ensure the comparison with simulation resulting a good correlation with experiment and simulation

In this research, the cloud of MRI data was used. In order to get the data of subject wearing the transfemoral prosthetic leg, subject need to lying on the bed inside the magnetic resonant device. Same procedure also applied to the subject in without prosthetic leg condition. The condition has set to ensure the quality of collected data fulfil the requirement. By this condition, the geometry of the residuum during standing position is can not be replicated. The limitation has affected the process of creating a 3D model because the model was created based on the MRI data`s specification. Therefore, in this research, we analyse the structure of residuum during inserted into the socket and compare it with result of donning simulation. The comparison can be one of the methods to justify the limitation of the taken MRI data.

In this research, MRI data was taken into consideration since it provides more level of distinguish between internal soft tissue of the residuum. In addition, the MRI image provide less harm compare to CT scan. Furthermore, the MRI data was not undergoing any filtration process to ensure the novelty of the methodology. Without the filtration, the data still provides distinguish between soft tissue such as fat, muscle and bone. With this distinction, the 3D model can be created with different internal part included.

Even though there is a certain limitation was faced during conducting the research and by the aid and help from other research reference, we able to solve the problem through out the research activity. The scope of study gave an opportunity to focus on the niche area of the research.

Chapter 2

Literature and Technical Review

In this chapter, a relationship with the past study will be explained. This chapter will review a technical study of finite element analysis (FEA) that act as a fundamental of the overall study. Also, the basic concept of creating the precise 3D model of residuum and prosthetic socket will be highlighted. This chapter also presents a revision of the previous studies. Some prevailing results of studies are also introduced to clarify the novelty of the contributions in this work.

2.1 Technical Review

2.1.1 B-Spline interpolation

B-spline is an acronym for basic spline which can be define as a curve line drew from one point to another point. B-spline have usually been used in designing various type of model based on the location of the point. A natural way to construct a curve from a set of given points is to force the curve to pass through the points or interpolate the points. There are various type of B-spline interpolation and the study has adopted the Bezier curve interpolation method as a basic algorithm for the three-dimensional (3D) model construction process.

2.1.1.1 Bezier Curve Interpolation

Bezier curves can be described as a polynomial curve and the method can avoid the problem of wiggles and bulges because all computations are true convex combinations. The segments of Bezier curves can easily be joined smoothly together to form more complex shapes. This avoids the problem of using curves of high polynomial degree when many points are approximated. Bezier curves are a special case of the spline curves. The smoothness of Bezier curves between neighbouring pieces was depended or controlled by the chosen control points. It turns out that by adjusting the construction of Bezier curves slightly, the production pieces of polynomial curves that automatically tie together become smooth. Here the Bezier curve interpolation or spline curve can be described with below equation:

$$p(\mathrm{t}|c_1, c_2; t_2, t_3) = \frac{t_3 - t}{t_3 - t_2} c_1 + \frac{t - t_2}{t_3 - t_2} c_2, \quad t \in [t_2, t_3] \tag{2.1}$$

where t and c denote as knot vector and control point respectively. By the setting $t_2<t_3$ and when $t_3=1$ and $t_2=0$, the curve equation become linear Bezier curve. The combination of multiple active point will be creating the piecewise linear curve **f** and described in equation 2.2.

$$\boldsymbol{f}(t) = \begin{cases} \boldsymbol{p}(\mathrm{t}|c_1, c_2; t_2, t_3), & t \in [t_2, t_3] \\ \boldsymbol{p}(\mathrm{t}|c_2, c_3; t_3, t_4), & t \in [t_3, t_4] \\ \quad\quad . & \\ \boldsymbol{p}(\mathrm{t}|c_{n-1}, c_n; t_n, t_{n+1}), & t \in [t_n, t_{n+1}] \end{cases} \tag{2.2}$$

The construction of spline curves can be generalized to arbitrary polynomial degrees by forming more averages. A cubic spline segment requires four control points c_{i-3}, c_{i-2}, c_{i-1}, c_i, and six knots $(t_j)_{j=i-2}^{i+3}$ which must form a nondecreasing sequence of numbers with $t_i < t_{i+1}$. The curve is the average of two quadratic segments,

$$\begin{aligned} \boldsymbol{p}(\mathrm{t}|c_{i-3}, c_{i-2}, c_{i-1}, c_i; t_{i-1}, t_{i-2}, t_i, t_{i+1}, t_{i+2}, t_{i+3}) \\ = \frac{t_{i+1} - t}{t_{i+1} - t_i} p(t|c_{i-3}, c_{i-2}, c_{i-1}; t_{i-1}, t_{i-2}, t_i, t_{i+1}, t_{i+2}) \\ + \frac{t - t_i}{t_{i+1} - t_i} p(t|c_{i-2}, c_{i-1}, c_i; t_{i-1}, t_i, t_{i+2}, t_{i+3}) \end{aligned} \tag{2.3}$$

with t varying in $[t_i, t_{i+1}]$. The two quadratic segments are given by convex combinations of linear segments on the two intervals $[t_{i-1}, t_{i+1}]$ and $[t_i, t_{i+2}]$. The three-line segments are in turn given by convex combinations of the given points on the intervals $[t_{i-2}, t_{i+1}]$, $[t_{i-1}, t_{i+2}]$ and $[t_i, t_{i+3}]$. Note that all these intervals contain $[t_i, t_{i+1}]$ so that when t varies in $[t_i, t_{i+1}]$ all the combinations involved in the construction of the cubic curve will be convex. This also shows that we can never get division by zero since we have assumed that $t_i < t_{i+1}$. The generalization of the spline curves of even higher degrees can be describe in equation 2.4.

$$\boldsymbol{p}_{i,k}^{s}(t) = \boldsymbol{p}(t \mid c_{i-k}, \ldots, c_i, t_{i-k+1}, \ldots, t_i, t_{i+s}, \ldots, t_{i+k+s-1}), \tag{2.4}$$

for some positive integer s, assuming that the control points and knots in question are given. The first subscript i $p_{i,k}^{s}$n indicates which control points and knots are involved (in general we work with many spline segments and therefore long arrays of control points and knots), the second subscript k gives the polynomial degree, and the superscript s gives the gap between the knots in the computation of the weight $(t - t_i)/(t_{i+s} - t_i)$. With the abbreviation (2.4), equation (2.3) becomes:

$$p^1_{i,3}(t) = \frac{t_{i+1} - t}{t_{i+1} - t_i} p^2_{i-1,2}(t) + \frac{t - t_i}{t_{i+1} - t_i} p^2_{i,2}(t). \tag{2.5}$$

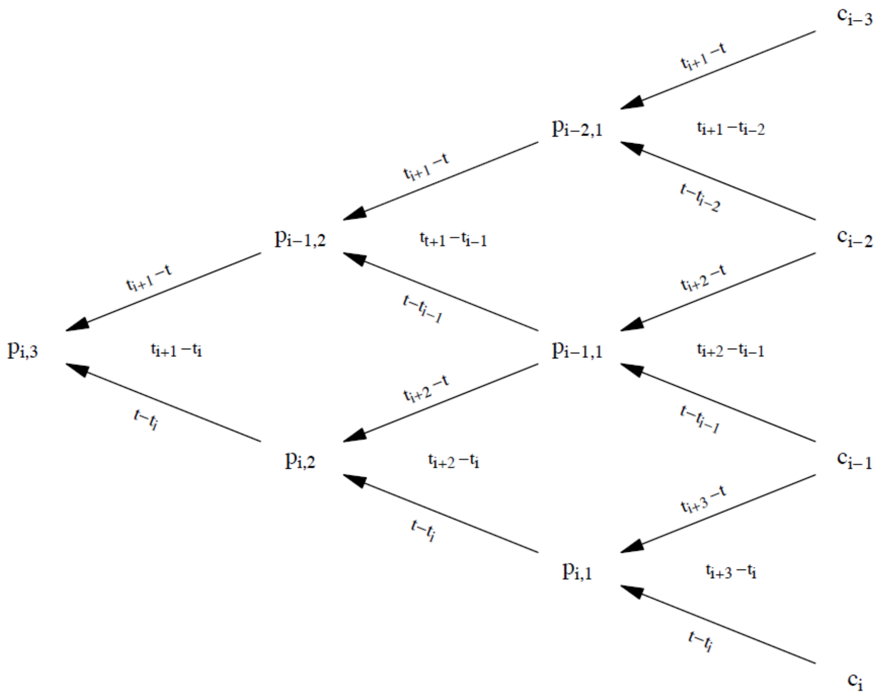

Figure 2.1 Computing a point on a cubic spline curve

The complete computations involved in computing a point on the cubic segment $p_{i,3}(t)$ can be arranged in the triangular array shown in Figure 2.1 (all arguments to the $p_{i,k}$ have been omitted to conserve space). A segment of a general spline curve of degree d requires d + 1 control points $(c_j)_{j=i-d}^{i}$ and 2d knots $(t_j)_{j=i-d+1}^{i+d}$ that form a nondecreasing sequence with $t_i < t_{i+1}$. The curve is a weighted average of two curves of degree d − 1,

$$p_{i,d}(t) = \frac{t_{i+1} - t}{t_{i+1} - t_i} p_{i-1,d-1}(t) + \frac{t - t_i}{t_{i+1} - t_i} p_{i,d-1}(t). \tag{2.6}$$

Because of the assumption $t_i < t_{i+1}$ we never get division by zero in (2.6). The two curves of degree d − 1 are obtained by forming similar convex combinations of curves of degree d − 2. For example,

$$\boldsymbol{p}_{i,d-1}(t) = \frac{t_{i+2} - t}{t_{i+2} - t_i}\boldsymbol{p}_{i-1,d-2}(t) + \frac{t - t_i}{t_{i+2} - t_i}\boldsymbol{p}_{i,d-2}(t), \tag{2.7}$$

and again, the condition $t_i < t_{i+1}$ saves us from dividing by zero. At the lowest level we have d line segments that are determined directly from the control points,

$$\boldsymbol{p}_{j,1}(t) = \frac{t_{j+d} - t}{t_{j+d} - t_j}\boldsymbol{c}_{j-1} + \frac{t - t_j}{t_{j+d} - t_j}\boldsymbol{c}_j \tag{2.8}$$

for j = i − d + 1, . . ., i. The denominators in this case are $t_{i+1} - t_{i-d+1}$, . . ., $t_{i+d} - t_i$, all of which are positive since the knots are nondecreasing with $t_i < t_{i+1}$. As long as t is restricted to the interval $[t_i, t_{i+1}]$, all the operations involved in computing $p_{i,d}(t)$ are convex combinations. The complete computerization is described below equation:

$$\boldsymbol{p}_{j,r}(t) = \frac{t_{j+d-r+1} - t}{t_{j+d-r+1} - t_j}\boldsymbol{p}_{j-1,r-1}(t) + \frac{t - t_j}{t_{j+d-r+1} - t_j}\boldsymbol{p}_{j,r-1}(t) \tag{2.9}$$

for j = i − d + r, . . ., i and r = 1, 2, . . ., d.

A spline curve of degree d with n control points $(c_i)_{i=1}^{n}$ and knots $(t_i)_{i=2}^{n+d}$ is given by

$$\boldsymbol{f}(t) = \begin{cases} \boldsymbol{p}_{d+1,d}(t) & t \in [t_{d+1}, t_{d+2}], \\ \boldsymbol{p}_{d+2,d}(t), & t \in [t_{d+2}, t_{d+3}]; \\ \vdots & \vdots \\ \boldsymbol{p}_{n,d}(t), & t \in [t_n, t_{n+1}], \end{cases} \tag{2.10}$$

whereas before it is assumed that the knots are nondecreasing and in addition that $t_i < t_{i+1}$ for i = d + 1, . . ., n. Again, we can express **f** in terms of the piecewise constant functions given

$$\boldsymbol{f}(t) = \sum_{i=d+1}^{n} \boldsymbol{p}_{i,d}(t) B_{i,0}(t). \tag{2.11}$$

The geometric construction of one segment of a spline curve, however elegant and numerically stable it may be, would hardly be of much practical interest was it not for the fact that it is possible to smoothly join neighbouring segments. The estimation of connection between intersection point between Magnetic Resonant Image (MRI) image and trajectory line are following the Bezier curve or B-spline interpolation. The ideal curve point will be discussed further in the next chapter. The relationship between number of curve point and b-spline curve interpolation will be discuss in chapter 3.

2.1.2 Finite Element Method

Finite element method (FEM) or finite element analysis (FEA) can be define as a numerical method for solving problem of engineering and mathematical physics. FEM has been utilized widely in engineering field especially in aeronautical engineering because one of its essential characteristics is the decomposition of a continuous domain into a set of discrete sub-domains. Such a characteristic provides a great advantage to employ local information comprehensively and to describe variation details, while much computation is needed.

The development of finite element methods for the solution of practical engineering problems began with the advent of the digital computer. That is, the essence of a finite element solution of an engineering problem is that a set of governing algebraic equations is established and solved, and it was only through the use of the digital computer that this process could be rendered effective and given general applicability. These two properties effectiveness and general applicability in engineering analysis-are inherent in the theory used and have been developed to a high degree for practical computations, so that finite element methods have found wide appeal in engineering practice.

In the study FEM has been utilized to create an environment where the connection between actual experiment and simulation can be realize. It is because mathematically, the finite element method is employed to find approximate solutions of partial differential equations as well as solutions of integral equations or their combinations. The solution approach is usually a numerically based simulation. However, the finite element simulation computational time are greatly affected by quantity of nodes and elements. This is because the symmetrical, banded stiffness matrix, which is a bandwidth is dependent on the difference in the node numbers for each element and this bandwidth is directly connected with the number of calculations the computer has to do.

In the modelling of the mechanical response of a soft tissue, the FEM has been employed to solve the established constitutive equation which describe the soft tissue behaviour. It is included the energy principle, hourglass phenomenon and energy dissipated during deformation of soft tissue. On the other hand, with the increase of the computation power of computers, the finite element-based modelling becomes an efficient and accurate technique in many applications.

2.1.2.1 Finite Element Solution of Mathematical Model Theory

The mathematical model of finite element is depending on various parameter. It included the geometry of the model, kinematic, material properties, material law, loading, boundary condition etc. Based on those parameter, numerical analysis will be conduct where it has been embedded inside the finite element simulation. In other hand, the finite element environment which is calculated based on the mathematical model is the solution that affected by the selection of certain parameter inside the model such as finite element quantity, mesh density, displacement, velocity, energy consumption, force etc. Based on the mathematical model and the environment, assessment of accuracy of finite element solution will be conducted. The feedback from the assessment will be used to refine the parameter such as mesh density etc. for creating an accurate simulation.

2.1.2.2 Nonlinear Analysis in Finite Element Method

In the research, a large deformation is hypothetically assumed happen in elastic material model. The linear elastic equation is not corresponded to the large deformation. When the problem came out of linearity of the equation such as the displacement of node is constantly changed or the force given to the model is unpredictable, the nonlinear analysis is required.

The linearity of a response prediction rests on the assumptions just stated, and it is instructive to identify in detail where these assumptions have entered the equilibrium equations in (2.12).

$$\mathbf{KU} = \mathbf{R} \tag{2.12}$$

The fact that the displacements must be small has entered the evaluation of the matrix **K** and load vector **R** because all integrations have been performed over the original volume of the finite elements, and the strain-displacement matrix **B** of each element was assumed to be constant and independent of the element displacements. The assumption of a linear elastic material is implied in the use of a constant stress-strain matrix C, and, finally, the assumption that the boundary conditions remain unchanged is reflected in the use of constant constraint relations for the complete response. If during loading a displacement boundary condition should change, e.g., a degree of freedom which was free becomes restrained at a certain load level, the response is linear only prior to the change in boundary condition.

Table 2.1 showed a classification of nonlinear analysis based on their description. An illustration of the type of this analysis shown in figure 2.2. noted that in a materially-nonlinear analysis, the nonlinear effects lie only in the non-linear stress-strain relation.

Table 2.1 Classification of nonlinear analysis [26]

Type of Analysis	**Description**	**Typical formulation used**	**Stress and strain measures**
Materially-nonlinear-only	Infinitesimal displacement and strains; the stress-strain relation is nonlinear	Material-nonlinear-only (MNO)	Engineering stress and strain
Large displacement, large rotations, but small strains	Displacement and rotation of fibres are large, but fibres extensions and angle changes between fibres are small; the stress-strain relation may be linear or nonlinear	Total Lagrange (TL) Updated Lagrange (UL)	Second Piola-Kirchhoff stress, Green-LaGrange strain Cauchy stress, Almansi strain
Large displacement, large rotations, and large strains	Fibres extensions and angle changes between fibres are large, fibre displacement and rotation may also be large, the stress-strain relation maybe linear or nonlinear	Total Lagrange (TL) Updated Lagrange (UL)	Second Piola-Kirchhoff stress, Green-Lagrange strain Cauchy stress, logarithmic strain

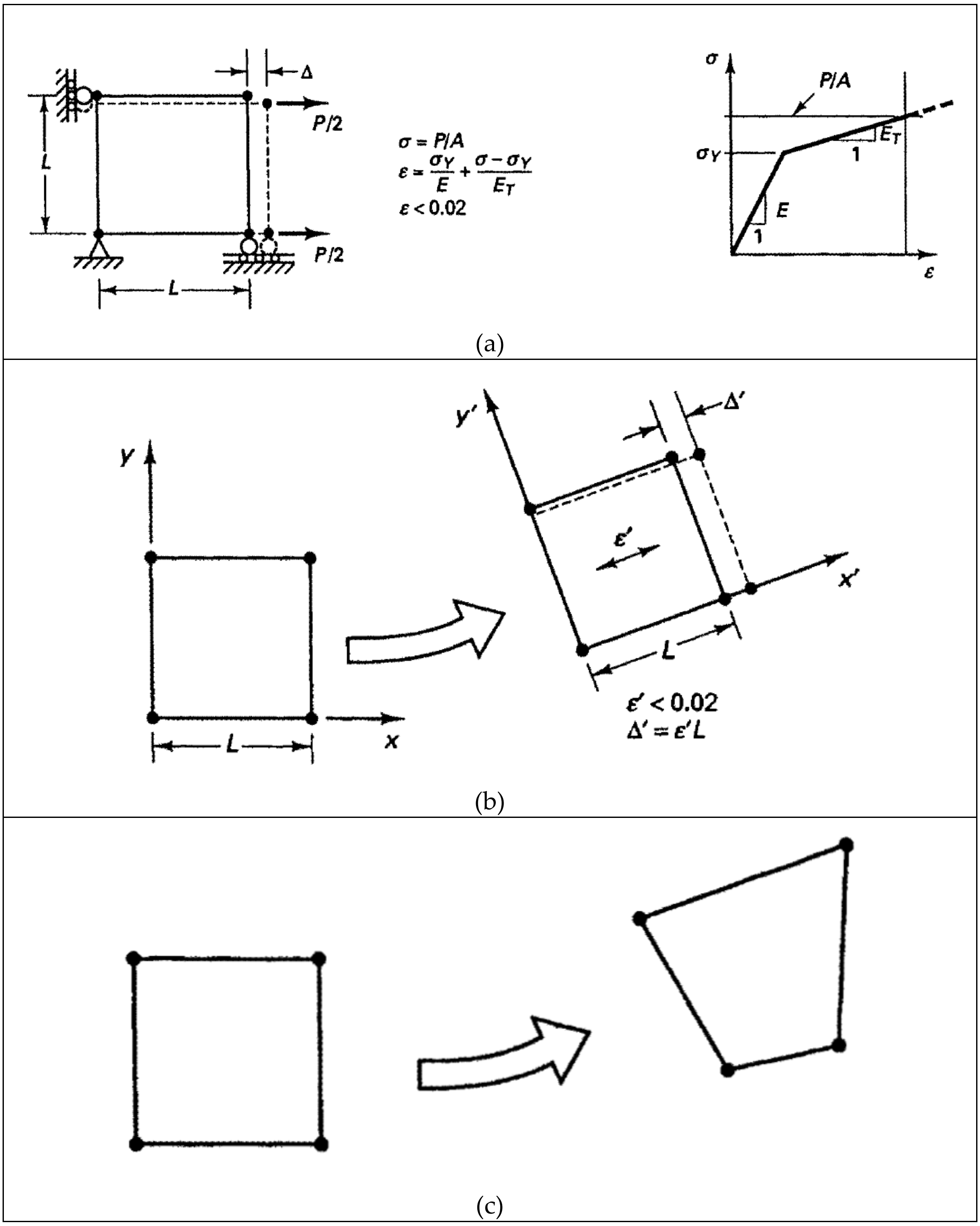

Figure 2.2 illustration of nonlinear analysis types. (a) Materially-nonlinear-only (infinitesimal displacements, but nonlinear stress-strain relation); (b) Large displacements and large rotations but small strains. Linear or nonlinear material behaviour; (c) Large displacements, large rotations, and large strains. Linear or nonlinear material behaviour [26]

In an analysis simulation software, the decision whether a problem falls into one or the other category of analysis will be calculated based on the setting of the function in the software. The settings will dictate which formulation will be used to describe the actual physical situation. Conversely, we may say that by the use of a specific formulation, a model of the actual physical situation is assumed, and the choice of formulation is part of the complete modelling process. Surely, the use of the most general large strain formulation "will always be correct"; however, the use of a more restrictive formulation may be computationally more effective and may also provide more insight into the response prediction.

2.1.2.3 Finite Element Analysis Stage

Generally, a finite element analysis (FEA) consist of three separated stages namely pre-processing, processing and postprocessing. A complete analysis is a logical interaction of these three stages.

I. Pre-processing

As the name indicates, pre-processing is something you do before processing your analysis. The pre-processing involves the preparations of data, such as nodal coordinates, connectivity, boundary conditions and loading and material information.

The preparation of data requires considerable effort if all data are to be handled manually. If the model is small, the user can often just write a text file and feed it into the processor, but as the complexity of the model grows and the number of elements increase, writing the data manually can be very time consuming and error-prone. Its therefore necessary with a computer pre-processor which help with mesh plotting and boundary conditions plotting.

For an example of a simple pre-processor, see the Java-applet on these pages. Her you can change loads, boundary conditions, mesh and element properties and material. All this is done graphically to minimize the chance of error. The only limitation is that you cannot draw your own geometry, you have to select one of the pre-generated geometries.

II. Processing

The processing stage involves stiffness generation, stiffness modification, and solution of equations, resulting in the evaluation of nodal variables. This is a typical" black box"-operation, as the user will see little of what's going on. You feed data from the pre-processor, and you get data out.

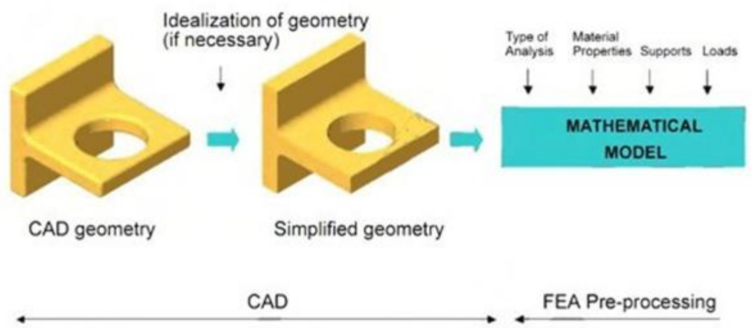

Figure 2.3 FEA Pre-processing (simplan.de)

III. Postprocessing

The postprocessing stage deals with the representation of results. Typically, the deformed configuration, mode shapes, temperature, and stress distribution are computed and displayed at this stage.

For an example of a simple postprocessor, see the Java applet on these pages. Here you can, after analysis of a model, view the deformed model, and inspect stresses and displacements, both in the centroid of elements and the nodal values, and see contour plotting of these data.

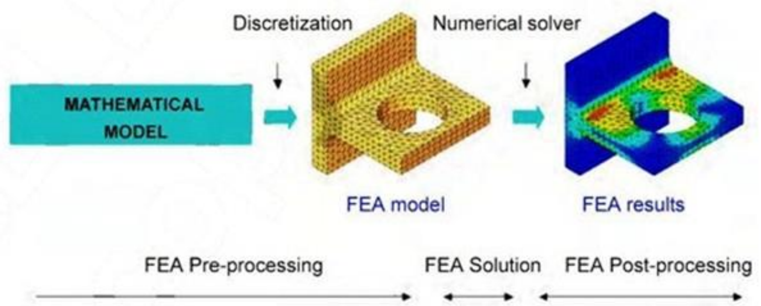

Figure 2.4 FEA postprocessing (simplan.de)

2.1.3 Computer Aided Drawing Software (CREO Parametric)

Creo is a computer aided drawing (CAD) software developed by Parametric Technology Corporation (PTC). Creo is a scalable, interoperable suite of product design software that delivers fast time to value. It helps teams create, analyse, view, and leverage product designs downstream utilizing 2D CAD, 3D CAD, parametric, and direct modelling. Creo is a powerful software which provide various function use in engineering field. Most common software used for CAD purpose is Creo Parametric. Creo Parametric is the standard in 3D CAD software.

It provides the broadest range of powerful yet flexible 3D CAD capabilities to accelerate the design of parts and assemblies.

Creo Parametric capable to create a 3D solid modelling with a precise geometry, regardless of model complexity. The technical surfacing method embedded in the software enable the user to develop a complex surface geometry with a single button click. There is a lot of `friendly` function in the software such as sweeps, blends, extends, offsets and many more to help the user creating a precise surface of a 3D model.

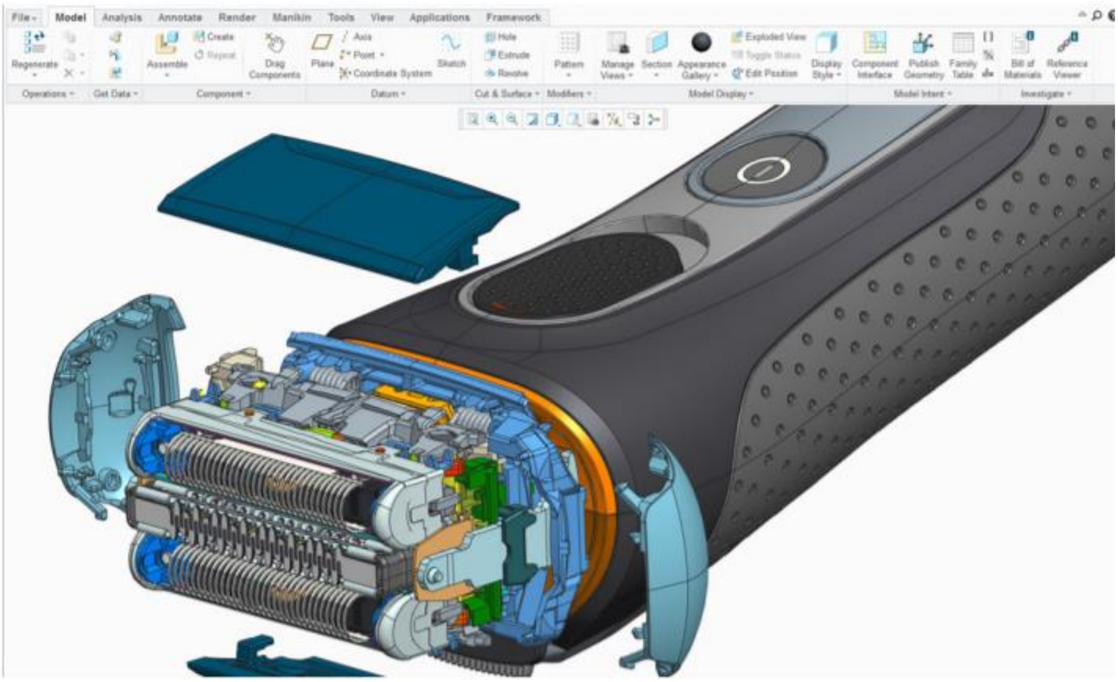

Figure 2.5 Creo Parametric environment and GUI (PTC Ltd.)

Creo Parametric also has an analysis features embedded. However, the features can only perform a basic static structural analysis on parts and assemblies. For that reason, this study must find an alternative to perform a dynamic analysis which can be synchronize a static and kinematic analysis in a same time. In other hand, one advantage that makes Creo Parametric was chosen for the study is the ability to convert a 3D model structure into a surface dimension standard file format including STEP, IGES, DXF, STL, VRML, AutoCAD DWG, DXF etc. Unite technology also was use in the software enable converting data from other CAD system including CATIA, Siemens NX, Solidworks, Autodesk and SolidEdge.

2.1.4 LS-DYNA 3D Solver

LS-Dyna is advanced general-purpose multi-physics simulation software developed by Livermore Software Technology Corporation. LS-Dyna is a Non-linear Explicit Transient Dynamic FE code, originated from the 3-D FEA program DYNA-3D developed by Dr.John.O.Hallquist at Lawrence Livermore National Laboratory, California in 1976.

The main application areas of LS-DYNA are crash simulations, metal forming simulations and the simulation of impact problems and other strongly non-linear tasks. LS-DYNA can also be used to successfully solve complex nonlinear static problems in cases where implicit solution methods cannot be applied due to convergence problems.

In conjunction of the variation of parameter embedded for dynamic analysis, the software was chosen to accomplish the objective of the study. LS-DYNA has embedded with encrypted keyword file namely K file to realize the simulation. K file consist of variety of keyword parameter that's define the simulation framework. Here, the discussion of utilized keyword that contribute to the research framework will be elaborated.

2.1.4.1 Prescribed Motion

Define an imposed nodal motion (velocity, acceleration, or displacement) on a node or a set of nodes [27]. Also, velocities and displacements can be imposed on rigid bodies. If the local option is active the motion is prescribed with respect to the local coordinate system for the rigid body (See variable LCO for keyword *MAT_RIGID). Translational nodal velocity and acceleration specifications for rigid body nodes are allowed and are applied as described at the end of this section. For nodes on rigid bodies use the NODE option.

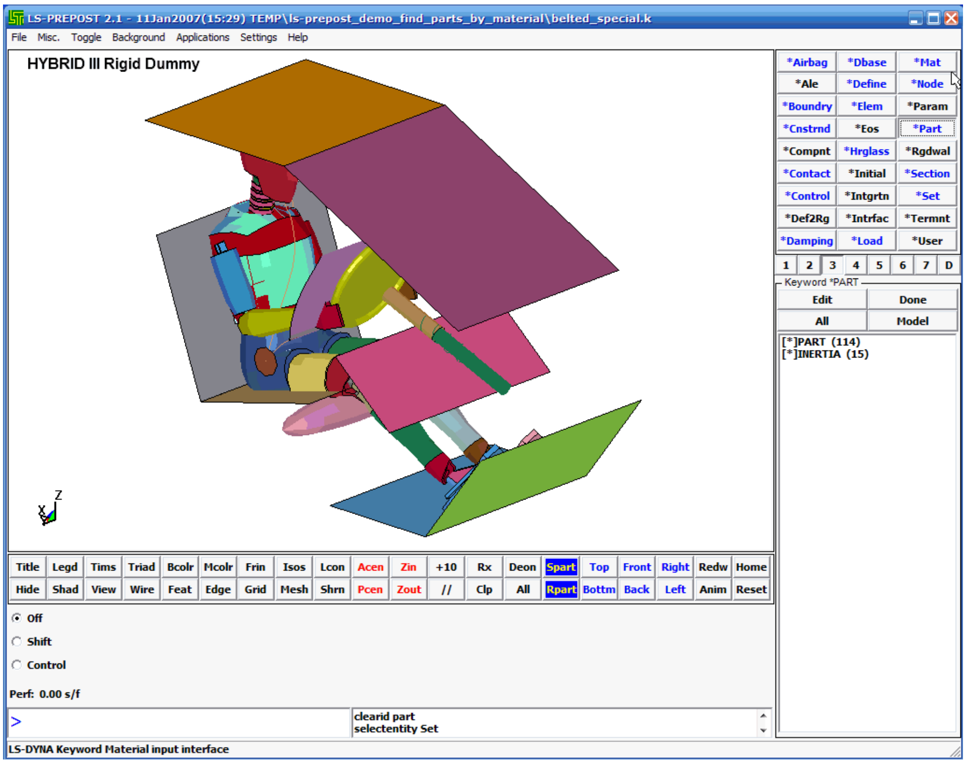

Figure 2.6 GUI of LS-Prepost (LS-DYNA) solver (Lstc.com)

2.1.4.2 Constraint

The constraint keyword provides a way of constraining degrees of freedom to move together in some way [27]. The keyword was used to define the constraint between a rigid body and non-rigid body. By this keyword, the non-rigid body will convert into a rigid body that posses a similar characteristic with attached rigid body. Extra nodes for rigid bodies may be placed anywhere, even outside the body, and they are assumed to be part of the rigid body. They have many uses including:

1. The definition of draw beads in metal forming applications by listing nodes along the draw bead.
2. Placing nodes where joints will be attached between rigid bodies.
3. Defining a node where point loads are to be applied or where springs may be attached.
4. Defining a lumped mass at a particular location.

2.1.4.3 Contact Definition

The keyword *CONTACT provides a way of treating interaction between disjoint parts. Contact definition is an important keyword to determine the output of the simulation [27]. The contact definition need to specifically defined such as static friction coefficient, dynamic friction coefficient, master and slave part, energy calculation equation and contact penalty value. Combining all the defined parameter, a smooth interaction between two or more model can be develop. The simulation will stop processing if the contact definition is not well tuned.

2.1.4.4 Loading Definition

The keyword *DEFINE provides a way of defining boxes, coordinate systems, load curves, tables, and orientation vectors for various uses. A definition of a curve [for example, load (ordinate value) versus time (abscissa value)], often referred to as a load curve. Curves are discretized internally with equal intervals along the abscissa for fast evaluation in constitutive models. Discretized curves are not used for evaluating loading conditions, e.g., pressures, concentrated forces, displacement boundary conditions, etc. [27].

2.2 Literature Review

2.2.1 Accuracy of 3D modelling

In this study, the accuracy of every created models is a precious benchmark towards achieving the ultimate research objective. Many studies have indicated that the accuracy of 3D model is defined by a method of creating the model.

Recent technological development has improved the method of creating a 3D model. For instance, in bio-mechanical engineering field, the utilization of machines and software, e.g Rodin 4D (Rodin 4D), Canfit™ (Vorum) and 3D Scanner has created an accurate 3D model with the complexity of the surface structure took into consideration. These technologies help manufacturer and therapist to develop a dummy model based on actual subject measurement. However, these technologies are quite complex and involves considerable workload, besides being difficult to apply in practice due to their unclear methodologies.

As mentioned by Ngon D. T. et. al [28], creating a 3D model of Globoid CAM with a complicated profile is quite difficult. However, Creo Parametric software can be used to create such model with precise measurement of curve equation. The features in Creo Parametric is simple and effective for user to determine the design parameters, compute operating- parameters, compute curve parameter and build a design profile using a single software. Based on the featured function in Creo Parametric, the software has been chosen to lead the study in designing the 3D model of the residuum and its socket.

In other studies, conducted by Giorgio Colombo et al. [29] where the construction of an amputee digital model using LifeMOD™ has been reported. LifeMOD™ is a biomechanical simulation package based on MSC ADAMS solver. The simulator is expensive and is not affordable for general users. The accuracy of created model was high due to it precision on calculating the residuum surface based on 3D scanner specification. To initialize the simulator, user need to have a lot of consideration such as financial stability etc. because the simulator is a very sophisticated and expensive to purchase. For this research, alternative method will be introduced to cover the financial problem. The method will be discussed detail in chapter 3.

Arun Dayal Udai and Amarendra Nath Sinha [30] reported the use of a combination of CAD and image processing tools to generate an accurate 3D model. The usage of MATLAB for filtering the Magnetic Resonance Imaging (MRI) image is necessary to determine the outer geometry of the image before it was used to construct the model. By the filtering technique, the accuracy of 3D model can be enhanced. The filtering technique also can be use not only in MRI image, but it also can be use in CT image and RGB image as usual. However, in their paper, the accuracies of the model's volume, shape, and composition of fat, skin, muscle, and bone were not evaluated. The accuracy of the 3D model is discussed by comparing the residuum model structure with outer geometry of the MRI image. In conjunction of the matter, this study has proposed a novel methodology to evaluate the accuracy of the 3D model.

2.2.2 Transfemoral Prostheses Socket Function

A lower-limb prosthesis is an artificial limb that is designed to mimic the natural function, structure, and aesthetics of a limb that is replaced. Different types of lower-limb prosthesis exist based on the levels of extremity of the lower-limb amputations. A transfemoral or above-knee prosthesis is an artificial limb for a case in which the knee joint is removed, and part of the femur or thigh bone remains intact. The socket is one of the most important parts of the transfemoral prosthesis because it acts as a connection between the residual limb and prosthesis. It protects the residual limb and appropriately transfers forces during standing and ambulation motions.

It is important that the subject feels comfortable while wearing the prosthetic device. Most physical changes are suffered by the residuum during gait when the body load is transferred to the socket. These changes can induce skin problem such as callosities, abrasions, and blisters [31]. A lot of research has been conducted to investigate the behaviour of residuum during gait cycle. They collected data for the manufacturer and physiotherapist to make improvement of their product or rehabilitation method. Most of the research focused on the surface pressure analysis of socket at certain point. Few studies focusing on trans-tibial or below-knee prosthesis utilized the finite element method to determine the stress distribution [32-33]. However, the measured change of volume in soft tissue was very low since the shape of residuum and socket were assumed to be the same.

Reference [31] used five sample subject data to perform the actual donning procedure. However, due to the similarity of the socket and residuum shape, the maximum contact pressure observed in the study (5.6 kPa) was lower than other studies. Reference [34] utilized a non-linear FE model with a homogenous and isotropic residuum contacted with socket. 80.57 kPa of maximum normal stress recorded at the distal end of the residuum. Their result difference from other in term of maximum stress on the residuum probably because the shape of the rectified socket was assumed to be the same as residuum. There are case studies on the behaviour of residuum [35-36], which characterized the mechanical condition of muscle flap of a trans-tibial patient for static load bearing. Here, the residuum model was divided into three parts viz., bone, muscle, and skin. The simulation revealed that the interface pressure between residuum and socket was 65 kPa, which has high correlation with the pressure obtained in clinical measurement.

2.2.3 Pressure Distribution in Prostheses Socket

The skin and soft tissue of a residual limb are subject to stress and excessive distortion during gait positioning [37] and are significantly higher during transfemoral prosthesis since a residual limb is comprised of complex soft tissue and experiences a large change in volume with the use of sockets. Thus, the prosthesis is unstable, and this makes it difficult for the patient. In order to evaluate the quality of socket design and fit, the pressure distribution at the interface between the residual limb and prosthetic socket is considered as an extremely important factor. An abnormal force transferred from the socket to a residual limb can cause unstable gait, pressure ulcers, and deep tissue injuries.

In conjunction of the matter, many studies have been conducted to investigate the possibility of theoretical analysis utilization to provide an alternative evaluation for pre-fabrication of prosthetic device. For instance, [38-41] were reported to investigate the stress distribution between residuum and prosthetic socket by utilizing finite element analysis. Even though the result were promising in term of the stability of the model geometry, the socket model was not realistically developed because the shape of the socket is similar with residuum shape. Thus, the geometrical changes of the residuum are not clearly seen.

Besides focusing on socket design and manufacturing methods, Sengeh et. al [42] was determined to investigate the effect of designing residuum model with multi-material towards an accuracy of actual residuum parameter. The residuum was modelled with subject-specific magnetic resonant (MR) image to allow the model being evaluated with numerical approach and its inspired this study to model the residuum with subject-specific parameter but with different methodology. Portnoy et. al [43] also reported that using subject-specific analysis of internal tissue loads in the residuum in real time is a practical tool for evaluating an internal stress inside residuum in clinical setting or outdoors.

2.3 Conclusion

In this chapter, the author has presented the fundamentals of basic spline interpolation, which is based on Bezier curve interpolation theory, finite element analysis (FEA), three-dimensional (3D) model creator by Creo Parametric software and its applied for development of precision 3D model using actual subject parameter. The application of FEA in LS-Dyna solver to simulate the interaction between residuum and socket also has been discussed. Simultaneously, many related studies have been reviewed to complement a panoramic view of the background. The concepts, terminologies, and equations in this chapter are very important for the subsequent chapters.

Chapter 3

Accuracy Evaluation on 3D Reconstruction of Transfemoral Residuum Model

In this chapter, a study on the accurateness of 3D reconstruction for transfemoral residual limb based on Magnetic Resonance Imaging (MRI) using basic spline (B-Spline) interpolation feature is discussed. Many researches have constructed 3D models by using the Non-Uniform Rational B-Spline (NURBS) approach; however, almost none of those studies have elaborated in detail the methodology used in the project and the accuracy of the model's volume against the residual limb volume. This chapter focuses on the optimization of the residual limb model's volume by investigating the effect of spline points on the volume value.

This investigation is divided into 3 phases, namely pre-segmentation, segmentation, and three-dimensional (3D) reconstruction. However, this study focuses on the segmentation phase in which four different spline point numbers are chosen, namely 72, 36, 24, and 12 points; Computer Aided Drawing (CAD) software CREO Parametric (PTC) was used for this process. As a hypothesis of this chapter, a higher number of spline points achieved greater accuracy for the model's volume. The volume [mm^3] of the 3D model with the specified number of spline points was evaluated by comparing it with the volume of the 3D model created by using image processing tools from MATLAB (Math Works). The outcome of this chapter can be used to indicate that CAD software, which is a technical drawing tool, can also be used in the biomedical field to design 3D models of the human anatomy with high accuracy, if the software includes a spline interpolation feature.

3.1 Introduction

Recent technological developments have improved the design of transfemoral prosthesis sockets, by using 3D models of the residual limb created with various type of machines and software, e.g. Rodin 4D (Rodin 4D), Canfit™ (Vorum), and 3D Scanner. These technologies help manufacturers and therapists to develop prosthesis and orthosis devices. However, these technologies are quite complex and involves considerable workload, besides being difficult to apply in practice due to their unclear methodologies, as mentioned by Ngon Dang Thien, Giang Nguyen Truong [28]. For instance, Giorgio Colombo et al. [29] reported the construction of an amputee digital model using LifeMOD™, which is a biomechanical simulation package based on MSC ADAMS solver. The simulator is expensive and is not affordable for general users. Furthermore, the simulator cannot measure the residual model volume for evaluation purposes.

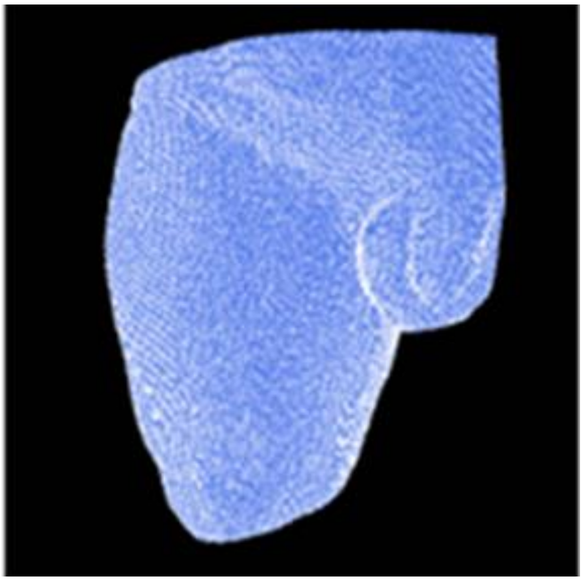

Figure 3.1 Residual Limb model created by LifeMOD™

Le Van Tuan et al. [44] mentioned the use of CAD and MATLAB software in constructing the geometry model of a residual limb (shown in Fig. 3.2); however, the methodology of creating the model was not described clearly. Moreover, the measurements of the created model were not compared with real amputee data, and the model was not evaluated in terms of the volume value.

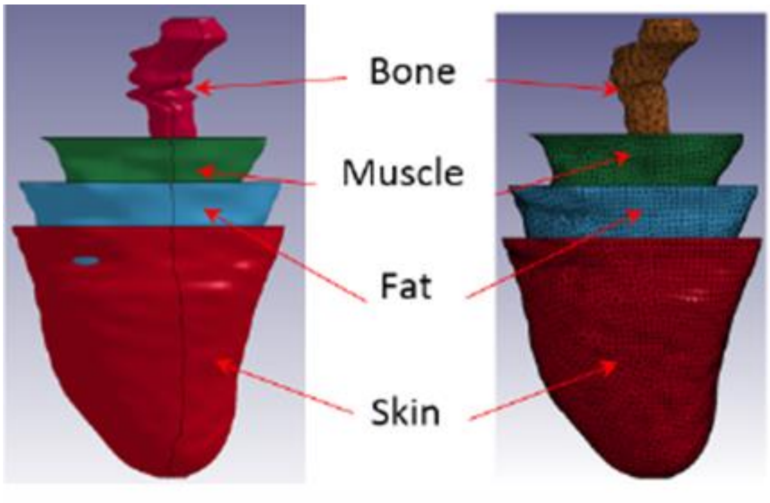

Figure 3.2 Geometry Model of Residual Limb [44]

Arun Dayal Udai and Amarendra Nath Sinha [30] reported the use of a combination of CAD and image processing tools to generate a 3D model. They have also mentioned the use of MATLAB for filtering the Magnetic Resonance Imaging (MRI) image before it was used to construct the model. However, in their paper, the accuracies of the model's volume, shape, and composition of fat, skin, muscle, and bone were not evaluated.

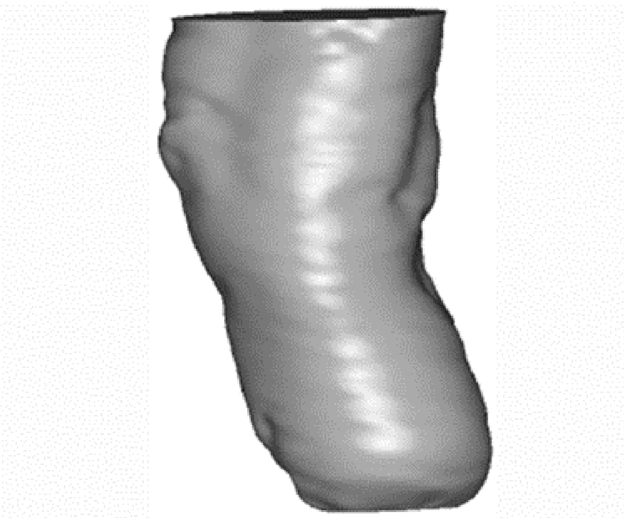

Figure 3.3 Completed Residual surface by Arun Dayal et. al [30].

The above-mentioned studies created models of the transfemoral residual limb using various methods; each of these methodologies has its own pros and contras. However, no measurements were made to evaluate the accuracy of the models in terms of the volume value. The accuracy of volume value in a residual limb model is a very crucial factor in the medical field, since it can help researchers to measure the density of residual limbs in future researches and investigate the muscle and fat changes.

The objective is to evaluate the accuracy of the created model by comparing its volume value with the measured volume of a model created using image processing tools from MATLAB (Math Work). The model is created with CREO Parametric (PTC) software by using the basic spline (B-spline) interpolation feature with 4 different spline point amounts (72,36,24, and 12 points). The volume of each model is compared with the image processing model, as its hypothesized volume has an almost similar value as that of a real residual limb. The methodology to create the model with different spline point amounts is proposed to achieve the objective.

3.2 Three-Dimensional Model Construction Methodology

In this section, a proposed method to design a residual limb model is presented. The proposed method must satisfy the following criteria:

- No extra features in CREO Parametric 3.0 (CREO 3.0) to maintain the novelty of the method.
- Simple and effective to use for physiotherapists and practitioners who are amateur users of CREO 3.0.

The transfemoral residual limb model was created using CREO 3.0 to meet the mentioned requirements. This methodology contains 4 phases, namely MRI data collection, pre-segmentation, segmentation, and 3D model construction.

3.2.1 Magnetic Resonant Imaging (MRI) Data Collection

In this study, MRI data of three (3) local transfemoral amputees are used. Data collection has been conducted ethically following the Declaration of Helsinki (DoH). The details of each amputee are given below:

Table 3.1 Profile of amputees

Measurement	Amputee		
	A	B	C
Weight (kg)	63	61	80
Height (cm)	169	167	162
Age (Years old)	35	47	56
Sex (M/F)	M	M	M
Amputated Leg	Left	Right	Right

MRI was used in order to obtain better images of the soft tissue and muscle boundaries [30]. Moreover, overdoses of Computed Tomography (CT) may prove to be harmful to the human body [44]. The MRI images were obtained using Siemens Magneton Symphony Maestro class 1.5 T. According to Chambers S et al. [45], MRI scanning image can reach 90.5% for the sensitivity, 89.5% for specific and 90.1% for accuracy. The MRI image of each amputee had a slightly different specification, as shown in Table 3.2.

Table 3.2 MRI image specifications

MRI Specification	Amputee	
	A, C	B
Pixels (mm)	0.78×0.78	0.8×0.8
Matrix Size (pixels)	512×512	512×512
Repetition Time (ms)	10.7	10.7
Echo Train Length	1	1

The MRI images were collected and stored in 3 different folders, indicating the 3 different amputees. Each file contains 30 MRI images of the sliced residual limb viewed from the z-axis.

3.2.2 Pre-segmentation

In this section, all the procedures are conducted using CREO 3.0 software. CREO 3.0 is a 3D CAD software, which provides the broadest range of powerful and flexible 3D CAD capabilities to accelerate the design of the parts and assemblies [46]. Table 3.3 shows some features of CREO 3.0 used to construct the 3D model using MRI images.

Table 3.3 Creo 3.0 features

Feature	Function
View/Model Display/Images	Export MRI images into CREO 3.0
Model/Plane	Create a plane where the MRI image will be located
Model/Sketch/Spline	Create a Non-uniform rational B-spline (NURBS) curve
Model/Sketch/Line	Create a horizontal line indicating the length of the model (Trajectory)

Model/Swept Blend	Create a 3D model, which is defined by two or more cross sections (Spline Curve) positioned along a trajectory
Model/Shell	Remove material from the inside of a fixed outside volume
Model/Pattern	Create a rotation replica of a line along the z-axis indicating the number of intersection points for spline curves
Model/Sketch/Offset	Offset the selected curve or line

In the pre-segmentation phase, the first step involves creating thirty planes where each plane is translated 5 mm from each other horizontally. In each plane, the MRI image is placed according to the sequence and scaled according to the pixel size, as shown in Fig. 3.4(a).

Next, the last image is chosen and all the images excluding the chosen one is hidden. In the image, a coordinate system is created at the centre of the bone. Then, a 150-mm line is drawn starting from the centre point of the coordinate system, and the pattern function is used to replicate the line, rotationally along the z-axis of the coordinate system (with a difference of 10 degree between each line), as shown in Fig. 3.4(b).

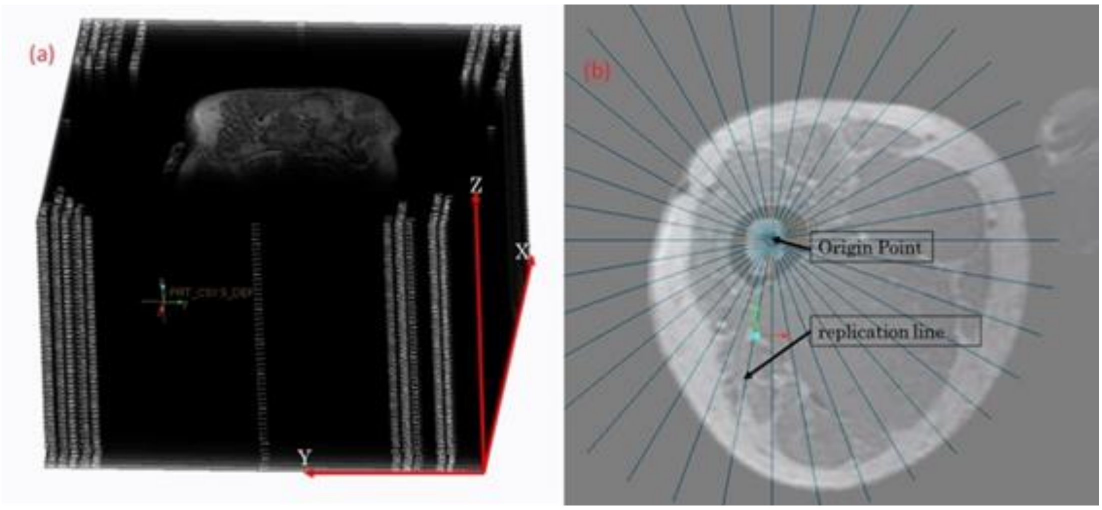

Figure 3.4 (a) Process of stacking MRI images in the z-axis, (b) Replication process in one layer of the MRI image

3.2.3 Segmentation

In the segmentation phase, basic spline interpolation (B-Spline) curves (or spline, as described in CREO 3.0) are used to connect the intersection between the replication line and the edge of each part. In this study, B-spline function is defined as generalization of Be'zier curve which is the combination of flexible line that passes through the number of spline point and create smooth curve for each slice of residual limb's MRI image. B-spline curves and surfaces are used in CAD and computer-aided geometric design (CAGD) not only to describe the mechanical parts but also to determine the offset curves and surfaces [47].

In this phase, the intersection between the replication line and the edge of each part is connected using the spline function. For one slice of residual limb, the estimation time to complete the segmentation for 12 spline point model is 40 s (±5 s) while 24 spline point model took 60 s (±5 s), 36 spline point model took 75 s (±5 s) and 72 spline point required 100 s (±20 s). The accuracy of the model's volume is investigated by creating the model with different spline point values, as shown in Fig. 3.5. The volume of each model is measured, and the percentage error for each model is calculated.

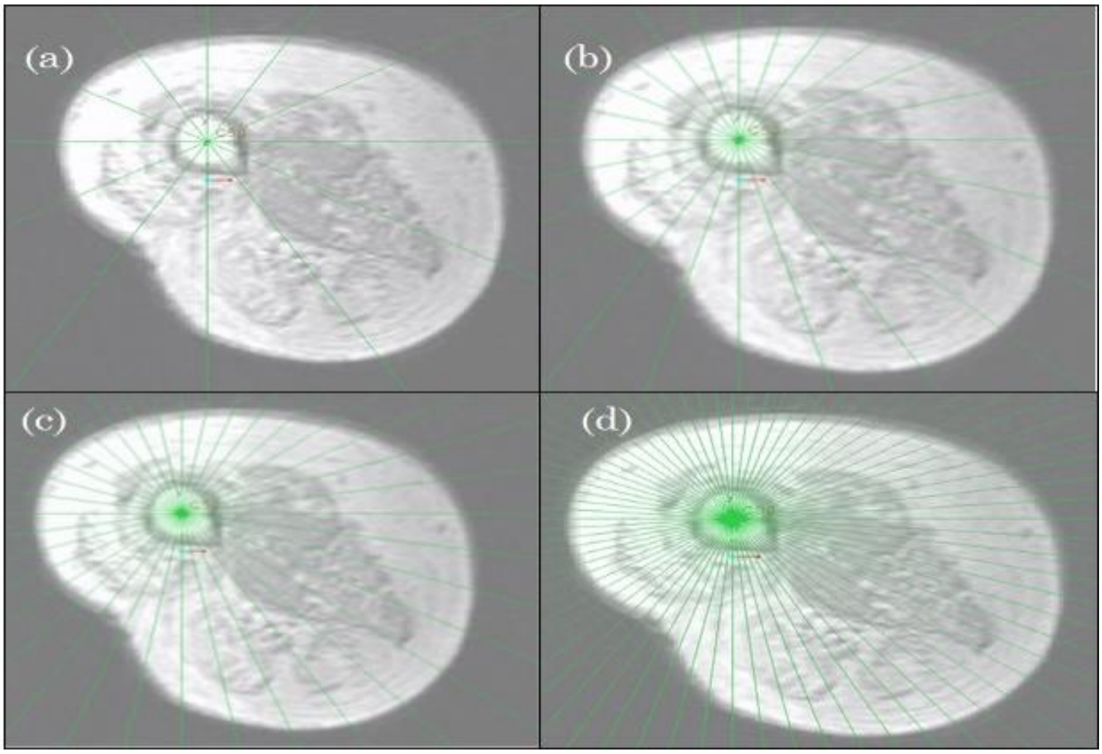

Figure 3.5 Process of segmentation in different spline point (SP). (a) 12 SP; (b) 24 SP; (c) 36 SP; (d) 72 SP.

3.2.4 Three-Dimensional (3D) Model Construction

Once a spline curve has been created in every plane, a single line is drawn along the z-axis of the created coordinate system, which acts as the trajectory. For 3D construction, Swept Blend (SB) features are necessary. SB is a function used to create a feature that is defined by two or more cross sections positioned along a trajectory. In this feature, the cross section is defined by a spline curve created previously. In SB, the first section is defined as the first spline curve, and it continues until the thirtieth section, which is defined as the thirtieth spline curve.

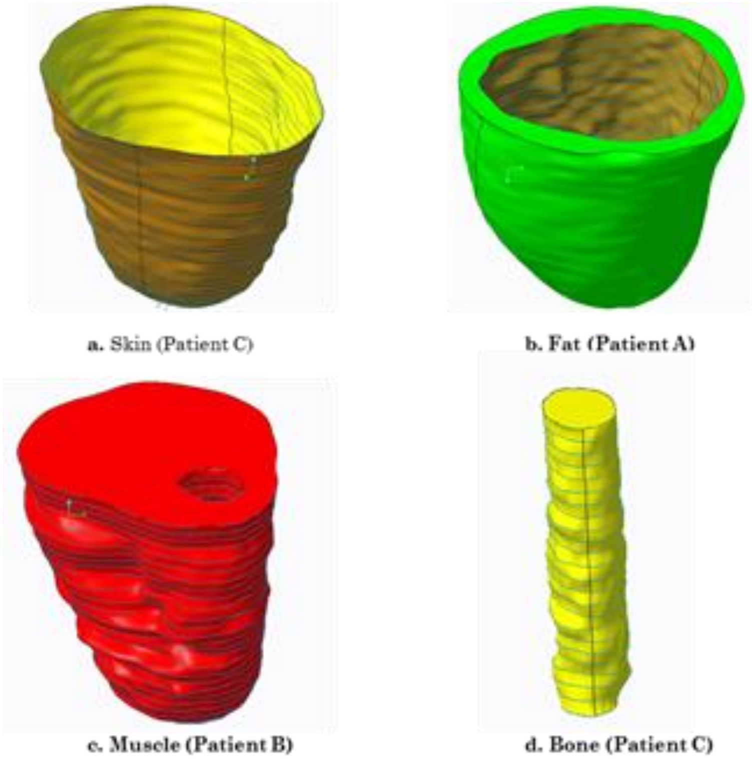

Figure 3.6 3D model constructed base on MRI image. (a) skin part; (b) fat part; (c) muscle part; (d) bone part.

3.3 Evaluation of the Residual Limb Model

The model is evaluated quantitatively by calculating the total volume of the model (equation 3.1), and it is compared with the total volume of the model obtained from the image processing method. The evaluation is made by assuming that the volume value taken from the image processing tools model is close or equal to the actual value of the residual limb's volume. This assumption is made to ensure the precision of the image processing model calculation.

$$\text{Volume} = \sum_{i=0}^{n} \frac{(A_n + A_{n+1})}{2} h\,[mm^3] \tag{3.1}$$

where A, h and n denote as spline curve area (mm^2), height between plane (mm) and number of plane (30)

The volume accuracy is evaluated by measuring the percentage error that occurs during comparison with the volume obtained from the image processing model using the error measurement equation (equation 3.2)

$$error = \left|\frac{Experiment\ Value - Simulation\ Value}{Experiment\ Value}\right| \times 100\% \qquad (3.2)$$

3.4 Accuracy Evaluation Result

The result of the total volume for each model is shown in Fig. 4. The result shows that each model produced total volumes similar to those produced by the image processing model for each amputee, with a correlation coefficient that is higher than 0.999 for all the models. The result shows that for amputee A, the 24-spline point model generated the smallest error (0.57%), while for amputee B, the 36-spline point model generated the smallest error (0.78%). For amputee C, the 36-spline point model produced an error of 2.1%, which is the smallest among the others.

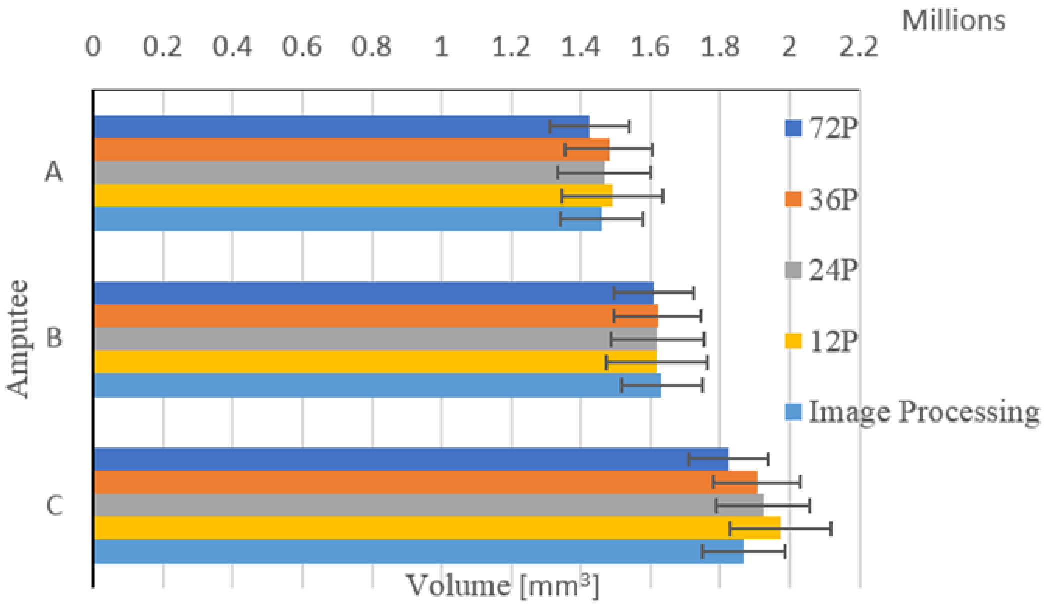

Figure 3.7 Comparison of total volume of each model for every amputee

Fig. 3.8 shows the results of the evaluation done by calculating the error percentage of volume for every 5-mm of the sliced MRI image. The result indicates that the 72-spline point model generated the smallest average error (6.36%) and has an acceptable value of consistency (<0.3).

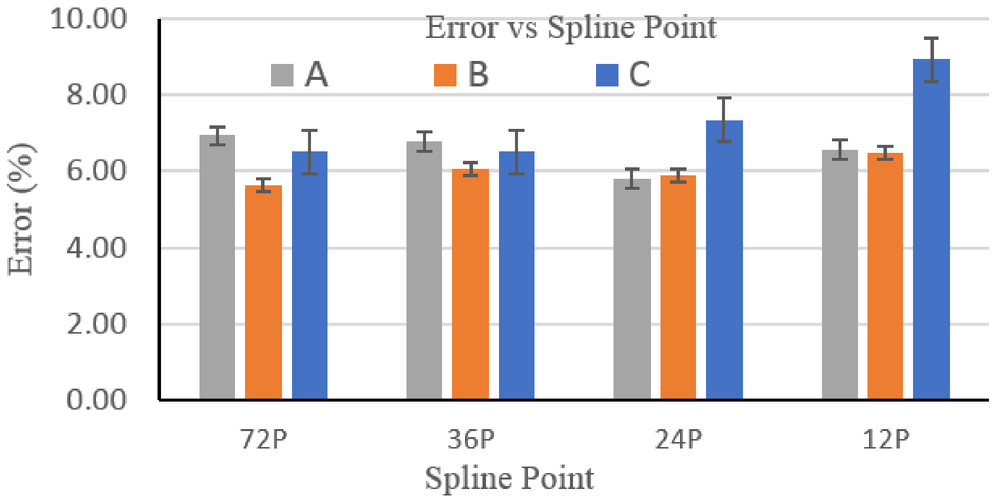

Figure 3.8 Average error of volume for each amputee with different spline point models

In order to calculate the difference, statistical tests are necessary. Based on the result, all the models satisfied the correlation coefficient value (>0.9). For the accuracy of the total volume, the 36-spline point model produced smallest error and has the highest accuracy rate. On the other hand, when the accuracy is evaluated for every 5 mm of the model height, the 72-spline point model was found to be the one with the highest accuracy, with the smallest error percentage and acceptable value of consistency.

3.5 Discussion

When the volume of every model was evaluated according to its height, the highest error occurred during the beginning of the model (0-mm), as shown in Fig. 3.9 with amputee B's result taken as an example (the results of all amputees have the same pattern).

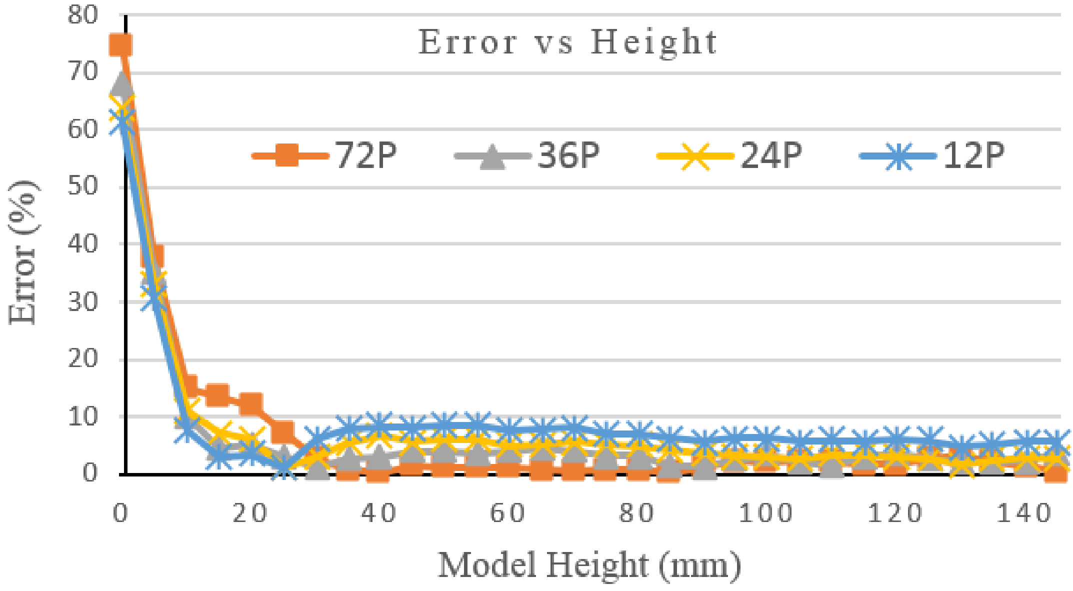

Figure 3.9 Error percentage of volume against height for amputee B

From 0 mm to 10 mm, the errors that occurred were high. It is due to the large difference in volume between the models, because for the calculation of the spline point model, it starts at 0 mm^3, while for the calculation of the image pro-cessing model, it starts at 74.22 mm^3. Starting from a height of 15 mm, the error is small (<10%) due to the similarities in volume between the models.

Parallax error could occur during the segmentation process, because the result of the plotting process mainly depends on human vision. Since the MRI image is not filtered due to the novelty of the methodology, some parts of the residual limb image cannot be seen clearly.

3.6 Conclusion

In this paper, the accuracy of the transfemoral residual limb model was evaluated by comparing the volume value of the model with the volume obtained from the image processing model. The result shows considerably high accuracy of the volume value for all the models with a very small error. To conclude, the model created with CREO 3.0 can be accepted as an alternative way to create a trans-femoral residual limb model. The error that occurred for the different spline models (<10%) indicates that the methodology can be used in any of the models (with different number of spline points) tested in this study. It is seen that the most accurate models are the ones with 72 and 36 spline points. The model created is yet to be tested for numerical calculation, but the model can be used for analysing the surface pressure and force by using Finite Element Methodology (FEM).

This chapter also shows that the CAD software with basic spline interpolation can be used an alternative method to create an anatomy model. In the bioengineering field, a high accuracy model is important for imitating real human anatomy in order to understand its characteristics.

3.7 Future Reference

The creation of precision 3D model in medical field is an important task. The accurate model of human anatomy helps doctors, nurses, bio-medical engineer etc. to understand the behaviour of the soft tissue externally and internally.

Even though recent technologies have discovered in-vitro etc. technology, the creation of MRI based 3D model also need to be highlighted. It is because, without undergone a surgery, the created model can describe and separate the internal soft tissue into different part. However, the model must undergo filtering technique before the model created and undergo intensive evaluation during post creation to enhance the accuracy rate of the model.

In the next chapter onwards, the method of creating the 3D model has been implemented and also will be used to perform several finite element simulations that will be discussed in particular chapter.

Chapter 4

Evaluation on Effect of Geometrical Changes of Prosthetic Socket Towards Transfemoral Residuum Model

This chapter presented the effect of prosthetic socket shape on the transfemoral residuum by using the finite element method. The effect of two Ischial-ramal-containment sockets (IRC) namely Manual Casting Compression Technique (MCCT) and University of California Los Angeles (UCLA) was evaluated during the donning process by predicting the qualitative measurement in a simulation. The simulation, mimicking the actual donning process, was done by creating a finite element model of residuum and socket based on the MRI image of subject`s residuum with and without socket. The change of contact surface pressure and geometry of the residuum were observed in the cross-section area along 170 mm from the distal end. This chapter provide a necessary information to help the engineer and prosthetist to understand the residuum behaviour during donning process. Moreover, it may help in modifying the socket shape to offer better comfort to the subject.

4.1 Introduction

The prosthetic devices have been used for most of the amputees to regain their self-confidence after accident or vascular disease. The device also acts as an assistive device for the amputees during their daily life activities. Nowadays, a high number of prosthetic devices are commercially available for different level of injuries. The transfemoral prosthesis is a typical lower limb above knee. It needs a socket to act as an interface between the subject's residuum and the prosthetic device. It is important that the subject feels comfortable while wearing the prosthetic device. Most physical changes are suffered by the residuum during gait when the body load is transferred to the socket. These changes can induce skin problem such as callosities, abrasions, and blisters [50].

A lot of research has been conducted to investigate the behaviour of residuum during gait cycle. They collected data for the manufacturer and physiotherapist to make improvement of their product or rehabilitation method. Most of the research focused on the surface pressure analysis of socket at certain point. Few studies focusing on trans-tibial or below-knee prosthesis utilized the finite element method to determine the stress distribution [48-49]. However, the measured change of volume in soft tissue was very low since the shape of residuum and socket were assumed to be the same. Reference [50] used five sample subject data to perform the actual donning procedure. However, due to the similarity of the socket and residuum shape, the maximum contact pressure observed in the study (5.6 kPa) was lower than other studies. Reference [51] utilized a non-linear FE model with a homogenous and isotropic residuum contacted with socket. 80.57 kPa of maximum normal stress recorded at the distal end of the residuum. Their result difference from other in term of maximum stress on the residuum probably because the shape of the rectified socket was assumed to be the same as residuum.

There are case studies on the behaviour of residuum [50-52], which characterized the mechanical condition of muscle flap of a trans-tibial patient for static load bearing. Here, the residuum model was divided into three parts viz., bone, muscle, and skin. The simulation revealed that the interface pressure between residuum and socket was 65 kPa, which has high correlation with the pressure obtained in clinical measurement.

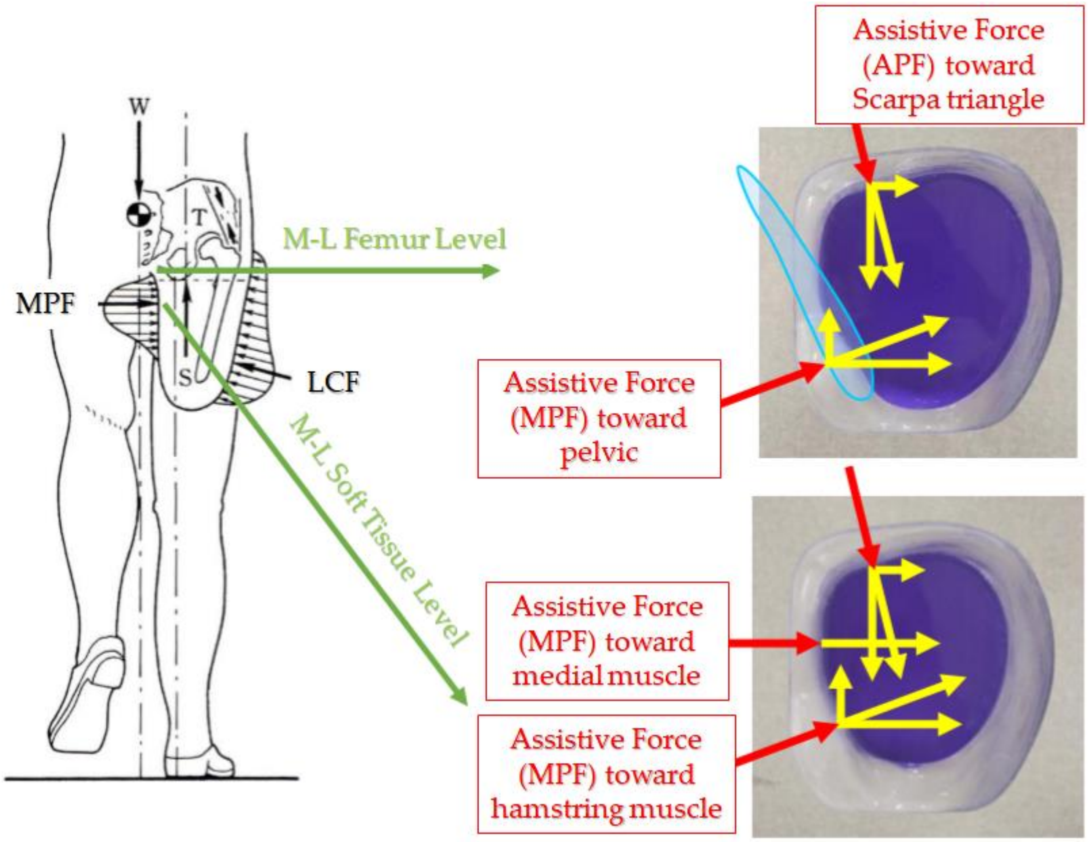

Figure 4.1 The transfemoral prosthetic MCCT socket. The assistive force distribution were highlighted to show the special characteristic of MCCT socket.

In the present study, the geometry change of residuum during donning procedure was efficiently evaluated by using a finite element analysis model. Two Ischial-ramal-containment (IRC) types of sockets (UCLA and MCCT) with significant difference in their shapes. The sockets were connected with single phase prosthesis knee and wood foot from different company. The Contour Adducted Trochanteric Controlled Alignment Method (CAT-CAM) used as a main method to create both of the socket [53].

Manual Compression Casting Technique (MCCT) socket was introduced by Prof. Yukio Agarie from Niigata University of Health and Welfare (NUHW) where the stability was improved in both anterolateral and sagittal direction of the UCLA socket. Unlike the previous researches done by others, our study used a new approach for designing the model and real measurement from magnetic resonance imaging (MRI) data. Since the real shape of socket and residuum were significantly different in two cases, the pressure acting on the interface between the socket and residuum was effectively detected during the simulation. At first, a three-dimensional (3D) model of residuum and both sockets were developed.

The model was then utilized in a donning simulation to determine the contact pressure between residuum and socket. Furthermore, an experimental verification of the simulation was conducted. Eight triaxial force sensors were placed on the socket surface to measure the forces generated on the skin of the residuum. The simulation and experimental results for two types of socket were then compared.

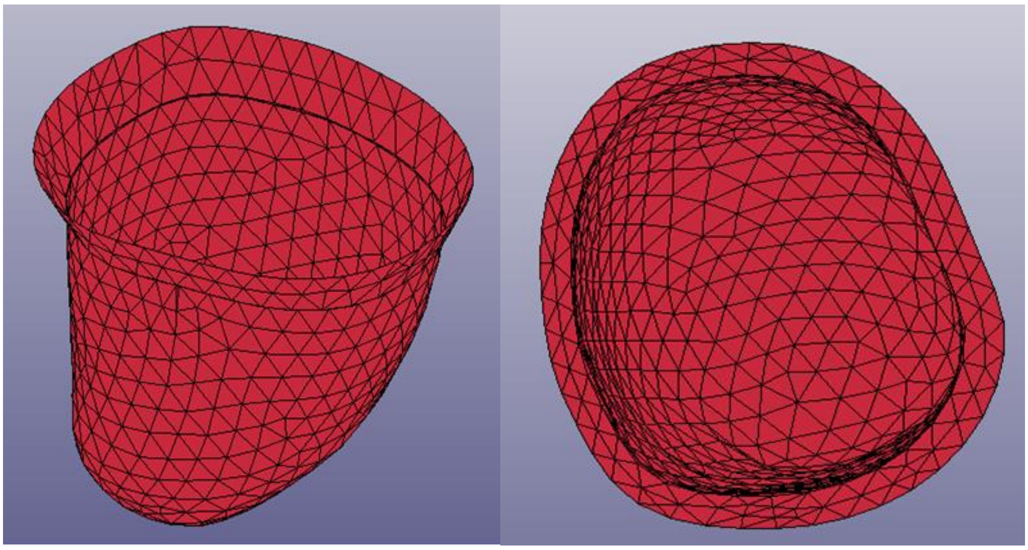

(a)

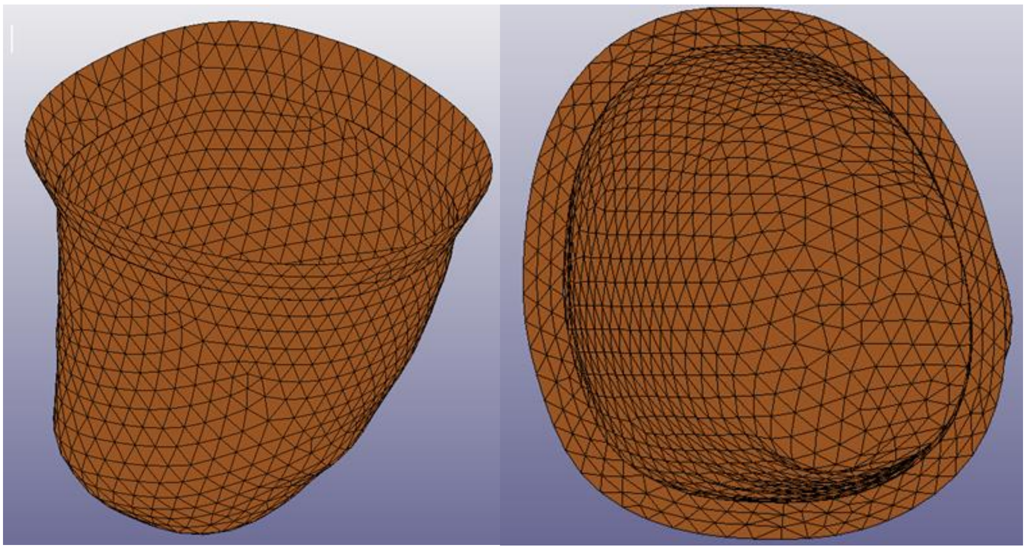

(b)

Figure 4.2 Three-dimensional (3D) model of (a) MCCT socket; (b) UCLA socket.

4.2 Finite Element Simulation and Method of Evaluation

The investigation of residual limb deformation was done by performing a simulation. Instead of using actual experiment, a simulation was chosen because its practicality and it can be performing a various type of simulation with less time consume. In order to conduct the simulation, a three-dimensional (3D) model has to be created. In this section, the method of creating a 3D model was presented and evaluation of the interaction between residuum model and its socket also presented.

4.2.1 Three Dimension (3D) Model Construction

The study involved a male subject (age 35, height 169 cm, and mass 63 kg without the prosthesis) with a left-side transfemoral amputation. An MRI image of the subject was used to obtain the residuum data with and without the prosthesis socket. The model was created with following four steps namely data collection, pre-segmentation, segmentation, and 3D model construction. The process of creating the model has been discussed in previous chapter. Here, the material properties and meshing technique will be discussed. Following the convention, the residuum model was consisted of two parts—bone and soft tissue [48-53]. The soft tissue model was considered as one entity due to the similarity in mechanical properties of skin, muscle, and fat. The model was meshed with tetrahedral element as it would generate similar results like theoretical ones [56].

The bone and soft tissue were meshed with 12000–19000 solid element depending on the subject`s residuum size. Both the sockets were meshed as a shell element with an approximate thickness of 3 mm (Figs. 4.2a and 4.2b). The mechanical properties of the bone and socket were defined as linearly elastic, following the Hooke`s Law, which stated the stress varies linearly with strain. The materials properties were assumed to be same on every point in all directions and considered as homogeneous. The Young Modulus and Poisson`s ratio for the bone defined as 17700 MPa and 0.3 respectively [57]. Both the sockets were fabricated with acrylic plastic [58]. Most studies use a linear isotropic model to represent the soft tissue mechanical behaviour. However, Fung used the viscoelastic formulation [58] and the parameter used is presented in Table 4.1, where C, S, T, and K denote the invariants of right Cauchy deformation, spectral strength, characteristic time, and bulk modulus of the material respectively.

Table 4.1 Mechanical properties of viscoelastic material

Name	**Density (kg/m^3)**	**C_1 (kPa)**	**C_2 (kPa)**	**S_1**	**S_2**	**T_1 (ms)**	**T_2 (ms)**	**K (MPa)**
Soft Tissue	906	0.186	0.178	0.968	0.864	10.42	84.1	20

4.2.2 Simulation Environment

The movement of residuum was toward the socket in vertical direction. The socket was only allowed to move linearly in the horizontal plane. The contact force, equivalent to half of the body weight applied to the residuum assumed subject standing with both of his legs. The pressure generated when the residuum was inserted into the socket. The contact surface pressure between the residuum and socket was observed.

The simulation was conducted for two sockets (UCLA and MCCT) with 10 N of force assumed as control force located at the outer surface of residuum. The force controlled the residuum movement during donning. At the end of simulation, the residuum geometry was changed and enable the residuum to be fitted into the socket. In this chapter, the contact pressure between socket and residuum was the main reason of residuum deformation. The contact surface pressure during donning simulation and the changes of the residuum geometry were recorded

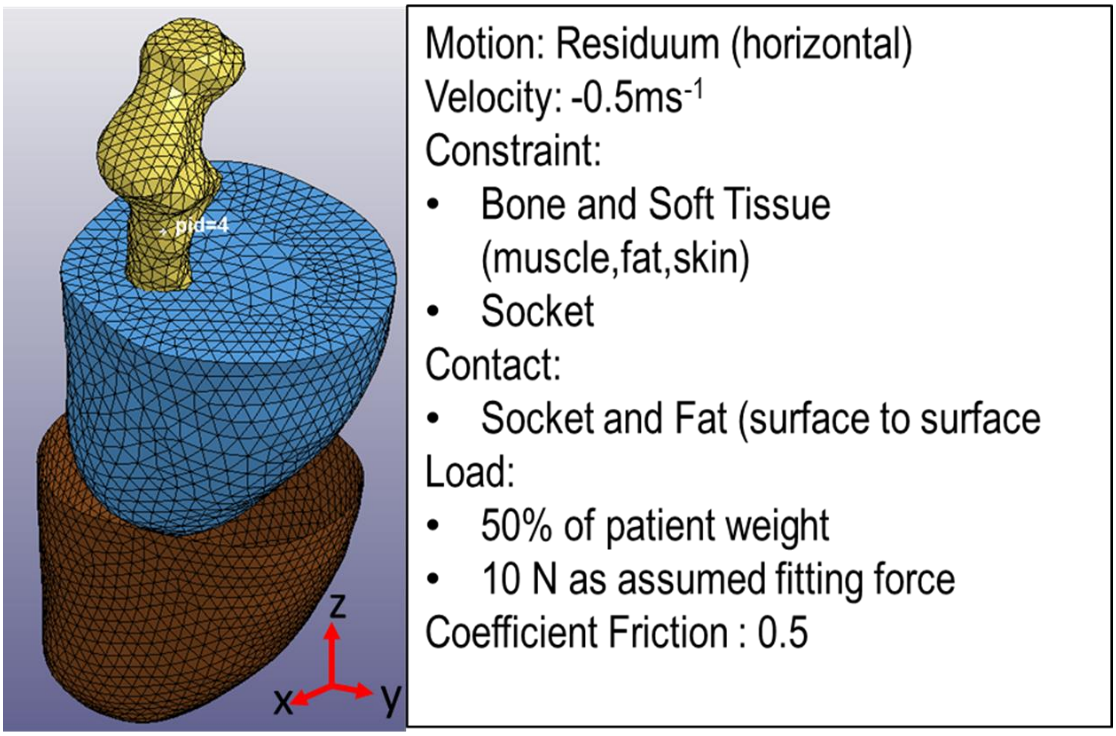

Figure 4.3 Simulation environment with parameter description.

The simulation was conducted mimicking the experimental measurement situation. The velocity of the residuum was set to 0.5 ms-1 to give enough time for the computer to calculate all the required data during the simulation. The contact between residuum and socket was set as surface-to-surface contact and a full penetration during contraction was allowed. The bone and soft tissue were set to be constrained in x and y axes. The body weight was located at the distal end surface of the bone.

4.2.3 Clinical Experiment

To ensure the validity of the simulation, clinical experiment has been conducted to confirm the outcome of the simulation by comparing the outcome with actual experiment results.

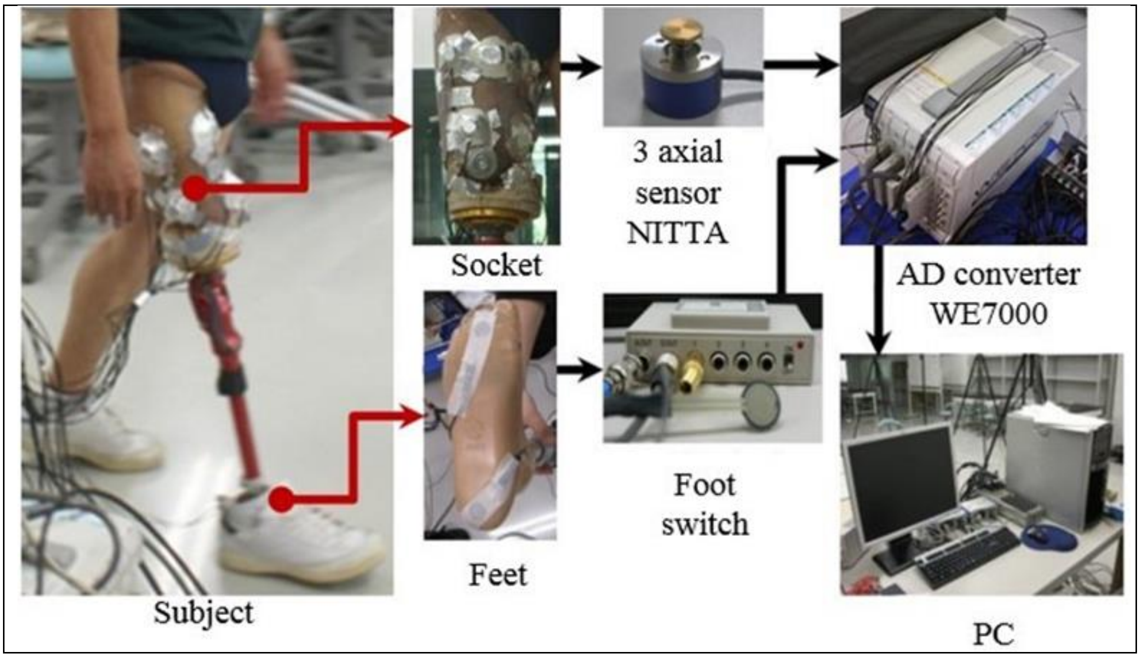

Figure 4.4 Experiment Diagram

The triaxial force sensors NITTA PD 3-32-05-015 [18] were used in experiments. These force sensors can resolve the force applied to their surface into three components, two shear components in orthogonal directions (in this study tangential to the skin surface) and one normal stress component (in this study normal to the skin). The schema of place which installed the sensors was shown on Figure 4.5. There are eight sensors correspond with eight areas of the socket were measured. Four sensors were defined on four directions are anterior, posterior, medial and lateral. The schema experiment was described in Figure 4.4 which include sensors on the socket of patient, analogue-to-digital converter, data acquisition software and computer. The direction of force along three axes of the sensor were described in Figure. The sampling frequency was 1000 [Hz]. After measuring the value of forces, the value of pressure was calculated by the equation as below:

$$\mathrm{P} = \frac{V}{C}\frac{g}{4.5^2\pi 10^{-12}} \tag{4.1}$$

where g, V, and C denote the acceleration due to gravity, voltage generated, and calibration coefficient respectively. 4.5 is the radius in millimetre unit of the sensor surface. This experiment, following the Declaration of Helsinki (DoH), measured the force when the subject was standing assuming that there was no environmental disturbance to affect the data.

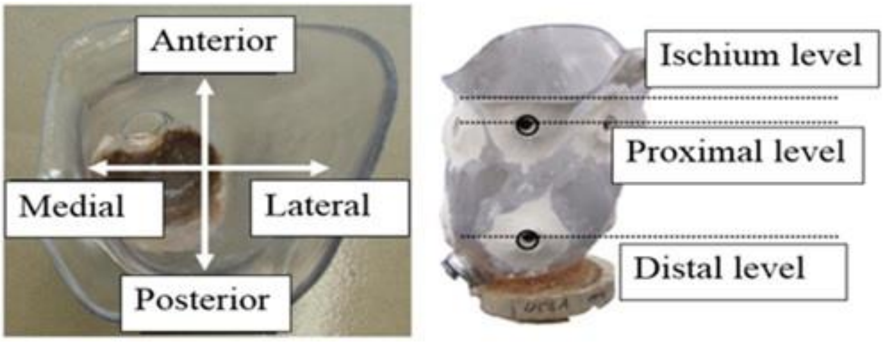

Figure 4.5 location of triaxial force sensor in the socket

4.3 Finite Element Simulation Outcome

The effect of transfemoral prosthetic socket towards the deformation of the residuum was measured quantitively by measuring the length changes of the residuum during complete donned stage. Figure 4.6 and 4.7 show the changes of residuum geometry for two types of sockets before and after donning simulation with the subject standing on one leg. Generally, the length of the residuum was increased after inserting it into the socket and the surface area of the soft tissue was decreased. Fig. 4.6 shows the change in residuum length until the residuum was completely inserted into the socket and figure 4.7 shows the deformation of soft tissues during donning simulation.

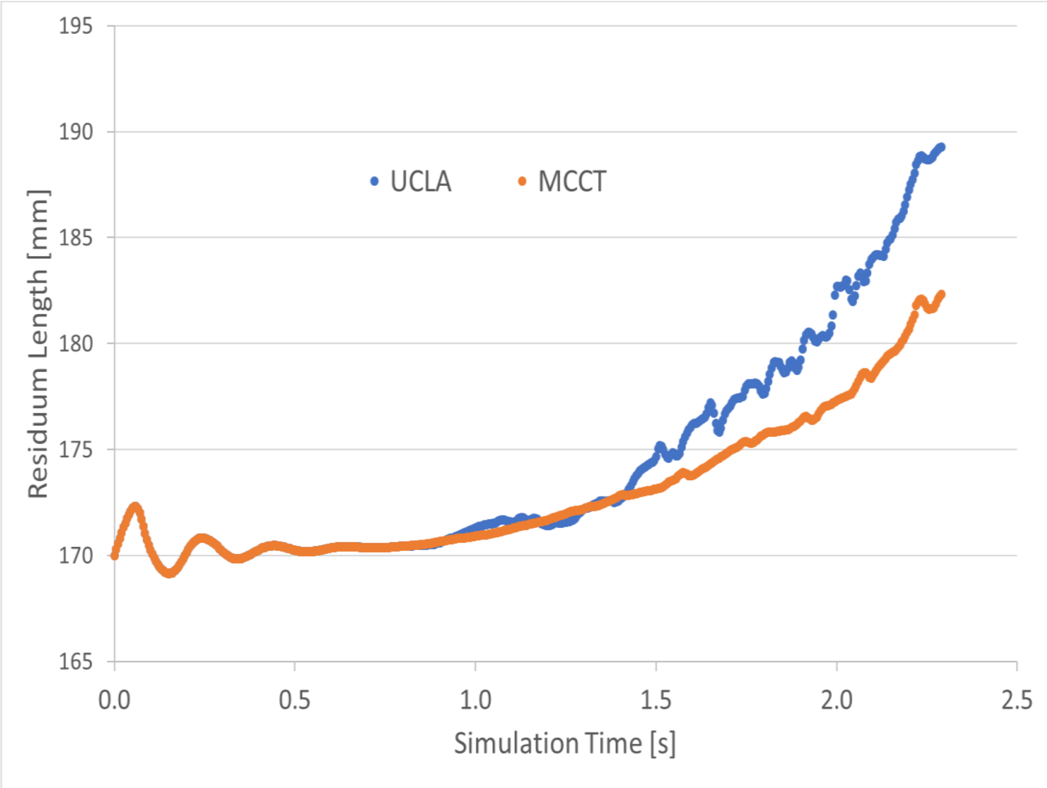

Figure 4.6 Residuum length transformation during donning

The residuum length increased 7.24 % and 11.32 % for MCCT and UCLA respectively. The soft tissue area decreased 6.06 % when inserted into the UCLA socket and 6.03 % when fully contacted with MCCT socket as shown in Figure 4.7.

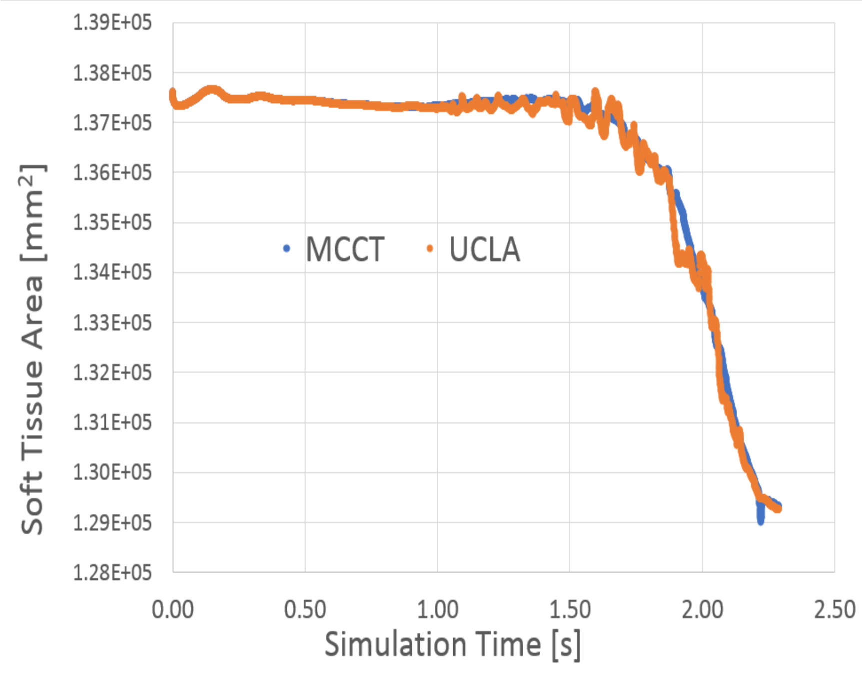

Figure 4.7 Residuum total area (without bone) transformation

The geometry of residuum also experienced large deformation as shown in Figure 4.8. The deformation was analysed during complete donned phase in four views of the simulation. For both cases, the total pressure at proximal area was higher than that at the distal area. The highest pressure was located at the Posterior Proximal (PP)—68.2 kPa and 14.3 kPa for MCCT and UCLA respectively.

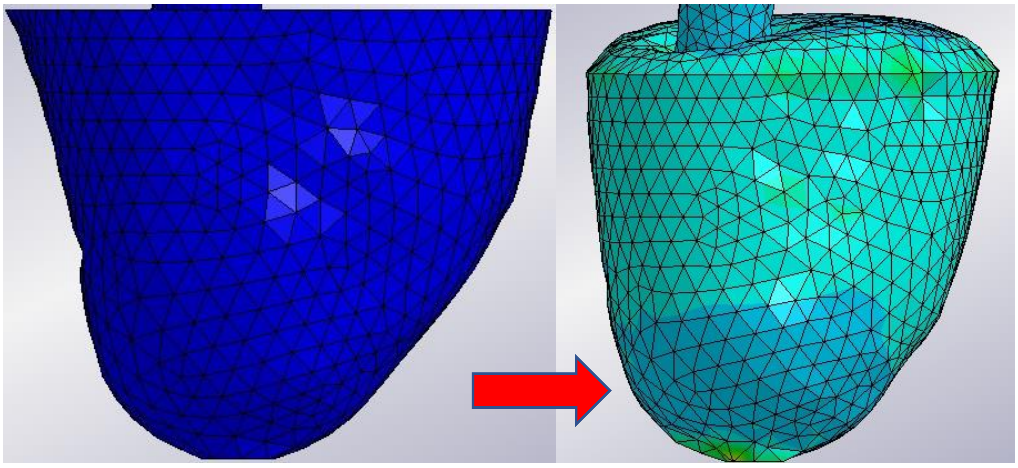

(a)

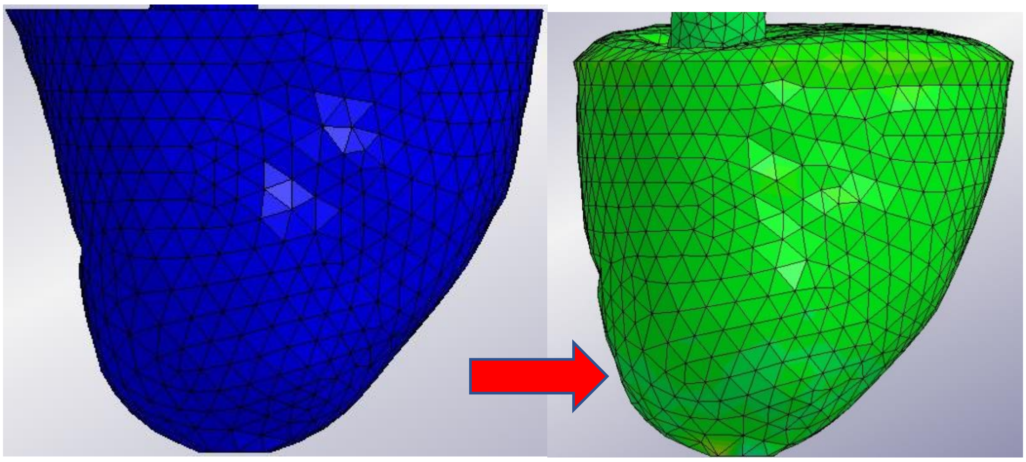

(b)

Figure 4.8 Residuum geometry transformation (a) transformation of residuum geometry during inserted in UCLA socket; (b) transformation of residuum geometry during inserted in MCCT socket. Both figures taken from lateral view.

4.4 Discussion

In this chapter, with the help of donning simulation, can predict the volume change in residuum for wearing the socket. According to the socket modelling theory, every residuum requires a high pressure in the upper socket division in order to make the residuum fix to the socket. The simulation results also showed that the pressure in the upper socket was higher. Moreover, the obtained pressure values from simulation and experiment were compared (See Figure 4.9).

Although the pressure values were different at all locations of the sensors, high correlation coefficient values were obtained between the simulation and experiment—0.717 and 0.976 for MCCT and UCLA respectively. Therefore, it can be concluded that the shape profile used in the simulation helped in obtaining an almost identical result. For both cases, a significant difference was observed at Lateral Distal (LD) where 44.32% and 10.71% of error were calculated for MCCT and UCLA respectively. This may be caused by the difference in soft tissue features in experimental cases. In this chapter, skin, fat, and muscle were all included in soft tissue and assumed to have a single property. However, every single part of the residuum has its own mechanical properties. Furthermore, the meshed element used in the simulation was limited to 20000 units and the size of the element could also be inappropriate. The mesh convergence was done within the limitation and the most accurate model was selected in this study.

The mean error was recorded to be 21.1 % and 4.93 % for MCCT and UCLA respectively. The mechanical properties of soft tissue, used in the simulation, were based on previous research where subjects with different age and health condition were used, and it was not equally distributed in the entire residuum. Therefore, the mechanical properties used in simulation were potentially suitable for general subject and not recommended to be used in specific areas. Here, the experimental and simulation pressure values were compared at eight places in the socket. However, in the simulation, the position of the measured element was not defined accurately, and it possibly introduced an error in pressure value observation.

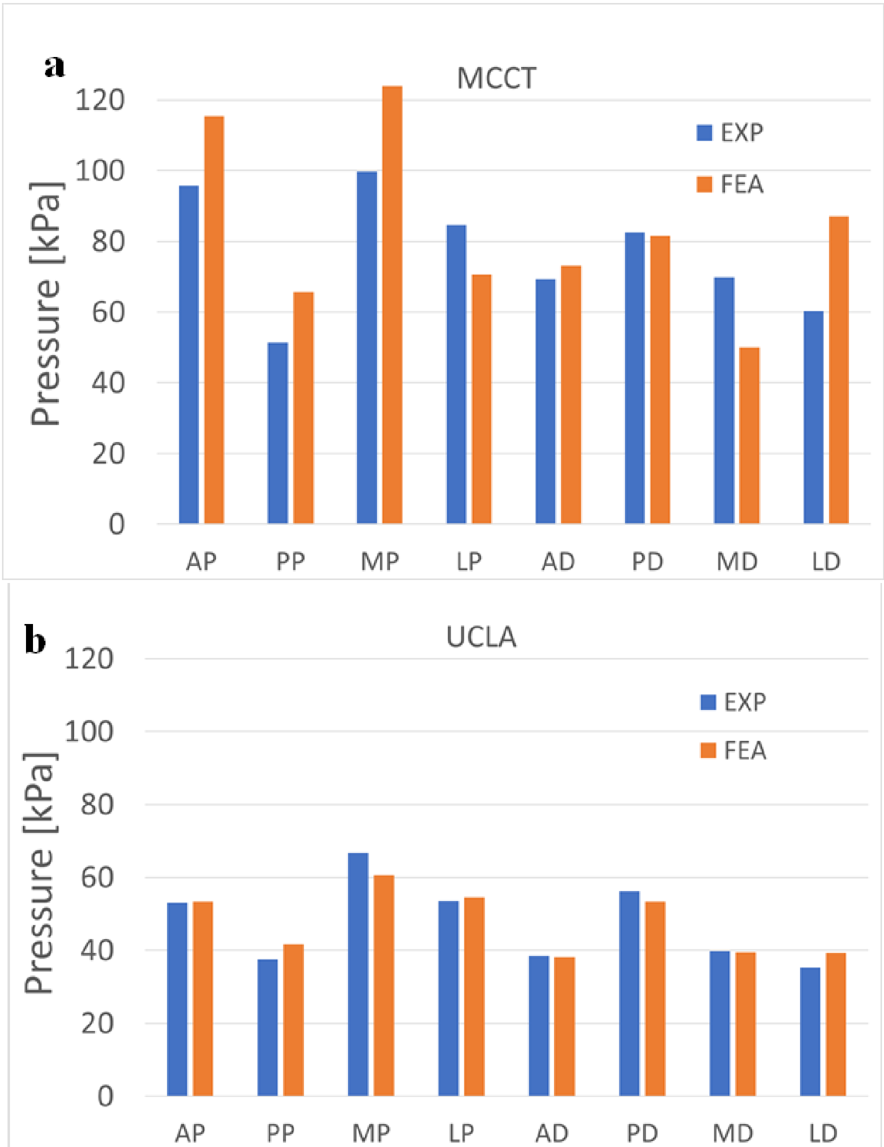

Figure 4.9 Pressure comparison between simulation and experiment based on the sensor location. (a) MCCT socket case; (b) UCLA socket case.

4.5 Conclusion

This chapter showed a high correlation between simulation and experimental donning process for transfemoral residuum. Moreover, it showed that the total pressure at proximal area was higher than that at the distal area, which is in accordance with the IRC socket modelling theory. The main objective of this research was to replace the existing methods with MRI image-based method and develop an assistive system to design a socket without the expertise of prosthesis. The result of this chapter supported the main objective of the research. The study also imitated a real condition of donning process with a real shape of socket and residuum. These conditions enhance the similarity of the simulation and experiment result because a large deformation occurred in the residuum when it was fitted into the socket amplify the pressure between the skin surface and socket.

In simulation, the total pressure at proximal area was lower especially in posterior (PP) for both cases, which indicated the advantage of IRC sockets. Furthermore, the pain threshold limit recorded to be 690 kPa [61] and the observed pressure levels showed in the simulation were significantly lower than the limit. The results also showed a good agreement between experiment and simulation with correlation value exceeding 0.7 for both cases. The correlation can be increased if the viscoelastic properties of the residuum are specified to the subject specific part. Besides, the results suggested dividing the soft tissue into 3 parts, skin, fat, and muscle that possess different mechanical properties can increased the understanding of soft tissue and bone movement in one part.

The comparison between MCCT and UCLA socket showed a similar pressure distribution throughout the entire residuum surface. However, the maximum pressure was higher in MCCT. The results indicated that better stability can be achieved in the anterolateral direction by reducing the area in upper part of the socket. However, it increases the pressure inside the socket.

In short, the current study indicated a high correlation between socket shape and residuum geometry. The results showed a pressure distribution inside the socket during donning process affecting the geometry of residuum. The higher socket wall in lateral area produced less pressure in anterior and medial brim. Moreover, a reduction of posterior socket wall may change the residuum length. The improvement made in the anterolateral and sagittal direction of the MCCT socket increased the total pressure inside the socket. The high correlation between experiment and simulation justified that the finite element method is a better method for validation compare to the conventional donning procedure and acts as a tool for evaluating the prostheses. This method may possibly reduce the subject's risk of getting tissue injury during socket fitting and help an engineer and health-care officer to reduce the socket repairing and editing time. Our future study will consider a separated soft tissue part to create an advanced geometry model for a better simulation analysis. In addition, the designing method of the 3D model using CAD software should be improved.

4.6 Future Work

In this chapter, the utilization of 3D model of residuum and its socket help to mimicking the actual socket donning process. With the nearly similar condition with actual donning process, the simulation environment can be adapted to achieve a better correlation between experiment and simulation result.

In the next chapter, the similar method of creating a 3D model will be used to conduct an analysis of pressure distribution inside the socket, walking gait analysis and many other analyses that related to interaction between residual limb and prosthetic socket.

Chapter 5

Analysis of The Pressure Distribution Inside Transfemoral Prosthetic Socket in Various Environment.

In this chapter, the estimation and validation of the pressure distribution profile between residuum and the two type of prosthetic socket for transfemoral amputee by utilizing finite element analysis is presented. Correct shaping of the socket for appropriate load distribution is a critical process in the design of lower limb prosthesis sockets. The pressure distribution profile provided the understanding of a relationship between socket design and level of subject comfortability. Estimating the pressure profile is an important task to help prosthesis by evaluating the socket design before undergoing fabrication process. The chapter focusing on utilizing Magnetic Resonant Imaging (MRI) based three-dimensional (3D) model inside pre-determined finite element simulation. The simulation was pre-determined by mimicking the actual socket fitting environment. This chapter outcome provided tremendous interest for the fabricator by utilizing a finite element model as an alternative method for pre-fabrication of prosthetic socket evaluation. In the future prosthetic socket fabrication, less intervention of prostheses is required to develop the socket and participation of subject for socket fitting session is not necessary. The contribution of the study is suggested to be expand by developing the overall pre-fabrication evaluation system to allow health-care providers and engineers to simulate the fit and comfort of transfemoral prosthetics.

5.1 Introduction

Achieving a proper residuum-socket interface by ensuring an optimum distribution of the interface loads is critical to a successful prosthetic fitting and rehabilitation of lower-limb amputees [61]. In Japan, there has been an estimated 22.4% yearly increase in amputees during the past 5 years owing to a high number of patients with a peripheral vascular disease [62]. The high demand for prosthetic sockets provides an opportunity to the fabricator to expand their socket manufacturing market. However, the design of a prosthetic socket is a time-consuming process, starting with measuring the subject amputee, creating a positive mould, shaping a socket, carrying out a socket fitting session, improvising the prosthetic socket, and finalizing the socket position using a knee joint mechanism. This process takes approximately 2 to 3 months before the socket can be used [62].

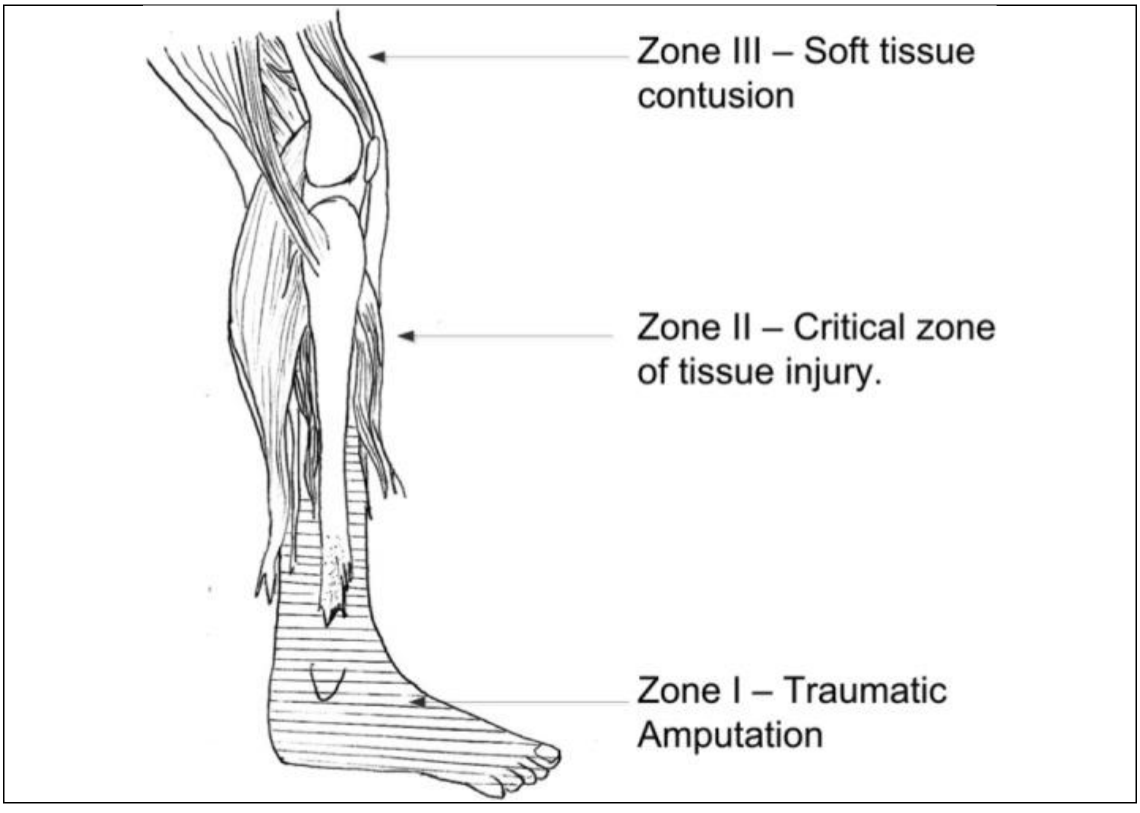

Figure 5.1 Zone of injury in lower limb injury

In conjunction with this, numerous studies have been conducted to investigate the possibility of utilizing a theoretical analysis to provide an alternative evaluation for a pre-fabrication of a prosthetic device. For instance, investigations into the stress distribution between the residuum and prosthetic socket by utilizing a finite element analysis have shown that, although the results have been promising in terms of the stability of the model geometry, the socket models were not realistically developed because the shape of the socket was similar with the residuum shape [63–66]. Thus, the geometrical changes of the residuum could not be clearly seen. In addition to focusing on the socket design and manufacturing methods, Sengeh et al. [67] investigated the effect on the accuracy of the actual residuum parameter in the design of a residuum model with multiple materials. The residuum was modelled using a subject-specific magnetic resonance (MR) image to allow the model to be evaluated through a numerical approach, which inspired a modeling of the residuum with a subject-specific parameter in the present study but with a different methodology. Portnoy et al. [68] also reported that using a subject-specific real-time analysis of the internal tissue loads in the residuum is a practical tool for evaluating the internal stress inside the residuum in a clinical setting or outdoors. In another aspect, Colombo et al. [69] managed to develop a computer-aided environment, namely, a socket modelling assistant (SMA), combining knowledge from prostheses and a 3D model simulation to create a prosthesis socket. Such research has resulted in the creation of a prosthesis socket using the additive manufacturing (AM) technique, although a compatibility analysis of the created socket has yet to be carried out.

This chapter focuses on an investigation into the interaction pressure of a patient-specific multi-material three-dimensional (3D) model and two types of ischial-ramal containment (IRC) socket when completely donned. One of the IRC sockets used is a UCLA socket (developed at the University of California, Los Angeles), which is a prosthetic socket that applies a contour adducted trochanteric controlled alignment method (CAT-CAM). This socket is based on a study conducted by Sabolich and inspired by research by Long [70]. Another IRC is a manual compression casting technique (MCCT) socket developed by Agarie. As the difference between the two sockets, the stability of the IRC–MCCT socket was improved through an adjustment of the anterolateral and sagittal directions of the IRC–UCLA socket [71]. In this study, an estimation of the pressure distribution during the interaction between the subject's residuum and both sockets were investigated. The pressure distribution profile was a key factor in determining the potential deep tissue injury from a prosthetics device [72]. Many subjects experience discomfort with their sockets owing to an improper fit, resulting in skin problems [73]. These issues are associated with a particular socket design. Such loading conditions, tissue stresses, and strains can be evaluated using a computational simulation [67]. Reynold et al. [74] proposed a simulation approach in modelling the contact interface between the residuum and rectified socket. However, the geometrical changes in the residuum were ignored because the socket used in the study was rectified from the outer layer of the residuum.

Many theoretical analyses use a finite element method (FEM) as a medium in quantitatively evaluating a bio-mimicking model [61, 65–68,71]. The FEM is a powerful tool to understand the load transfer between the interaction of the human anatomy and a prosthetic device. The FEM also provides a better understanding of the effects of the socket modification of the prosthetics [73, 74] and offers a prediction of the stress, strain, and motion at any location of the model, as well as proficient parametric studies [66]. In conjunction with this, we propose utilizing the FEM combined with an image processing (IP) method in evaluating the estimation of the pressure distribution profile of transfemoral amputee subjects. The study is motivated by the lack of a quantitative analysis system for evaluating a pre-fabricated prosthetic socket. The evaluation is aimed at improving the socket design of the prosthesis according to the stress distribution profile of the individual subjects. The process can provide an opportunity for each subject to own a stress reduction prosthetic socket.

5.2 Development of Donning Simulation via Finite Element Method

5.2.1 Designation of three-dimensional model based on MRI data

This study focuses on utilizing a subject-specific MR image to create a multi-material residuum model. The MR images for the subjects were obtained using a Siemens Magneton Symphony Maestro class 1.5 T. The residuum model created through this study is categorized into three main parts, namely, fat, muscle, and bone.

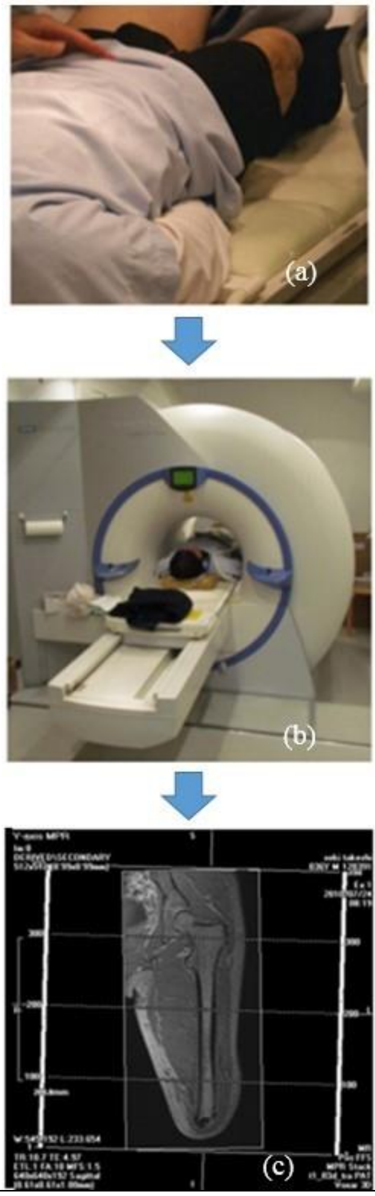

Figure 5.2 Process of creating the MRI image. (a) subject standby in a desired posture; (b) Image taken by magnetic resonant imaging machine; (c) MRI image created.

The clouds of 30 MR images were arranged vertically layer by layer with a 5 mm spacing between images. The center point of bone part was selected and used to create 36 trajectory lines surrounding the residuum image. The intersection points between the trajectory line and residuum perimeter were connected by creating multiple cross sections in a single layer. Then, every cross section was linked to cross sections of the other layers to construct the 3D model. The construction was made using the Swept Blend (SB) function in Creo software (PTC Ltd., Boston, USA). The same procedure will be applied to create the socket model using a different cloud of MR images. In this study, LS-DYNA software (Livermore Ltd., Livermore, USA) was also used to initiate the meshing procedure for each model. Figure 5.2 shows an example of a subject residuum meshed model with both sockets.

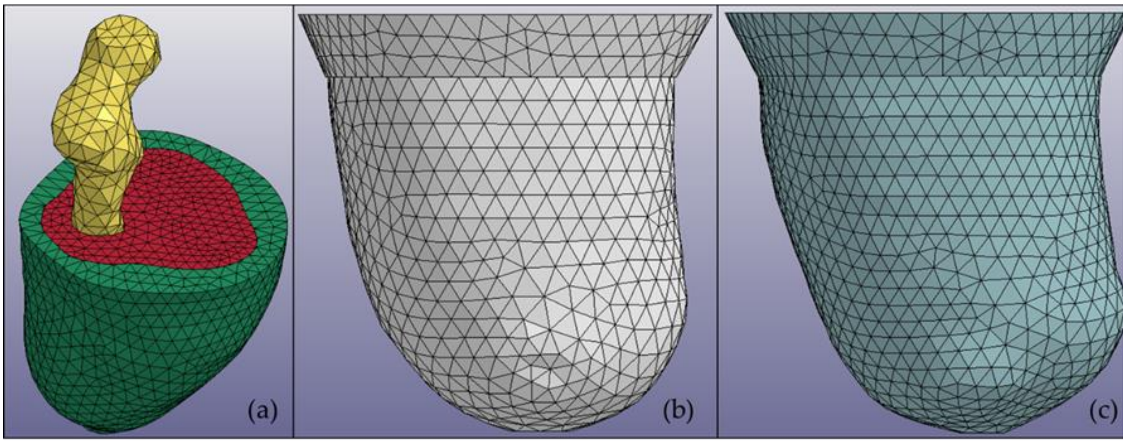

Figure 5.2 (a) Multi-material 3D model of residuum which every part is distinguished by colour. Bone (yellow), muscle (red) and fat (green). (b) 3D model of MCCT socket. (c) 3D model of UCLA socket.

The materials of the parts were modelled as isotropic with uniform elastic properties in all directions and were assumed as homogenous with consistent material properties. Soft tissue was considered a composite material comprised of collage fibers embedded in a softer isotropic material. Based on previous studies [76–78], a viscoelastic material was chosen to represent the soft tissue material, which was formulated using the strain-energy function based on the quasi-linear viscoelastic (QLV) theory. Calibration of the QLV material was conducted in a previous study and showed a good agreement with the cadaver data in terms of the maximum force and displacement [78]. The QLV material properties were selected because they have a better biofidelity than the linear elastic property in low-speed impact tests [78]. The soft tissue material function was formulated by Weiss [76], and is expressed through Equation (5.1) below:

$$\mathrm{W} = W_1 + W_2 + W_3 \tag{5.1}$$

The first term models the ground substance matrix as a Mooney-Rivlin material expressed as Equation (5.2):

$$W_1 = C_1(I_1 - 3) + C_2(I_2 - 3) \tag{5.2}$$

where I_1 and I_2 are invariants of the right deformation tensor. The second term $W_2 = F(\lambda)$ is defined to capture the behaviour of the crimped collagen under tension, and the term is inapplicable to the materials because the direction of the fibers (muscle and fat) is not defined in the model. The role of the third term in the strain energy function is to ensure a nearly incompressible material behaviour.

$$W_3 = \frac{1}{2}K[\ln(J)]^2 \tag{5.3}$$

where J = det F is the third invariant of the deformation tensor, and K is the bulk modulus. In this study, terms 1 and 3 of the function were used to express the viscoelastic properties for the soft tissue. The reduced relaxation function for the soft tissue material G(t) was represented through a Prony series [78]:

$$G(t) = \sum_{i=1}^{3} S_i exp\left(\frac{-t}{T_i}\right) \tag{5.4}$$

Two terms in the strain energy function were used to define the reduced relaxation function of the skin, fat, and muscle owing to ignorance regarding the second term because the directions of the skin, fat, and muscle model were undefined. The formulation parameters used in the simulation are listed in Table 5.1, where C, S, T, and K denote the hyperelastic material constants, spectral strength, characteristic time, and bulk modulus, respectively [79].

Table 5.1 Mechanical properties of viscoelastic material

Part	**Density (kg/m^3)**	**C_1 (kPa)**	**C_2 (kPa)**	**S_1**	**S_2**	**T_1 (ms)**	**T_2 (ms)**	**K (MPa)**
Skin	906	0.186	0.178	0.968	0.864	10.43	84.1	20
Fat	906	0.19	0.18	1	0.9	10	84	20
Muscle	1051	0.12	0.25	1.2	0.8	23	63	20

The bone and socket were categorized as a solid material. The bone was modelled using the density of the femur with a Young's Modulus (YM) of 17,700 MPa and a Poisson’s Ratio (PR) of 0.3. The actual socket was designed using an acrylic plastic with a YM of 1,885 MPa and PR of 0.39.

5.2.2 Pre-determined Environment for Finite Element Simulation

In this chapter, the simulation was generated by replicating the socket fitting session. During the actual socket fitting, the subject was required to stand to accurately measure the comfort level while wearing the socket. During the simulation, 50% of the body weight of the subject was used as an indicator that the subject is standing. Because the geometrical shape of the residuum and socket are different, the distance during the donning process was taken into consideration. The ideal velocity is suggested to be 0.5 mms^{-1} and must be constant starting from the initial position until the residuum reached the distal end of the socket.

The definition of contact used in the simulation is divided into two parts. The first contact between the residuum and socket was defined as a surface-to-surface contact. A coefficient of friction of 0.5 was assigned as an interaction property for the contact surfaces based on that used in another study [80]. The second contact definition applied corresponded to a tied contact between the bone and muscle, which is a simple way of permanently bonding surfaces and preventing slave nodes from separating or sliding relative to the master surface. This method of contact was obtained from a previous study [81]. The definition of contact is based on the hypothesis applied to the connection between the skin and fat, and to the fat and muscle, in which the relative motion was neglected.

The basic principle of the simulation relies on the fact that the residuum should move toward the socket. In the residuum, 50% of the body weight is at the top to emulate a bipedal stance. Regarding the socket, the horizontal movement is constrained to realize contact between the residuum. Figure 5.3 shows a graphical overview of the simulation environment.

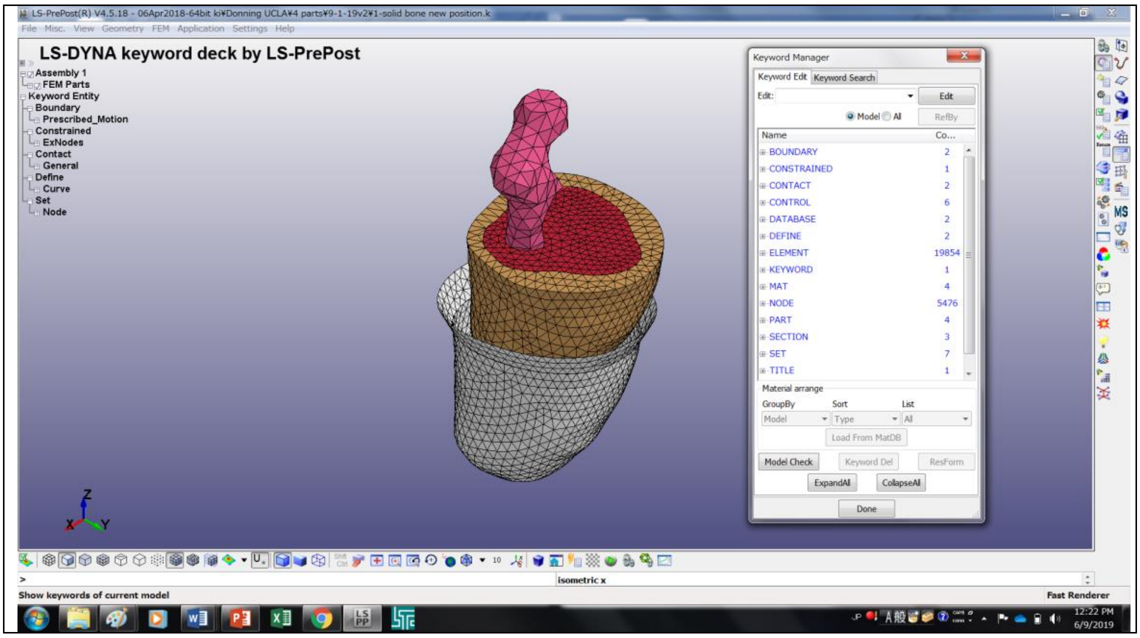

Figure 5.3 An overview of simulation environment. Residuum is moving vertically with 50% of body weight located at the top of the bone. The socket has been constrained in vertical direction to allow connectivity with residuum during complete donned.

5.2.3 Experimental Analysis

The triaxial force sensors NITTA PD 3-32-05-015 [22] were used in the experiments. These force sensors can resolve the force applied to the surface into three components, two shear components in the orthogonal directions (tangential to the skin surface) and one normal stress component (normal to the skin). Eight sensors corresponding to eight areas of the socket were applied for the measurements. Four sensors were applied in four directions, namely, the anterior, posterior, medial, and lateral directions. A schematic of the experiment is shown in Figure 3, which includes sensors on the socket of the patient, an analogue-to-digital converter, data acquisition software, and a computer. After measuring the forces, the pressure was calculated using the equation 3.1 in chapter 3. The schema experiment was described in Figure 5.4 which include sensors on the socket of patient, analogue-to-digital converter, data acquisition software and computer.

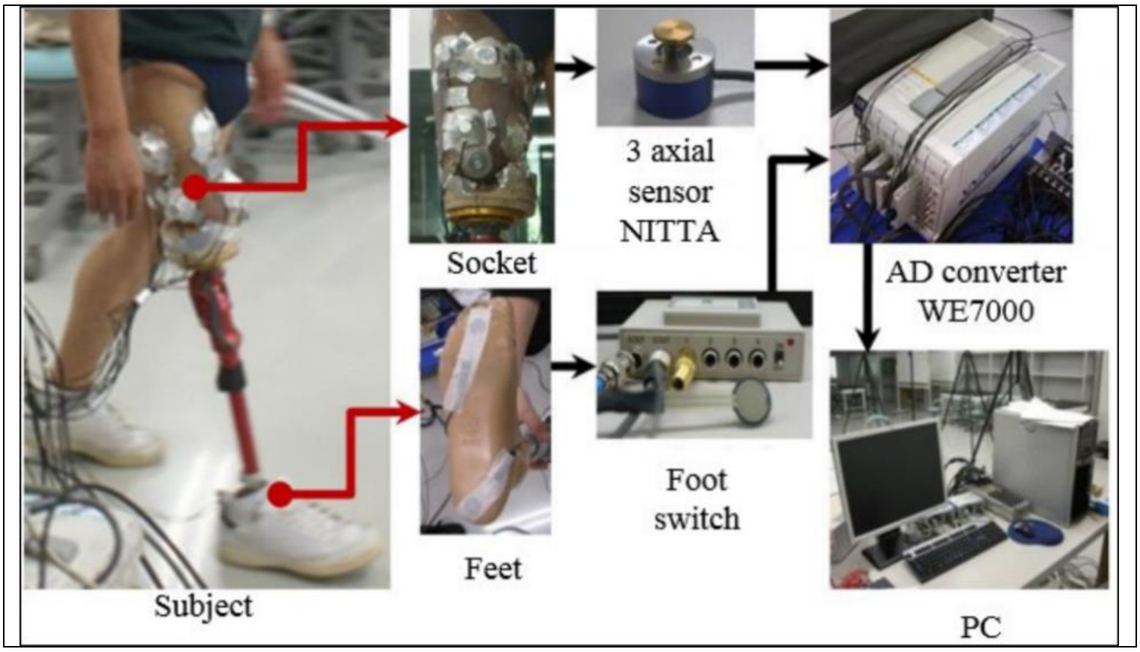

Figure 5.4 Bi-pedal stance experiment. 50% of body weight was assumed transferred to amputee and interact with the socket

5.3 Quantitative Evaluation of Finite Element Donning Simulation

In this chapter, corresponding to the number of subjects, a two tetrahedral finite element model was created. Subject A is a male, 35 years in age, wearing a socket on the left leg, with 7 years of history wearing a socket. Subject B, also a male, 47 years in age, is a right-leg amputee with 5 years of experience wearing a prosthetic socket. Both subjects were provided with two prosthetic socket models, namely, the UCLA and MCCT sockets. For each subject, a donning simulation was applied using an LS-Dyna Solver (Livermore, Ltd., Livermore, USA) as a simulator medium to observe the pressure distribution during the complete donning stage. The time of the computation varied for both subjects, but the average time was recorded as 6 h using a single Intel Xeon CPU 2.8 GHz device. During the complete donning the stage, the pressure distribution was assumed to be similar to the actual pressure when wearing the socket. Figure 5.5 shows the results of the pressure distribution for each subject during the complete donning of the UCLA and MCCT sockets. The pressure was determined in eight locations of the residuum, namely, the anterior proximal (AP), posterior proximal (PP), medial proximal (MP), lateral proximal (LP), anterior distal (AD), posterior distal (PD), medial distal (MD), and lateral distal (LD). A comparison with the experiment results was also made at similar locations of the sensors used in the simulation.

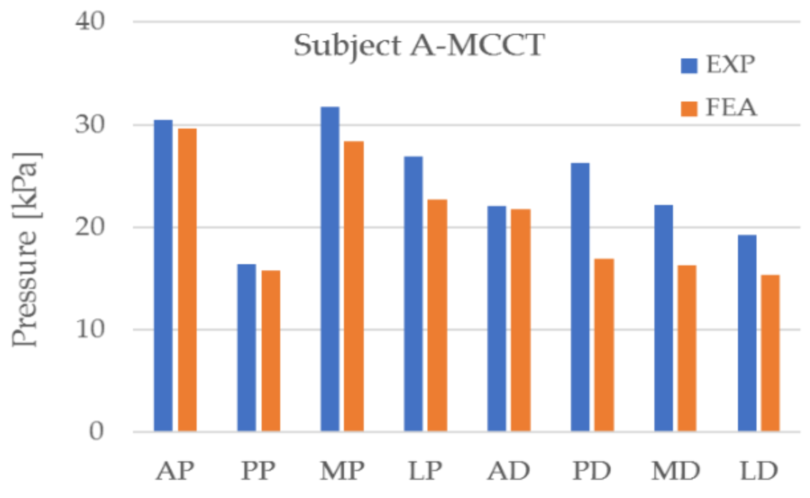

R^2= 0.8482

(a)

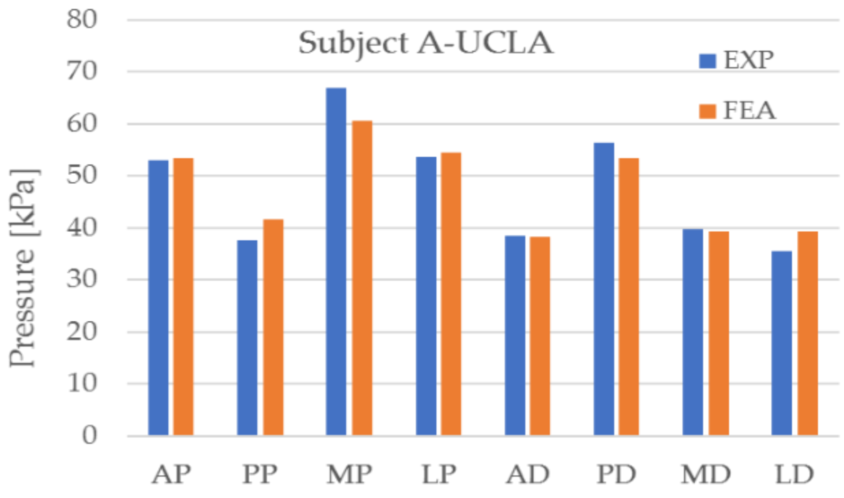

R^2= 0.9767

(b)

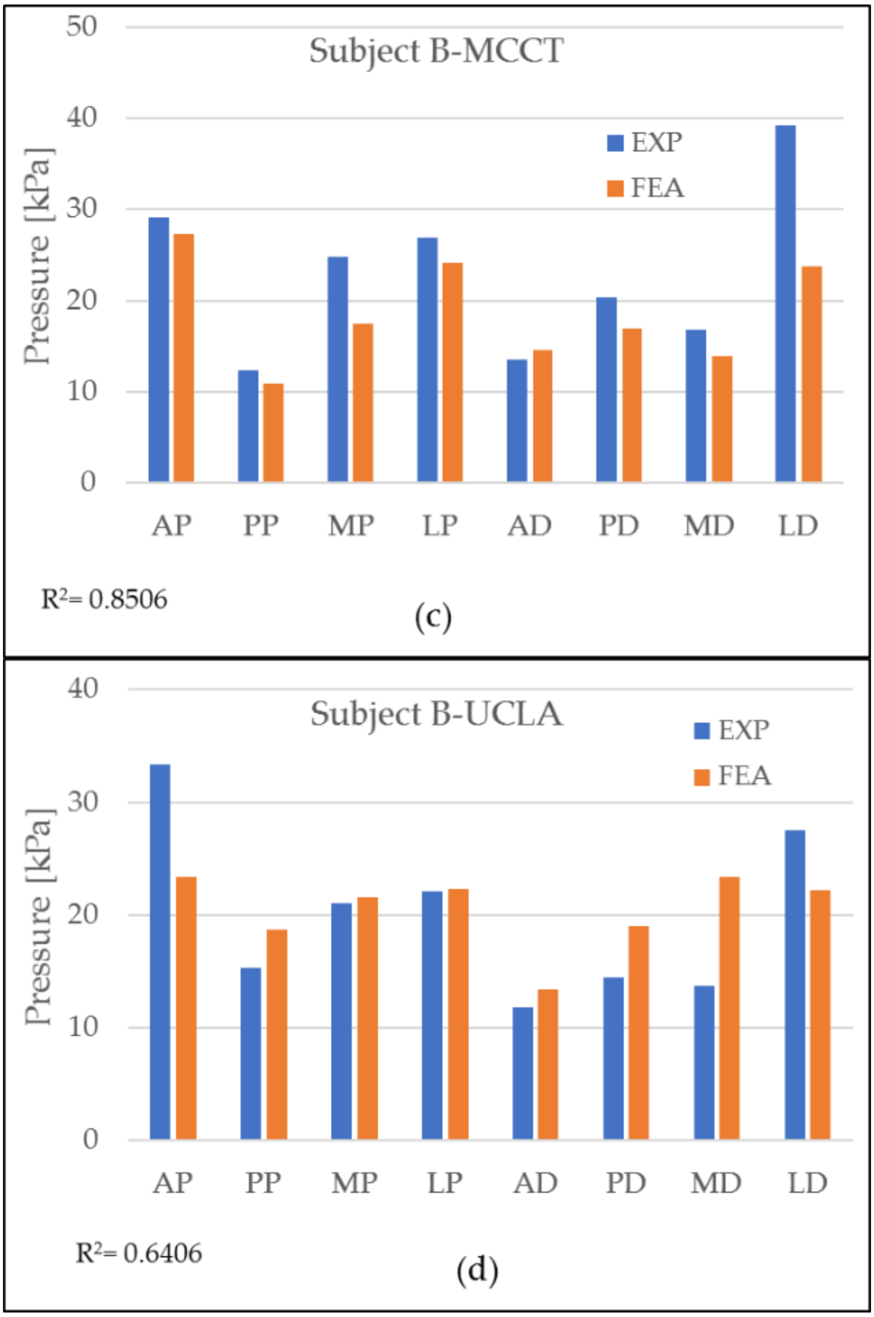

Figure 5.5 Pressure distribution in simulation (FEA) and comparison with experimental data (EXP) for each subject in both sockets at eight different locations. (a) pressure distribution for subject A in MCCT socket; (b) pressure distribution subject A in UCLA socket; (c) pressure distribution for subject B in MCCT socket; (d) pressure distribution for subject B in UCLA socket.

Validation of the simulation results was conducted by comparing the pressure in the eight locations of the residuum model with the clinical experiment data, as shown in Figure 5.6. A high correlation was observed throughout most of the comparison. However, in the results of the subject B-UCLA, the correlation was lower than 0.8, although this is considered a positive correlation because the average error for the measurement was considered to be small (<10%).

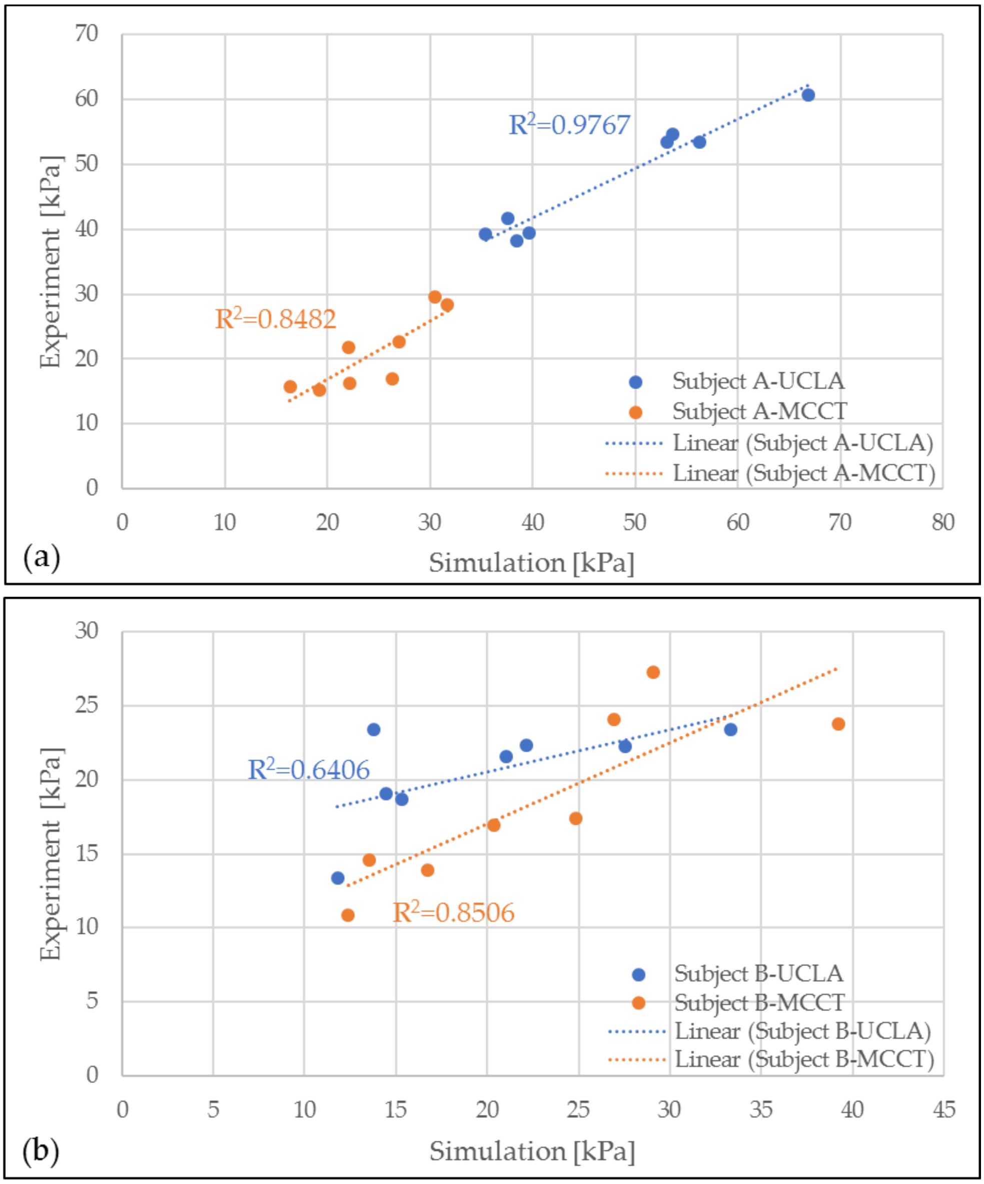

Figure 5.6 Correlation between experiment (EXP) and simulation (FEA) result in MCCT and UCLA socket for; (a) subject A and (b) subject B.

In addition to the pressure measurement occurring in the eight locations of the sensors, a pressure mapping occurring inside the socket was also observed. Figure 5.7 shows the pressure mapping occurring in the anterior and posterior views. The number in the mapping indicates the location of the sensor during the experiment.

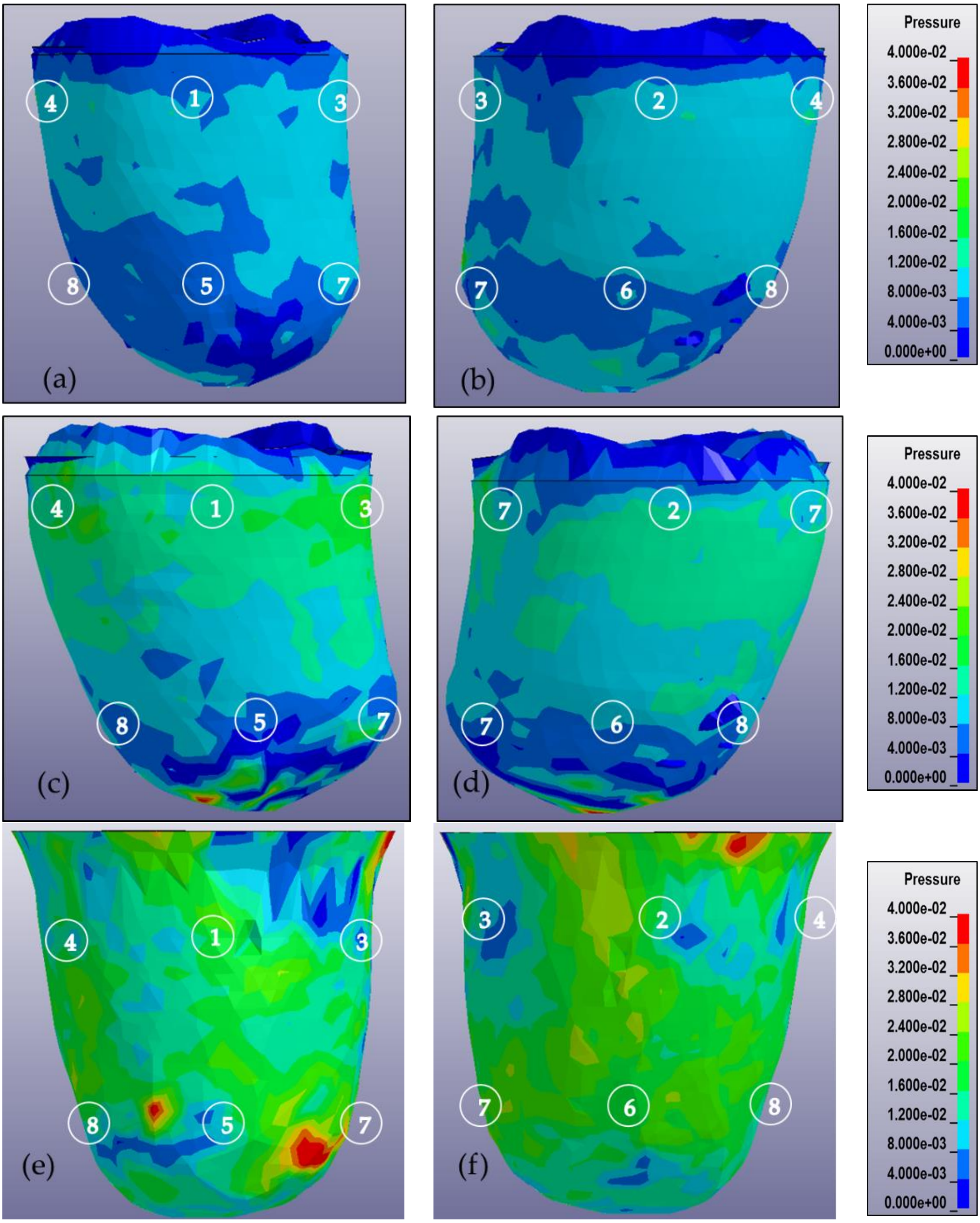
(a)
(b)
(c)
(d)
(e)
(f)
Pressure
4.000e-02
3.600e-02
3.200e-02
2.800e-02
2.400e-02
2.000e-02
1.600e-02
1.200e-02
8.000e-03
4.000e-03
0.000e+00

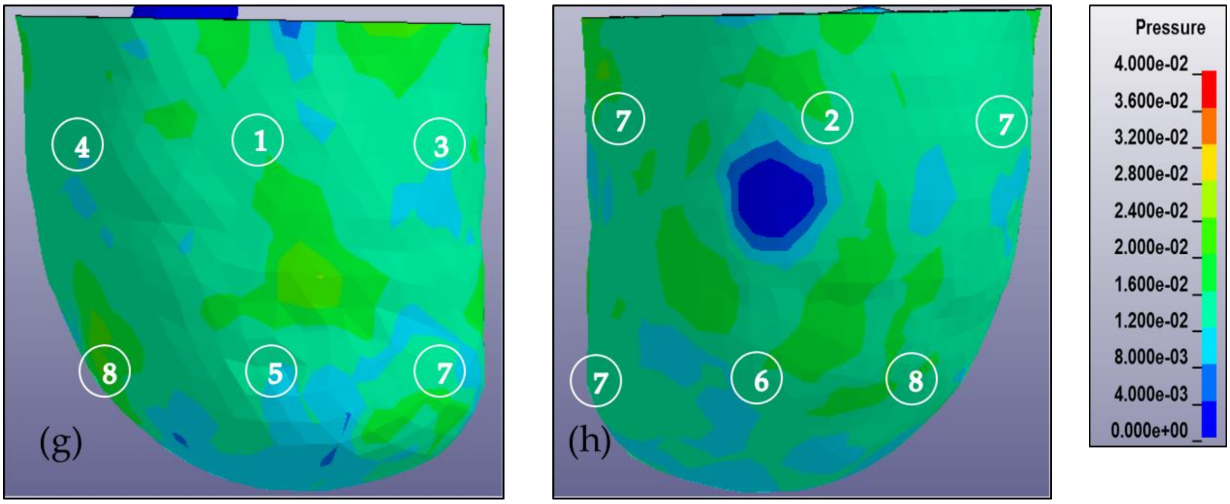

Figure 5.7 Pressure mapping of residuum during complete donning stages calculated from 0–40 kPa and observed from the anterior and posterior views. The sequence of numbers on the mapping denotes the location of the sensor, namely, AP, PP, MP, LP, AD, PD, MD, and LD, respectively. (a) Anterior view of residuum pressure mapping for subject A in MCCT socket. (b) Posterior view of residuum pressure mapping for subject A in MCCT socket. (c) Anterior view of residuum pressure mapping for subject A in UCLA socket. (d) Posterior view of residuum pressure mapping for subject A in UCLA socket. (e) Anterior view of residuum pressure mapping for subject B in MCCT socket. (f) Posterior view of residuum pressure mapping for subject B in MCCT socket. (g) Anterior view of residuum pressure mapping for subject B in UCLA socket. (h) Posterior view of residuum pressure mapping for subject B in UCLA socket.

A high correlation coefficient was generally observed in most of the models compared. Most of the simulation results are lower than the experiment data. In the subject A-MCCT socket case, the total pressure was recorded as 166.72 kPa in the FEA, whereas in the EXP, the number was 18.45% higher. In the UCLA case, the total pressure was recorded as 84.11 kPa, and for the experiment, a 44.19% increment was achieved. The pressure occurring in the AP was the highest among both the FEA and EXP for the MCCT socket case, whereas the pressure in the MP was higher than in the UCLA socket case for both the FEA and EXP results. The comparison of the pressure between the distal and proximal areas in the simulation was made for subject A, whereas the pressures in the distal and proximal areas in the MCCT case were recorded as 78.53 and 118.95 kPa, respectively, and in the UCLA case, the pressures for these areas were recorded as 36.68 and 45.43 kPa.

In the subject B-MCCT socket case, total pressures of 148.84 and 183.11 kPa were recorded for the FEA and EXP, respectively. In the UCLA socket case, the total pressure was recorded as 127.53 and 159.41 kPa for the FEA and EXP, respectively. In the MCCT socket for the subject B case, there is a significant difference in pressure detected in the LD position for the FEA and EXP. The highest pressure was detected in the LD, which occurred in the distal area for the MCCT socket case. However, in the UCLA socket case, the higher pressure was detected in the AP, where it occurred in the proximal area. When the comparison was made between the pressure distribution in the proximal and distal areas in the MCCT-FEA, pressures of 69.16 and 79.68 kPa were detected. In the UCLA-FEA case, the pressures were recorded as 86.20 and 41.33 kPa for the distal and proximal areas, respectively.

5.4 Analysis of The Simulation

The tendency exhibited by the pressures obtained in the results for both the MCCT and UCLA sockets is almost the same for both subjects. This indicates that the shape profile of the two types of sockets ensures that the behaviour of the residuum for each subject is almost identical.

Differences in the measurements of the FEA and EXP were observed in all locations at the sensors. However, the values exhibited a high correlation. In most cases, the measurements recorded in the FEA were lower than the EXP measurements. The reason for this phenomenon could be the period during which the subject wore the socket. Both subjects have more than a 5-year history of wearing a socket, and the soft tissue of the residuum tends to reduce it elasticity. According to Sanders et al. [83], a mature residuum (>18 months postamputation) will continue experiencing daily fluctuations in volume and shape owing to a reduction in the muscle elasticity. A reduction of the soft tissue elasticity contributes to maximizing the triaxial force sensor ability by increasing the contact force between the residuum skin and the force plate of the sensor, as illustrated in Figure 5.8. As for the FEA, the residuum model was set to be isotropic and homogenous, and the elasticity of the model remained constant.

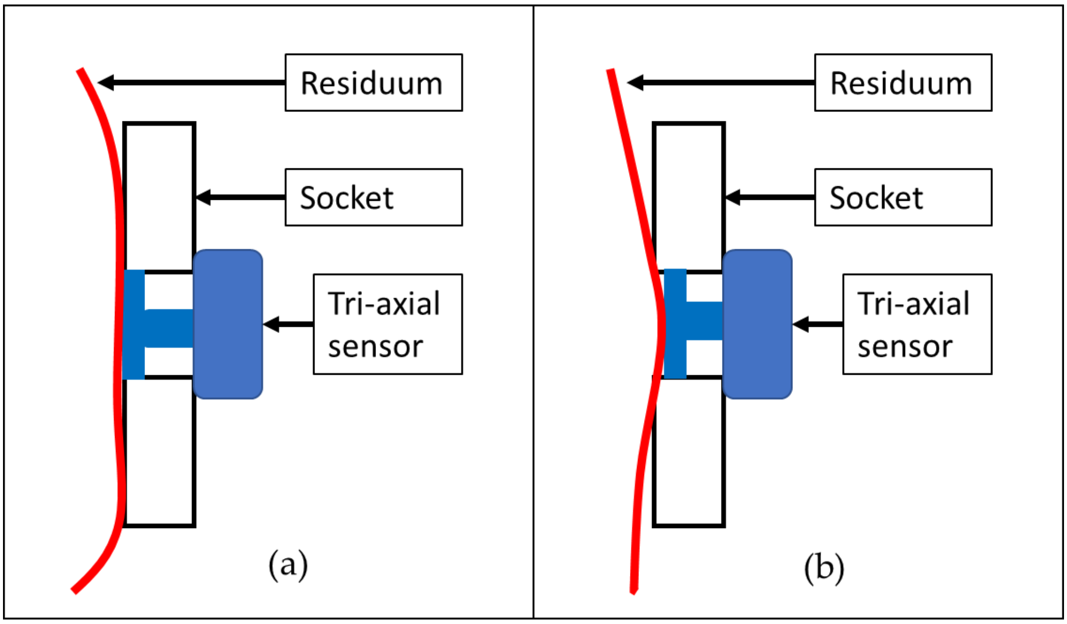

Figure 5.8 Illustration of contact surface between tri-axial force sensor and residuum skin in a socket. (a) The contraction of residuum with normal elasticity. (b) the contraction of residuum with less elasticity.

The pressure observed in the proximal area was higher than in the distal area in most of the cases studied. The selection of different shapes between the residuum and socket model increases the tendency of the residuum geometrical deformation. During the complete donning stage, a high amount of volume deformation occurred in the proximal area because the prosthetic socket was created using a small cross section in the proximal area to allow the socket to fit the subject residuum well [71]. The shrinking of the residuum increased the pressure occurring in the proximal area.

In other areas of the residuum that were not measured by the sensor, the distribution of the pressure was clearly observed by the FEA results. The results showed that the pattern of the pressure distribution on the surface was almost identical in both the MCCT and UCLA sockets. However, the amount of pressure occurring in the UCLA socket was higher compared to that of the MCCT socket in most cases.

Although a considerably realistic 3D model of the residuum was created in this study, which distinguishes soft tissue into fat and muscle parts, the separation of the muscle type of the residuum and its precise geometry is said to be more realistic and enable an internal pressure analysis to investigate the pressure ulcer and deep tissue injury (DTI) in an accurate environment [84]. The relative motion between the fat and muscle parts can be considered by enhancing the model in a realistic manner.

5.5 Pressure Analysis Summary

In this study, the pressure distribution profile of two subjects wearing UCLA and MCCT sockets was analysed through a utilization of the finite element method (FEM). The analysis results showed that the measurement in the FEA exhibited a high correlation with the actual pressure distribution inside the socket during a standing phase. Although not all FEA measurements achieved similar results with the EXP, the results were considered promising because only a small average error (<10%) was determined during the FEA-EXP comparison. This error may be caused by an abnormality in the actual residuum features where scars and tissue injury in the actual residuum skin were not measured during the simulation. Furthermore, the mechanical properties used in the simulation were considered to be general, whereas the geometrical shape of the residuum is based on the subject-specific profile.

A comparison of the results of the proximal and distal areas showed that the pressure distribution on the surface of the proximal area in both the MCCT and UCLA sockets was higher than in the distal area. The results showed that the prosthetic socket was designed by minimizing the pressure in the distal area such that the post-operation wound and scars in the residuum will not be affected, while at the same time maximizing the pressure in the proximal area to make the socket properly fit the subject's residuum [71].

The main objective of this study involving an estimation of the pressure distribution profile using the FEM was achieved. The results of the current study along with those of previous research studies indicate that the FEM is a suitable method for investigating the residuum deformation behaviour by measuring the pressure developed inside the socket. The pressure distribution profile helps the prostheses estimate the comfortability level of the subject while wearing the device. Thus, an adjustment can be made to the socket design before it has been fabricated. Although the calibration of a 3D model was previously conducted [85], the details, particularly the scar from the post treatment at the distal end, were not highlighted. In a future study, increasing the number of subjects will be our top priority for enhancing the statistical analysis and considering a subject-specific material property through an advanced finite element (FE) model creation.

Chapter 6

Evaluation System for Magnetic Resonance Imaging (MRI) Based Three-Dimensional (3D) Modelling of a Transfemoral Prosthetic Socket Using Finite Elements Method

An evaluation system to measure the accuracy of a subject-specific 3D transfemoral residuum model during the interaction with the socket in conjunction with the application of finite element methods is presented in this chapter. The proposed system can be used in future validations of socket fabrication. The evaluation is based on the measurement of the residuum's soft tissue deformation inside two types of prosthetic sockets. In comparison with other studies, the 3D models were constructed with magnetic resonance images (MRI) with the aid of computer-aided design (CAD) software. The measurement of soft tissue deformation was conducted based on the measurement of the volumetric value of fat, muscle and skin in the pre- and post-donning phases. The result yielded a promising correlation coefficient value between the simulation and the experiment in the soft tissue deformation evaluation. The relation of the muscle–fat ratio in the residuum is extremely important in the determination of the ability of the prosthetic to deform. The environment during the socket fitting session was similar to that defined by the set boundary conditions in simulations. In view of the promising results of this proposed system, the evaluation system is considered reliable and is envisaged to be used in future research.

6.1 Introduction

Prosthetic device manufacturing has increased tremendously owing to an increased demand in recent years. This demand has been driven by the increase of amputees that require the prosthetic device to perform their daily routines. In Japan, the proportion of amputees increased to 22.4% compared to the statistic reported five years ago because the number of patients with peripheral vascular disease has increased [84]. Conventional prosthetic device manufacturing has been depended on hand craftsmanship, expertise skills and experience. As a result, current socket design and fitting are inconsistent and vary among prosthetic manufacturers. Furthermore, the process requires considerable time before the end product is obtained and it is really exhausting for the patients who are mostly elderly citizens [85].

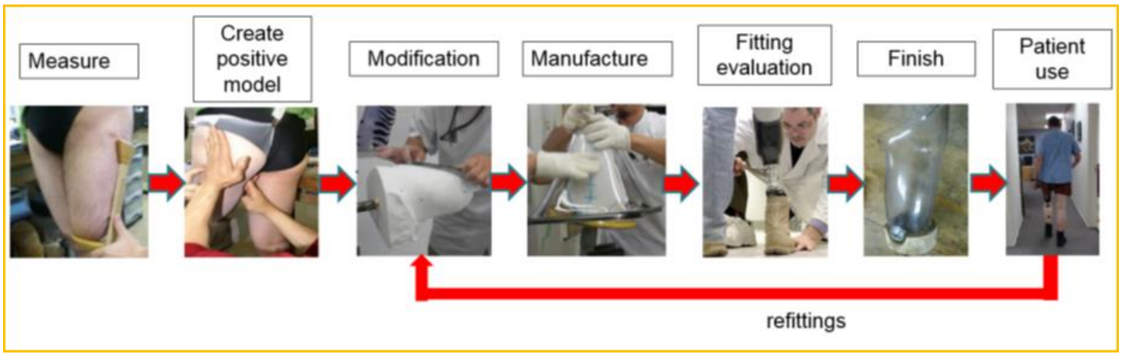

Figure 6.1 Conventional method of socket manufacturing

Recent developments and applications in biomechanics introduced the utilization of a three-dimensional (3D) printing system to enhance the process of socket design. As reported by Zuniga [86], 3D printers have been utilized to develop prosthetic devices using antibacterial filaments. The investigation found that the 3D printer is capable of developing effective antibacterial finger prosthesis. Furthermore, the potential of 3D printing in the fabrication of the transfemoral prosthetic socket has also been discussed. According to Nguyen et al. [87], the design and 3D printing of the transfemoral prosthetic socket required less time compared to conventional methods. However, the evaluation for 3D printing prefabrication has not been discussed in most of the previously published research studies [86,88-90].

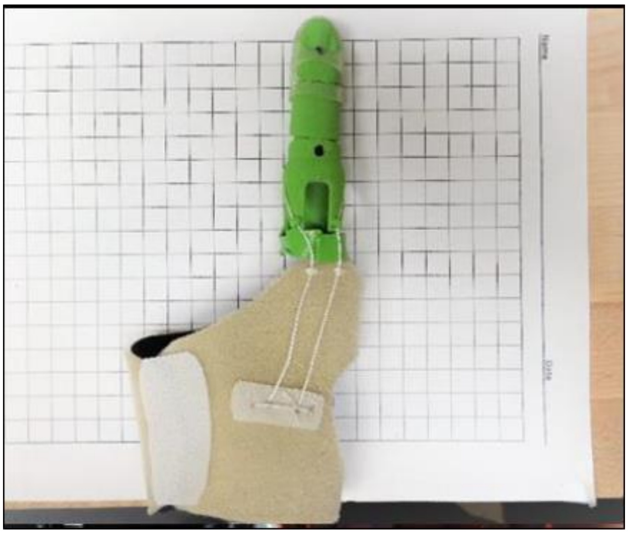

Figure 6.2 3D printed finger prostheses [86]

Finite element analysis (FEA) is extensively used in the evaluation of human anatomy models. For example, in Reference [88], internal strains of transtibial prosthetics have been investigated during load bearing using FEA. Furthermore, investigation of specified prosthetic socket interactions with the transfemoral residuum was also conducted with the same method by measuring the interface pressure on the surface of the residuum [89]. In addition to the prosthetic and orthotic field, FEA was also extensively used in dentistry to develop a future implant. In Reference [90], the development of finite element models from medical images was presented using automated methods. As a result, the proposed methodology revealed its potential to solve linear elasticity problems in two-dimensional (2D) and 3D implementations.

Figure 6.3 3D printed arm forged (PrinterPrezz)

Even though the FEA method was extensively used in the evaluation of a 3D model in terms of the stress distribution [91], strain measurement and mechanical properties, the geometrical and volumetric changes in the simulation can also be analysed. For instance, in Reference [92], an approach to modelling the contact interface between transtibial residuum and prosthetic socket has been developed. However, the presented model was used to investigate the stress distribution along the residuum and no indication of comparison with experimental comparison were observed. Volumetric changes constitute an important quantitative factor for the determination of the level of comfort during the period the prosthetic socket is worn. In Reference [93], they concluded that patient-specific analyses of the residuum were important for evaluation of potential deep tissue injury as a result from soft tissues changes inside the prosthetic socket. The outcome enables the expert designer to modify the prosthesis and thus improve the stability and durability of the prosthetic socket. Combination of the FEA method with image processing allows the development of a geometrical model system for pre- and post-fabrication evaluation of prosthetic devices.

In this study, we propose an overall evaluation scheme of two 3D transfemoral prosthetic socket models constructed using magnetic resonance images (MRI) (based on the UCLA and manual casting compression technique (MCCT)) in conjunction with a finite element method (FEM). The evaluation is based on the geometrical and volumetric changes of a residuum model before and after the simulation of the donning procedure. The geometrical model is compared with the model developed with precise image processing (IP) software that was considered as most accurate model to the real residuum. The procedure adopted in this study includes the following steps. First, the finite element models of the residuum and prosthetic socket were developed using MRI with the aid of CAD software using a construction methodology created by our team. The donning simulation was then performed which was created based on real-fitting conditions. The simulation results are converted to cross-sectional data along the z axis and reconstructed to imitate the MRI image specifications. The soft tissue volume is calculated based on the reconstructed simulated images. Finally, the volume calculations are compared with the experimental outcomes. The study is motivated by the high demand for the prosthetic socket in recent years, but the process of socket fabrication requires special treatment and craftmanship from prosthesis and an alternative method of pre-fabricated socket evaluation is necessary to shortening the overall process.

6.2 System Evaluating Method

The system evaluation involved three subjects. The main criteria of the selected subjects are that they must have a single above knee (transfemoral) amputated leg. All selected subjects have more than 5 years of experience wearing the prosthetic socket. The subjects are a volunteer and have no conflict of interest in the research. The magnetic resonant (MR) images for the subjects were obtained using a Siemens Magneton Symphony Maestro class 1.5 T. The MR image was chosen owing to its ability to generate excellent soft tissue contrast and to differentiate soft tissues and muscle boundaries [91,94].

In Reference [95], MR image also has been used to create the resemblance of residuum model. However, the created model only utilized the outer area of the residuum cross section image. Residuum model created in the study is categorized into 3 main parts namely fat, muscle and bone. The adipose tissue part is assumedly merged with the fat part because of the similarities of their mechanical properties. Two Ischial–Ramal–Containment (IRC) socket types—namely UCLA and MCCT—were used in this study. The IRC–UCLA socket is a standardized transfemoral prosthetic socket that is extensively used, while the IRC–MCCT is a socket introduced by Professor Yukio Agarie. The socket was inspired and created based on the standard IRC socket. The difference between the two sockets is that the stability of the IRC–MCCT socket was improved by the adjustment of the anterolateral and sagittal directions of the IRC–UCLA socket [96], as shown in Figure 6.4 and the method used to produce the IRC–MCCT socket uses MCCT.

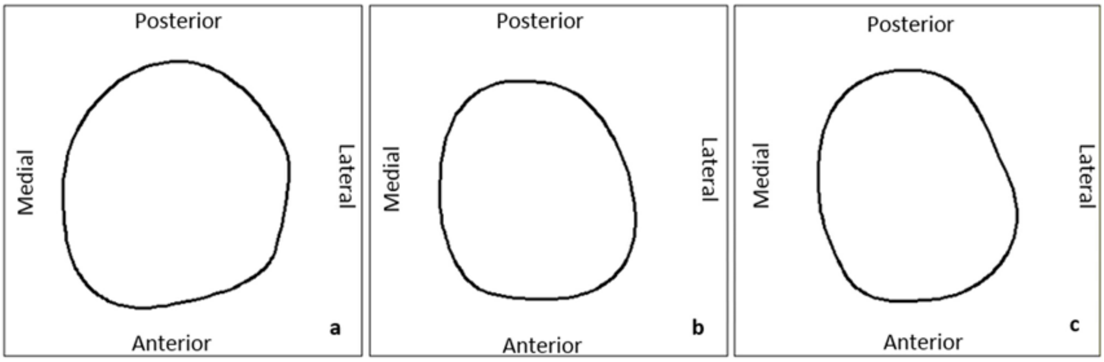

Figure 6.4 Profile at the cross section from distal end of (a) residual limb, (b) UCLA socket, and (c) MCCT socket at 180 mm

6.2.1 Finite Element Model Construction

As mentioned in previous chapter, to realize the interaction between socket and residuum, the 3D model of residuum and its socket must be created. Instead of using a 3D scanner, this study has proposed a low-cost, accurate method where computer-aided design (CAD) Creo software (PTC Ltd., New Delhi, India) has been used to construct the transfemoral residuum and its socket. The utilization of MR images is recommended because its provided distinction between muscle, fat, skin inside the soft tissue image [94].

Each subject provided 30 MR images which are aligned in the vertical direction with 5 mm spacings between successive images. In every image, 36 trajectory lines were drawn from the centre point of the residuum slice every 10°. Every intersection between each trajectory line and the residuum slice is plotted and connected with a spline curve function using CAD software to generate a cross-section for the image. Finally, every cross-section will be combined to construct the 3D model of the residuum. The same procedure will be implemented to create the socket model. The socket model was created using the real size of the prosthetic and not a residuum shape offset as practiced in most previous research studies. The design method has been discussed in detail in Reference [97].

Creo 3 (PTC Ltd.) is a CAD software used to generate a surface dimension file format such as an initial graphics exchange specification (IGES) file and standard triangular language (STL) file and it enabled the meshing process to be conducted directly without file conversion. In this study, the model is required to be meshed using Ls-Prepost software (Livermore Ltd) with a tetrahedra element is set to be the main element type.

6.2.2 Simulation Environment

The fitting procedure is an effort used to maximize the comfort and functionality of a prosthetic limb and to achieve an appropriate fit. It is effectively a trial-and-error method used to determine the socket volume and shape. This study has used the fitting procedure condition as a benchmark for the simulation condition. The basic principle in the simulation relies on the fact that the residuum ought to move toward the socket. In the residuum, 50% of its body weight is at the top to emulate the bipedal stance, as shown in Figure 6.5a. Regarding the socket, the horizontal movement has been constrained to realize the contact between the residuum, as shown Figure 6.5b. The first contact was defined as the surface-to-surface contact between the socket and residuum with a coefficient of friction of 0.5, as suggested in Reference [96,98]. The second contact was defined as the tied contact between bone–muscle and muscle–fat. The contact defined the base on the hypothesis of relative motion between skin–fat and fat–muscle was neglected [99].

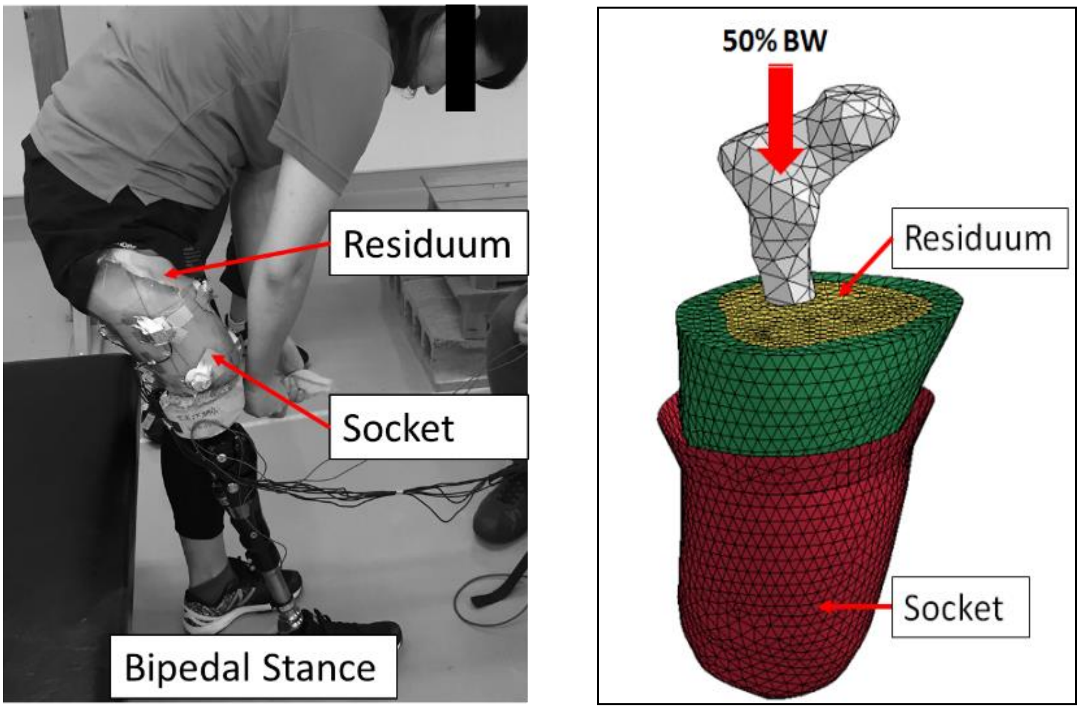

(a) (b)

Figure 6.5. Simulation boundary condition. (a) Actual fitting session and bipedal stance. (b) Donning simulation of the fitting session with 50% of body weight (BW).

6.2.3 Mechanical Properties of Material for Residuum and Socket

The material properties were classified into solid and viscoelastic. The bone and socket were categorized as solid materials and were defined as homogenous and linearly elastic, according to Hooke's law, based on which stress varies linearly with strain. The bone was modelled with a Young's Modulus (YM) of 17,700 MPa and a Poisson's ratio (PR) of 0.3 [99]. Acrylic plastic was used to construct both sockets with YM and PR values equal to 1885 MPa and 0.39, respectively. Viscoelastic materials are representative for skin, fat and muscle and where defined as soft tissues. The viscoelastic formulation parameter used in the simulation was listed in Table 5.1 where C, S, T and K, respectively denote the invariants of the right Cauchy deformation tensor (stiffness), spectral strength, characteristic time and bulk modulus [100,101,102].

6.2.4 Simulation and Acquisition Outcomes

For simulation purposes, LS–DYNA software (Livermore Ltd., California, US) was used to generate the nonlinear dynamic donning simulation. The simulation was conducted in the case of donning with the MCCT and UCLA sockets in the bipedal stance position. At the end of the simulation, the shape of the residuum was deformed and was fitted to the socket. The analysis of the geometrical and volume changes was conducted at the end of the simulation.

First, the completed simulation model was sectioned horizontally every 5 mm from the bottom of the model. The sliced model was trimmed and converted into a binary image. Binary images were used to calculate the area of the residuum's cross-section (A_i) during the donning process. The volume of the residuum was calculated with Equation (6.1), where A and h respectively denote the cross-sectional area and the height between successive cross-sections.

$$V_{i(i+1)} = \left(\frac{A_i + A_{i+1}}{2}\right) h \tag{6.1}$$

To calculate the pixel ratio of the simulation image, a raw volume ratio was calculated for both the simulations and experiments. The volume ratios (R_V) for the simulations and experiments were determined based on Equation (6.2), whereby V_P and V_s respectively denote the volume of the part and cross-section in a single image. Fixed average volume ratios of simulations and experiments are shown in Equation (6.3), whereby R_{SV}, R_{EV} and n, respectively denote the simulation volume ratios, experiment volume ratios and numbers of utilized images.

$$R_{Vi(i+1)} = \left(\frac{V_{pi(i+1)}}{V_{si(i+1)}}\right) \tag{6.2}$$

$$R_{FA} = \left(\frac{\sum_{i=1}^{n} \frac{R_{SVi(i+1)}}{R_{EVi(i+1)}}}{n}\right) \tag{6.3}$$

The actual volume of the simulation was determined by multiplying the average volume ratio (R_{FA}) with the cross-sectional volume for every layer of the model. Finally, the model volume was compared with the value obtained from the image processing (IP) analysis.

IP analysis was calculated by Matlab (MathWork) by summarizing an area of cross section from the filtered MR image. The image was converted into the desired scale and transformed into a binary image. In the binary image, every white pixel's area was summarized. The calculation was continually performed in every MR image. The volume of the IP model was calculated by inserting the calculated area into Equation (6.1).

6.3 Simulation Result and Comparative Evaluation of the System

In this chapter, a three tetrahedral finite element model was created corresponded to the number of subjects. Every subject provided with two prosthetic socket model corresponded to UCLA and MCCT socket. Table 6.1shows the list of number of element and nodes for each of the subject and their socket.

Table 6.1 List of Element and nodes unit.

Model		Number of Elements	Number of Nodes
Residuum	Subject A	17,693	13,250
	Subject B	19,576	14,020
	Subject C	19,725	5017
MCCT Socket	Subject A	1703	880
	Subject B	299	181
	Subject C	328	190

UCLA Socket	Subject A	2161	1158
	Subject B	337	199
	Subject C	234	246

Table 6.3 showed the list of subjects' profiles involved in the study. The study focused on the transformation of the geometrical model based on the donning simulation. The result was collected from three parts of the model before and after donning was completed. Figure 6.6a shows an initial environment for the donning simulation, while Figure 6.6b shows the simulation result after the donning process is completed. The complete residuum model was then sectioned in 30 cross-sections along the z axis, binary images were generated, as shown in Figure 6.7, which shows the fat part of subject A as an example.

Table 6.2 subject profiles

Measurement	**Subject**		
	A	B	C
Weight (kg)	63	80	61
Height (cm)	169	162	167
Age (YO)	35	56	47
Gender (M/F)	M	M	M
Amputated Leg	Left	Right	Right
History Socket Usage (Years)	7	40	5

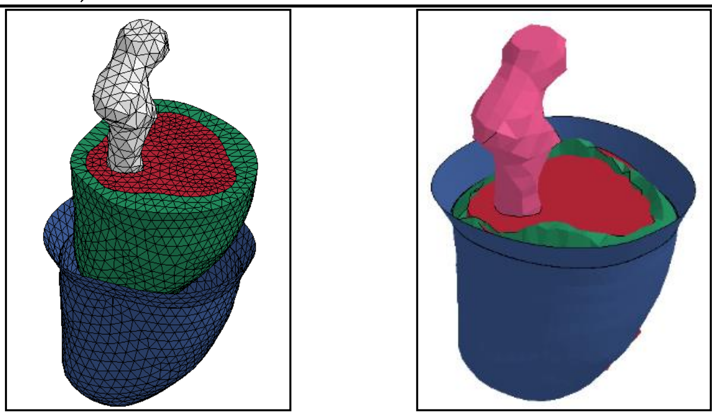

(a) (b)

Figure 6.6 (a) Initial condition of donning simulation. (b) Results of complete donning simulation for subject A.

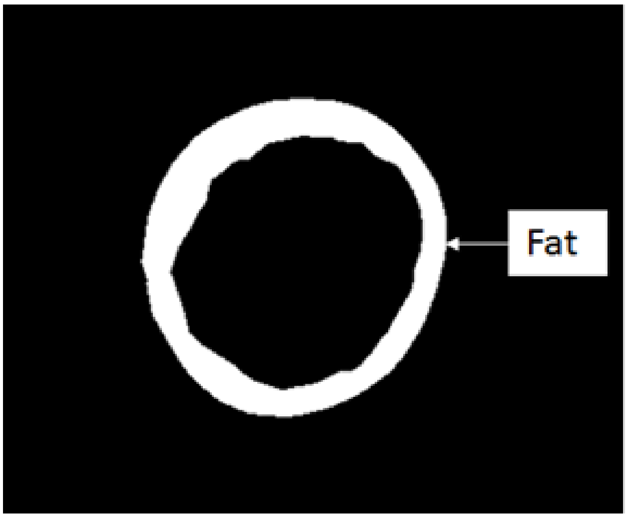

Figure 6.7 Sample of binary image created from subject A to complete the donning process.

All the part volumes were determined layer-by-layer for each subject, as shown in Figure 6.8. The results consist of the image processing measurement (IP) and finite element simulation (FEA) outcomes for the three subjects with errors between both measurements. The volume measured before donning is denoted by the NO symbol. The corresponding volumes after the residuum was donned in both the MCCT and UCLA sockets are denoted with the symbols MCCT and UCLA, respectively.

Increased correlation coefficient values (R^2) were obtained in most of the models and the errors (Err) which occurred for the total volumes are acceptable, as shown in Table 6.3. Increased correlation values (>0.9) indicate the similarities of the FEA model to the actual residuum. This is attributed to the fact that the IP model yielded the most accurate volume measurements. All the FEA models yielded average errors which were less than 9% for each layer.

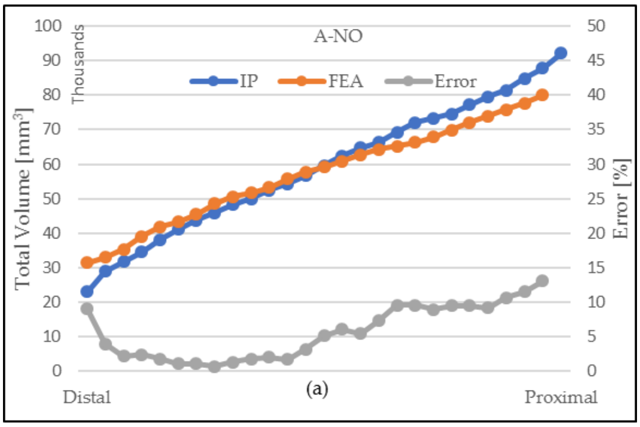

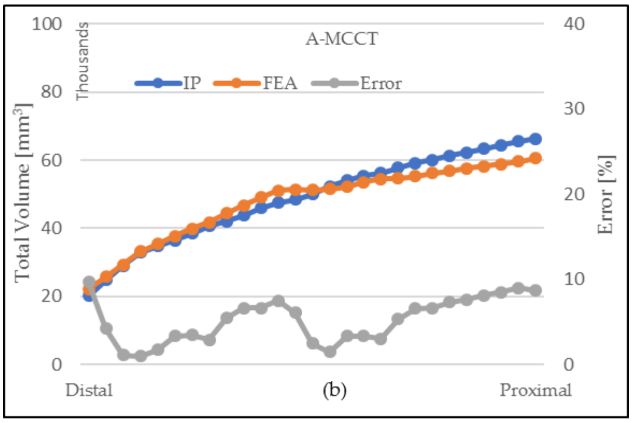

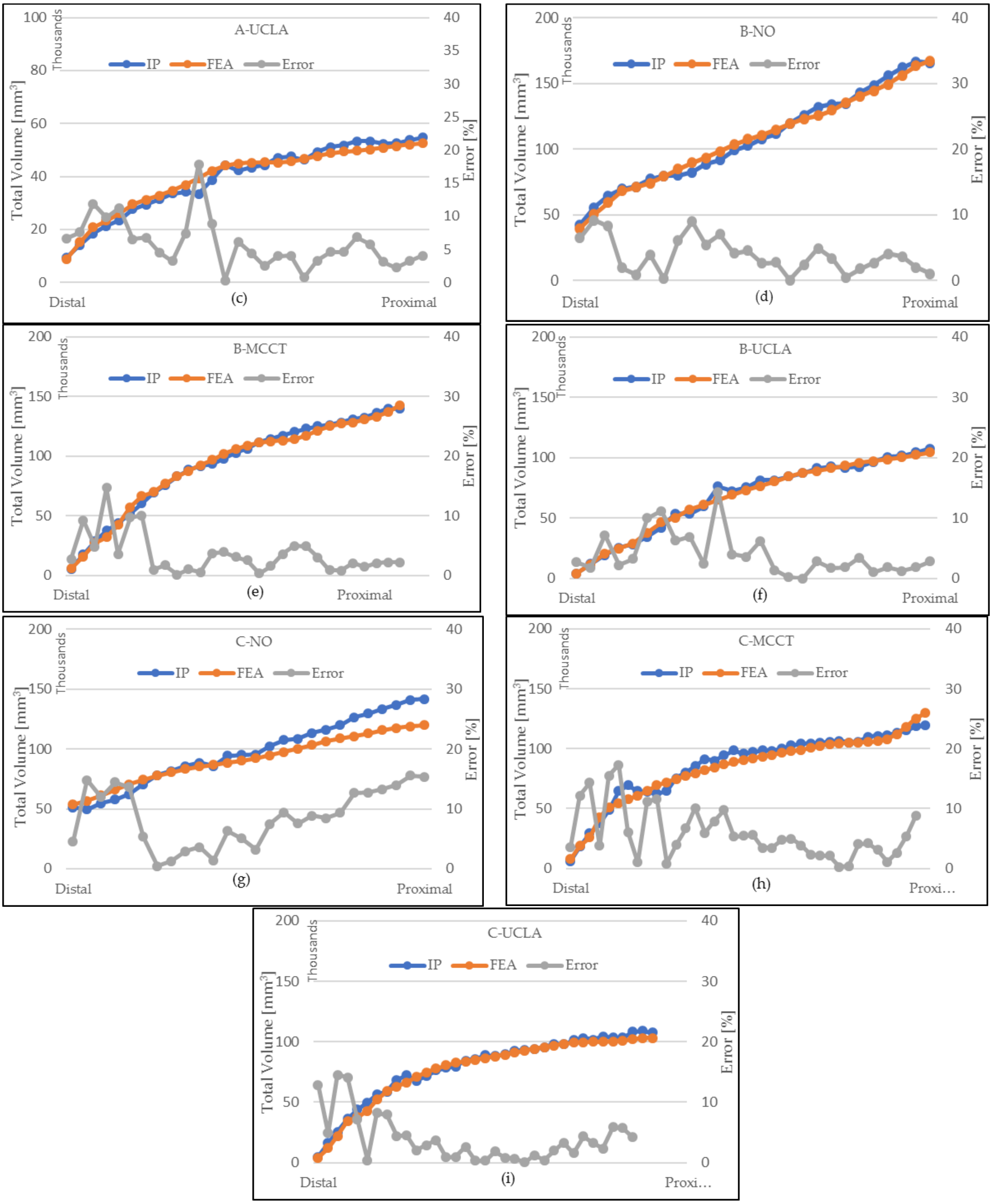

Figure 6.8 Volumes of all parts in every layer for each subject. IP denotes the measurement of volume from image processing method, finite element analysis (FEA) denotes the measurement of volume from a simulation and Error denotes the

percentage of differences between image processing (IP) and FEA measurement. (a) Volumes for subject A without socket and with (b) MCCT and (c) UCLA sockets. (d) Volumes for subject B without socket and with (e) MCCT and (f) UCLA sockets. (g) Volumes for subject C without socket and with (h) MCCT and (i) UCLA sockets.

Table 6.3. Correlation coefficient values of residuum volumes for the FEA and IP models and average errors.

	Part	A			B			C		
		NO	MCCT	UCLA	NO	MCCT	UCLA	NO	MCCT	UCLA
R^2	**Fat**	0.962	0.949	0.890	0.980	0.981	0.982	0.915	0.686	0.702
	Muscle	0.994	0.968	0.965	0.979	0.982	0.980	0.987	0.977	0.994
	Bone	0.492	0.658	0.658	0.539	0.539	0.539	0.934	0.934	0.934
Error (%)		A			B			C		
		NO	MCCT	UCLA	NO	MCCT	UCLA	NO	MCCT	UCLA
	Fat	2.305	0.419	2.594	2.288	0.703	0.199	0.529	0.066	3.207
	Muscle	7.580	4.528	6.777	0.518	2.864	2.916	10.954	5.230	8.179
	Bone	0.521	0.069	0.069	0.483	0.483	0.483	1.681	1.681	1.681

Figure 6.9 shows the anterior cross-sectional views of the FEA residuum models of the three studied subjects before and after the penetration of the residuum models inside the sockets. It is clearly shown that the residuum has changed into the socket shape after its complete penetration. The movement of the soft tissue during the process is not controlled by the user. In other words, the changes of the soft tissue depended on the simulation boundary condition.

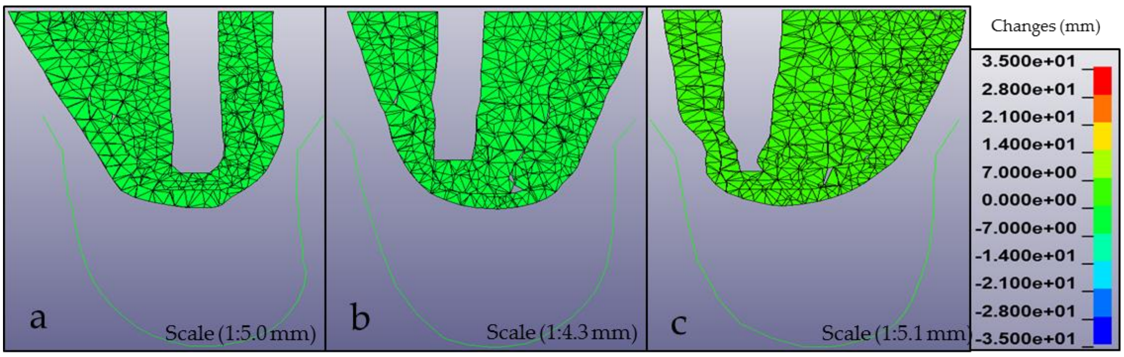

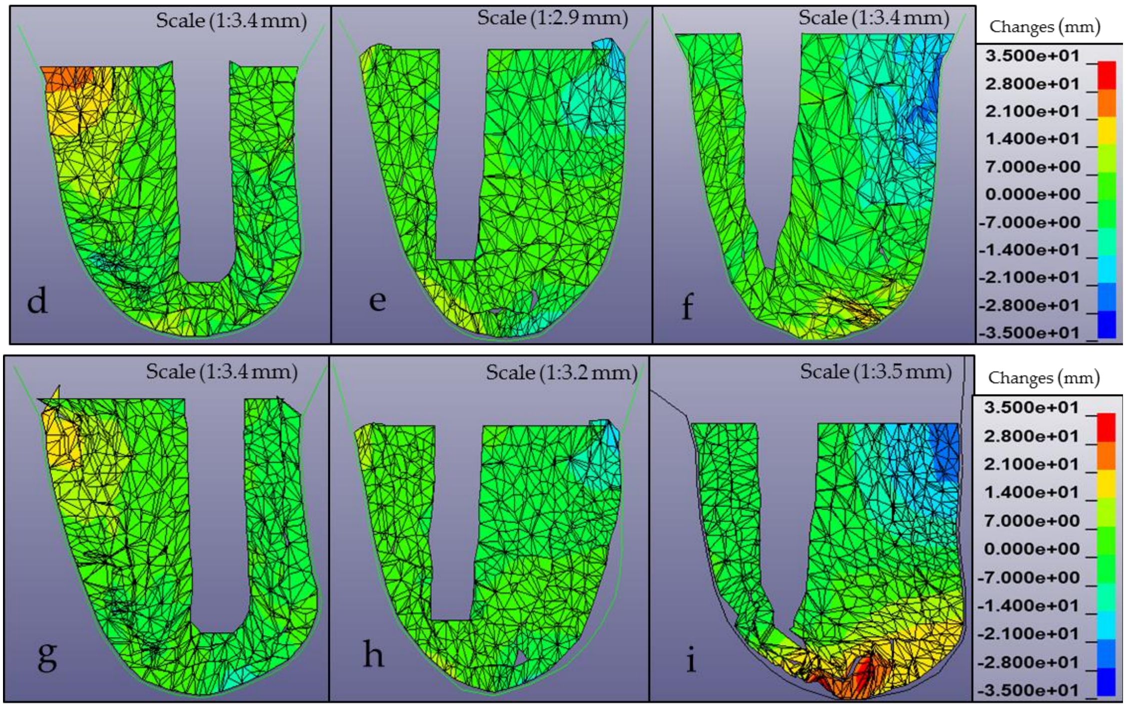

Figure 6.9. Heat map of a residuum deformation from anterior cross-section view before and after the donning process. (a–c) Residuum models shown before the donning process for subjects (a) A, (b) B and (c) C. (d–f) Results of complete donning into the MCCT socket for subjects (d) A, (e) B and (f) C. (g–i) Corresponding results of the complete donning into the UCLA socket for subjects (g) A, (h) B and (i) C.

Volumetric changes were observed for soft tissue parts only when the bone part was considered as solid and unchanged. Figure 8 shows the deformation graph of the residuum during the insertion into the MCCT and UCLA socket for both simulations and measurements. The measurement included the deformations of the total soft tissue, fat and muscle. The error bars indicate different volume values for IP and FEA data. The positive and negative values indicate that the volumes respectively increased or decreased during the complete donning process. The correlation coefficient between simulations and measurements remained high. In most cases, fat changes are significant compared to muscle and they mostly contribute to the total soft tissue deformation.

In the cases of subjects, A and C, the fat and muscle volume decreased in the distal area while they increased in the proximal area in both socket types. However, the fat rapidly changed in the proximal area and corresponded to the enlargement of the muscle. The maximum increase of fat volume occurred in the distal end, whereby during the fitting session, the residuum was theoretically pushed toward the distal end before the socket was vacuumed. The decrease of the volume corresponded to the increase of the residuum length. When the fat was pushed downward, the residuum was shrunk to fit the socket and the total length of the residuum pushed the distal fat. The result supported the assumption that during socket penetration, the residuum tended to shrink to fit the socket shape by pushing the soft tissue downward and thus allowed the length of the residuum to increase.

Figure 6.10 Variations of the volumes of deformed soft tissue for total soft tissue, fat and muscle. (a) Results for subject A with the MCCT socket. (b) Results for subject A with the UCLA socket. (c) Results for subject B with the MCCT socket. (d) Results for subject B with the UCLA socket. (e) Results for subject C with the MCCT socket. (f) Results for subject C with the UCLA socket.

The simulation (FEA) results for subjects A and C indicate that the fat increases in the distal area of the MCCT socket are 18.5% and 23.69%, respectively shown in Figure 6.10. Additionally, in the distal area of the UCLA socket, the fat respectively increased by 6.63% and 1.68%. However, in the proximal area, the fat respectively decreased by 7.53% and 3.67% in the MCCT socket and by 11.96% and 1.99% in the UCLA socket. Based on the evoked outcomes, we can verify that the fat volume increased in the distal area and decreased in the proximal area of the residuum. The increase of the fat's volume in the distal area led to the increase of the residuum length.

6.4 Discussion

In this chapter, the geometrical changes had a primary role in the determination of the efficiency of the overall evaluation system. In order to check the result of donning simulation, a special process for taking the MRI data wearing the developed sockets is necessary. This process is a burden for the subjects, so we limited the number of subjects when we applied to the ethical committee of our university. Even though the number of subjects participating in the study is low, it is enough to accomplish the geometrical changes observation objective.

6.4.1 Geometrical Changes

In the cases where geometrical changes occurred, the correlation coefficient value was high in most cases. However, in most cases, low differences of the volumetric value occurred between simulations and measurements.

During the complete donning process, a higher deformation was observed in the fat part. The deformation of the fat part represented almost 70% of the total deformation and the changes were mostly in the distal area where the muscle volume was low. The effects of the mean muscle density on deformation were more pronounced than those for fat and the lower volume of the muscle allowed the fat to deform in an easier manner.

The simulation results from subject B showed a unique pattern of deformation based on the hypothesis that the fat volume decreased by 21.03% and 15.18%, respectively, in both the proximal and distal areas of the UCLA socket. The increased muscle–fat volume ratio in the residuum most likely affected the deformation because the density of each material affected the movement of the fluid inside the residuum.

Subject B had the highest soft tissue volume among all the tested subject residuum values. As a result, the volume of the fat in the distal area has not significantly changed during the complete donning process. Even though subject B is the shortest in height among the others, the diameter of the residuum of subject B is the highest. There is no significant difference in the comparison of the simulation and measurement results for both sockets and a high-correlation coefficient value is estimated for these sets. Subject B has a history of wearing the socket. In this respect, the muscle has become used to the local environment and the elasticity of the residuum is likely to be low and tends to shrink during its insertion into the socket.

Figure 6.11 shows the error distributions of soft tissue volumes between FEA and IP measurements in every layer for each subject with and without sockets. The differences detected in the measured and simulated values are most likely caused by the fact that in the simulation cases, the muscle and the fat part are considered as one entity, while in real cases both parts are connected to each other. Furthermore, the internal fat inside the muscle was ignored in simulations, which led to fat volume decreases.

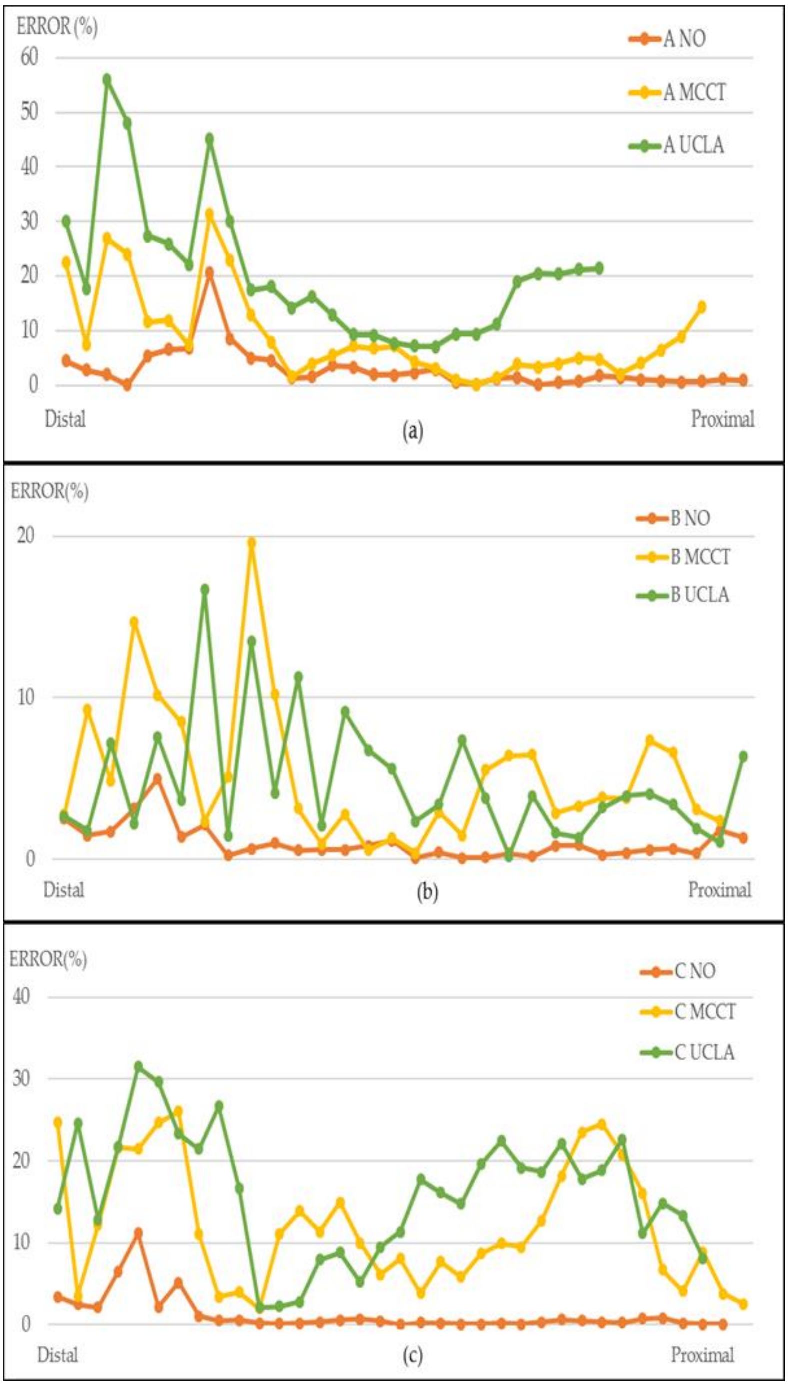

Figure 6.11 Error distributions of soft tissue volumes between FEA and IP from the distal end to the proximal area with and without sockets. Results for subjects (a) A, (b) B and (c) C.

6.4.2 Error Analysis

The highest error observed in the distal area of all part models is shown in Figure 6.12. Specifically, the average errors for the distal areas were respectively equal to 2.88%, 9.33%, 11.92%, 1.04% 13.07%, 13.1%, 1.26%, 12.02% and 20.09%, for subjects A, B and C, without the socket and with the MCCT and UCLA sockets. The error in the proximal area was 32% lower than the average distal area in every model.

A significant error was observed in the distal area, most probably because the simulation model was designed from a visually clear, large planar area in the distal end, while the IP measurement was based on the differentiation of a small area which was very precise. In addition, the limitation on the meshing mechanism which was restricted to 20,000 units elements also affected the volume measurement in the FEA model. Furthermore, the boundary condition in the simulation reflected the result whereby most of the body weights of the subjects were located at the top parts of the residuum at which the force was not well distributed within the distal area because the soft tissue material had a high elasticity and density. As a result, the deformation in the distal area was not significant compared to the deformation in the proximal area.

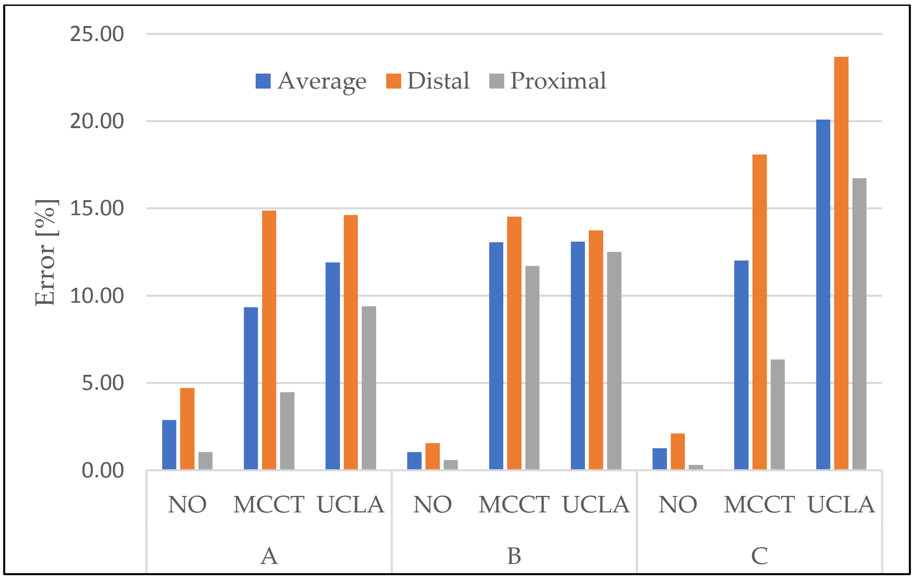

Figure 6.12. Comparisons of average errors of IP–FEA for every tested model within the average, distal and proximal areas.

The graphical comparison between the FEA model and the actual MR images of the residuum is shown in Figure 6.13. The comparison is discussed in two parts and includes the position on the bone and the geometrical structure of the soft tissue. From the results, we can confirm that the FEA model was created at its actual inner position. Specifically, for subject A, the bone position was on the right side of the model, thus indicating that the residuum should be on the left. By contrast, for subjects B and C, the bone positions were on the left side, which indicates that the location of the residuum should be on the right side. After the complete penetration, the fat part of the FEA model tended to combine inside the muscle part owing to the fact that the density of the fat was lower compared to muscle. Correspondingly, this allowed the fat to deform easily compared to other tissues.

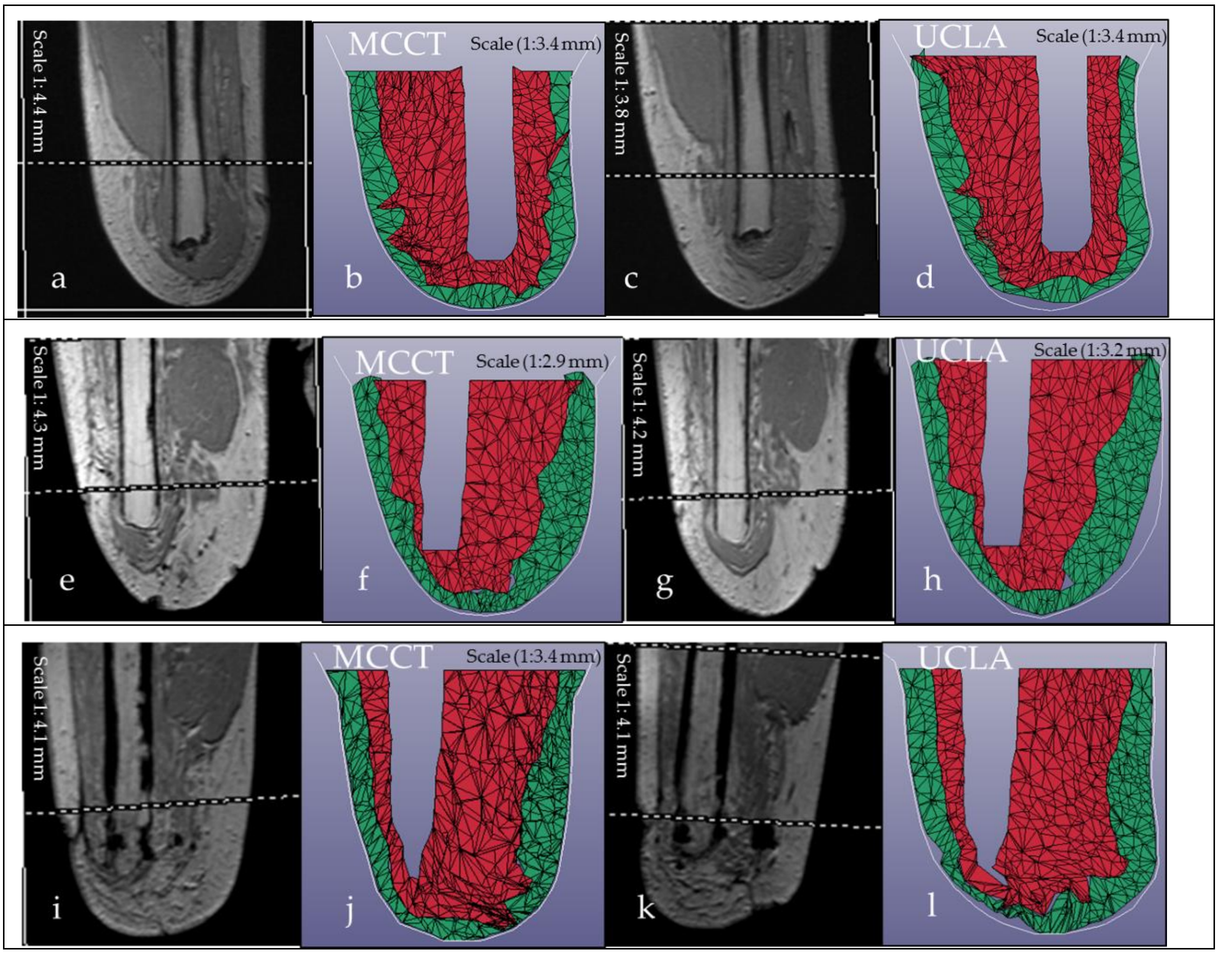

Figure 6.13 Graphical comparison of FEA model and MRI during complete donning. (a,c) MR images of the residuum for subject A in the (a) MCCT and (c) UCLA sockets. (b,d) FEA simulation results for subject A after the completion of donning inside the (b) MCCT and (d) UCLA socket. (e,g) MR images for the residuum of subject B in the (e) MCCT and (g) UCLA sockets. (f,h) FEA simulation results of subject B after the completion of donning inside the (f) MCCT and (h) UCLA sockets. (i,k) MR images for the residuum of subject C in the (i) MCCT and (k) UCLA socket. (j,l) FEA simulation results of subject C after the completion of donning inside the (j) MCCT and (l) UCLA sockets.

6.5 Summary of the Evaluation System

In this chapter, the overall qualitative evaluation of the MCCT and UCLA sockets was presented in terms of the effects of the socket on the residuum's geometrical changes. The results showed that the simulations and measurements for every subject exhibited considerable correlations and similarities. The FEM model created by the suggested method possessed various similarities with the real residuum.

The differences detected were attributed to post operation scarring and to some merged skin on the residuum that cannot be created by the meshing method in the 3D construction. The calculation of geometrical changes was completed based on the bipedal stance condition, which has been extensively used in previous studies [96,99]. The increased correlation of the FEA and IP pressure outcomes confirmed that the finite element pressure distribution was reliable and could support the research objective.

The study also showed the efficiency of the FEM model created by the proposed method as an evaluation tool for the socket before its fabrication with 3D printing. The system was initiated to help engineers and manufacturers undergo an evaluation procedure before the transfemoral socket was fabricated by the 3D printer. Even though the simulation ignored the relative movement between each part inside the residuum, the results are still promising because the deformation of the residuum depends on the fluid movement inside the soft tissue parts [103].

The system is low-cost and low-maintenance and has user friendly interfaces with an added value for prostheses and fabricators to run as an evaluation system. The system was also able to reduce the time consumption during the fitting sessions and the number of sessions required for each subject. According to the promising results of this study, the system can potentially serve as an alternative method to the evaluation of the prefabricated socket.

The use of the system and its capabilities is envisaged to allow the pursuit of numerous other research studies to evaluate the transfemoral socket and their uses for the determination of the level of deep-tissue injuries that occur inside the socket and in any other soft tissues of the human anatomy involved with the application of external forces.

Chapter 7

Conclusions and Future Works

7.1 Conclusions

An accurate three-dimensional (3D) is an important role in designing a subject-specific human model. There are many methods that's has been introduced in a past decade to accomplish the important task. However, when there is an alternative method, there also will pro and cons for those methodology. In this work, the author has proposed, develop and validate the method using combination of b-spline curve interpolation and finite element analysis (FEA) for analysing a dynamic function of transfemoral prosthesis. The author also has provided an alternative way to evaluate a transfemoral prosthesis socket for pre-fabrication process.

In the author perspective, finite element analysis is a very strong method for applications engineering. Especially, in design and simulate the product which relate to the human. Because, it is difficult to have experimented or test with subjects as a human. The best solution is designed and simulation with the support of computer (CAD-CAM-CAE technology). The utilization of commercialize software such as CREO etc. gave an opportunity for the general user to conduct or using the evaluation system.

The successful result of creating an MRI based 3D model of residuum and its socket shown that the calculation of b-spline interpolation inside CREO is reliable to imitate an actual model of transfemoral socket. The successfulness of creating the socket 3D model are depending on the spline curve point during the segmentation stage in a 3D model construction process. The low error measured during comparison with image processing (IP) volumetric value indicate that the quality of the created model can be accepted. By using the commercialize software such as CREO, the objective of this study was achieved which is developing the three-dimensional (3D) model of residuum with precise parameter of actual residuum where the model consist of multi-material properties includes: skin, fat, muscle and bone.

The interface pressure between socket and residual limb was computed by finite element method, the experiment was also conducted for confirming the results of simulation. The successful results of simulation shown that the finite element analysis is reliable enough for the evaluation shape of the socket. This means that, the prosthetist and the designer can use the results of the simulation for observing the behaviour of residual limb when it was put to the socket. The interface pressure generated on the surface between socket and residual limb can use to evaluate the quality of socket. The development of donning also utilizes the material properties of nearly similar to actual material of residuum. Event though the material is different, but the result gained was promising. By the development of the donning simulation, including interaction between socket and residuum, combination of multiple material properties and similar environment mimicking actual socket fitting session, the study has achieved the second objective which is designing a simulation mimicking an actual donning process to improve the evaluation fitting of transfemoral prosthesis socket in stance phase of gait.

Combining the accurate 3D model, suitable simulation environment and appropriate selection of material properties, the study has provided an alternative way to evaluate a pre-fabrication socket. The method is proposed to be used before the 3D printing prosthetic socket are created. This method helps to reduce the sequence of conventional socket manufacturing method by reducing the number of socket fitting session. In chapter 6, the overall process of the evaluation has been described and the outcome of the analysis showed good correlation between environment that was created in a simulation and an actual socket donning stage. The comparison of volume changes between simulation and image processing experiment also showed a promising correlation and very small error occurred between both of it. The objective of the study was achieved by creating an evaluating system for transfemoral prosthetic socket that created based on MRI data.

However, there are some limitations set cause the study conditions and devices. First, the experiment and MRI data that used in the study was only three subjects. Usually, with the larger number of subjects, the results of the experiment will be more valuable and more reliable with a good standard of variation. Furthermore, the data of subject with a classified age, sex, amputation levels and so on will help the results study more detail and accuracy. Second, the study only considers the movement of the transfemoral prosthesis in sagittal plane. The forces appeared on hip and knee joint, ground reaction forces, the moment is inadequate all directions. Third, the ischial zone in the socket was ignored in the study due to limitation of the MRI data of the subject.

7.2 Future Work

The study has given a new dimension to create a 3D model based on MRI data and an evaluation system for the transfemoral prosthetic socket geometry was presented. Even though the validation, analysis and evaluation done in the study achieved a promising result, there are several works can be done in the future as opportunity for improvement.

First, the model created in study utilize an MRI data of subject starting from distal end until the residuum reached 180 mm of height. It considered a minimum requirement of the study since the height of attached triaxial force sensor was measured 180 mm toward distal ends. As an opportunity of improvement, it is suggested to increase the height of residuum model and consider to adding a pelvis bone model in the simulation. It is because, by adding the height residuum model and socket, the analysis of pressure in proximal area can be measured and the behaviour of residuum that not interact with socket also can be observed. Furthermore, by adding the pelvis bone structure in the simulation, the pressure that developed in ischial zone of the socket can be measured and analysed. The analysis of the ischial zone pressure can enhance the evaluation of transfemoral prosthetic socket function.

Second, material properties used in the study are based on the other studies that's related to the environment of donning process. Its recommended to utilize the subject-specific material properties. The subject-specific database is more likely depending on actual age, gender and amputee condition during the experiment. The experiment for evaluating the soft tissue material need to conduct. The range of parameters of soft tissue material is long and difficult to choose the comfortable value. By the experiment for human soft tissue, the value of material properties will confirm, and the input parameters of finite analysis will approach with the real value.

Third, the number of subjects is recommended to be increased. The larger number of subjects increase the number of analysis and the statistical analysis can be more accurate and reliable.

Fourth, parametric optimization analysis was considered as a future work for this study. The optimization analysis consists of optimizing the parameter such as, material properties, socket velocity etc. to enhance the possible result in the simulation. The analysis should be done by considering the current numerical setup in the simulation is well tuned.

Fifth, the analysis the dynamics of transfemoral prosthesis in the gait cycle was considered as a future work. The result of the analysis is valuable and useful for the designer and health supporter. The analysis is recommended by considering some of the factor such ass, the quantity of subject, the detail of the knee joint and the utilization of full model of human model. It is because:

- The more quantity of subject with classified of type as age, sex, amputation levels will help the data of study more valuable and reliable. The data of patient are very different with individual cases. By classifying the patient into groups, the data are easy to evaluate and get the helpful conclusions.
- The knee joint need to describe in fully model, include joint properties. The fully model of knee joint helps the movement of the transfemoral prosthesis more reality and get the accuracy results. Furthermore, the dynamics of the knee joint can be disclosed for the calculation and optimization the knee joint.
- The full model of the human body which include all parts of the human body are intact limb, upper limb, head and chest abdomen. By using all human body parts in computation, almost the parameters which were considered in the design and optimization the structure of the transfemoral prosthesis can be disclosed by simulation.

7.2.1 Transfemoral Prosthetic Gait Cycle Simulation Proposal

A dynamic analysis of walking simulation or gait cycle for amputee subject is an important element in order to investigate the pressure distribution inside socket during the gait. Moreover, the pressure distribution contributes a better understanding of the behaviour of a fat and a muscle during the walking. A person with a transfemoral amputation must compensate for the loss of both the knee and ankle joint [104]. The gait cycle is affected by the quality of the surgery, the type and alignment of prosthesis, the condition of the stump and the length of the remaining muscular structure and how well these are reattached [105]. The main focus of the gait cycle is to prevent the knee from buckling during stance phase. A fixed knee prosthesis will counteract this issue. A free knee will need to remain in extension for longer throughout the stance phase approx. 30-40% to ensure buckling does not occur. This extension causes prolonged heel strike and the body will move forward over the prosthetic leg as one unit for stance phase. The hip extensors on the prosthetic side will work to stabilise the limb in During swing phase of the prosthetic limb the hip extensors and calf muscles on the non-prosthetic side help to generate force for the non-prosthetic limb to gain swing forwards. Hip flexors on the prosthetic limb must generate the same force required during normal gait.

7.2.1.1 Kinematic Gait Analysis

There are several types of method to analyse the human gait. The Mac3D motion caption for example is widely used in the lab scale to analyse the gait. The system consists of six to twelve cameras that will be used to record all the movement of a marker that attached in human body. Then the recorded data will be connected to each other depending on the movement of the human and where the marker was located. The system can generate three-dimensional (3D) coordinate where it enables the user to analysis the movement in various angle and positions.

Figure 7.1 Subject with a marker in the Mac3D motion capture system

In this proposal, a low-cost method has been introduced to analyse the gait where open source software was introduced to calculate the coordinate of the walking gait in two-dimensional (2D) environment. Kinovea software is an open source software used by the researcher to analyse the movement of a human especially in sport field. Kinovea software is a video analysis, which is a free software application for the analysis, comparison and evaluation of sports and training, especially suitable for physical education teachers and coaches. Some advantages of this software are: observation, measurement, comparison of videos, etc. This software also can perform the analysis without use physical sensors or by means reflective markers and it is uncomplicated to use. The overview function is a summary image of the video. It creates a composite picture where you can see the motion at a glance by sample images from the video at regular interval.

For this study, a video of walking for subject has been analyse. The subject in this study was a woman with a right-side trans-femoral amputation. She was aged 35, 167 cm in height, and weighed 61 kg without her prosthesis. Her prosthesis incorporated a MCCT socket, a Nabco prosthesis, and an Ottobock foot. The video of walking will be analysed by repetitively marking every joint movement of the prosthetic leg. The movement will be marked every 0.03 second per frame. The distance of x and y axis will be recorded for every joint and coordinate system for the movement will be created base on the distance of x and y axis for every joint. Based on the coordinate system, a joint angle will be calculated by using equation 7.1 below to determine the joint parameter for the simulation.

$$\theta = tan^{-1}\left(\frac{x_{i+1} - x_i}{y_{i+1} - y_i}\right) \qquad (7.1)$$

where x is an x axis coordinate in the system, y is a y axis coordinate in the system and i is a number of a frame.

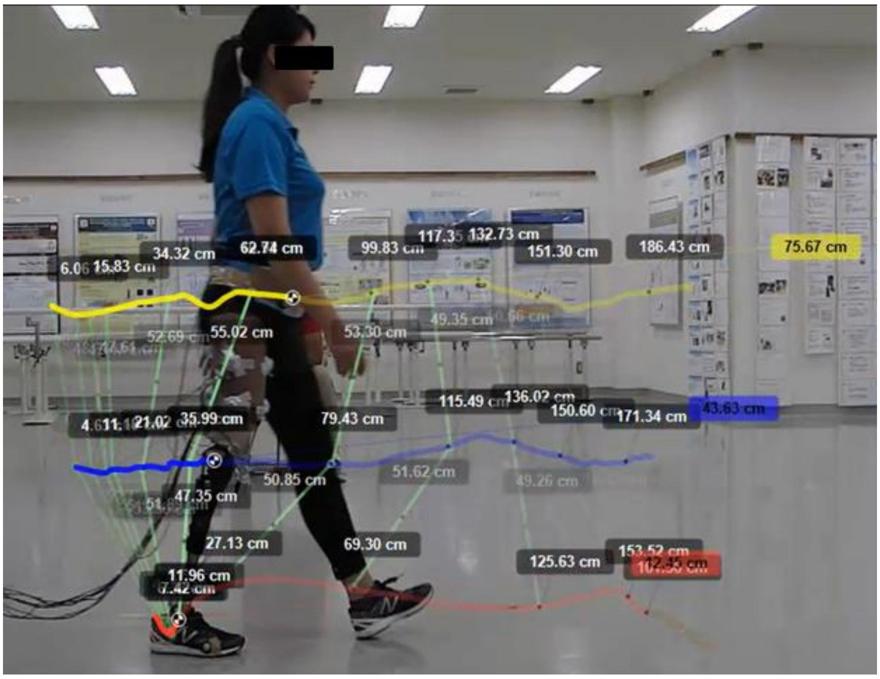

Figure 7.2 video analysis in the Kinovea software.

Based on the video analysis, the coordinate data was recorded and converted to CSV file. The file will be rearranged in the Excel software to determine the necessary parameter for the simulation.

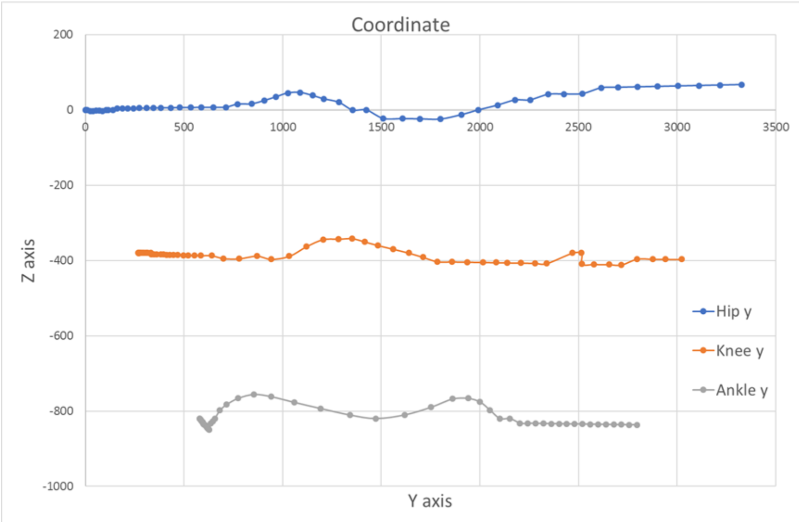

Figure 7.3 coordinate system based on the video analysis

The angle of every joint movement can be calculated based on the coordinate system. The joint angle was determined to observe the rotation movement occur in every joint. The joint can be utilized in the future research where when replacing the knee joint with an automated motorized knee joint mechanism, the torque of the motor can be calculate based on the angle joint generated.

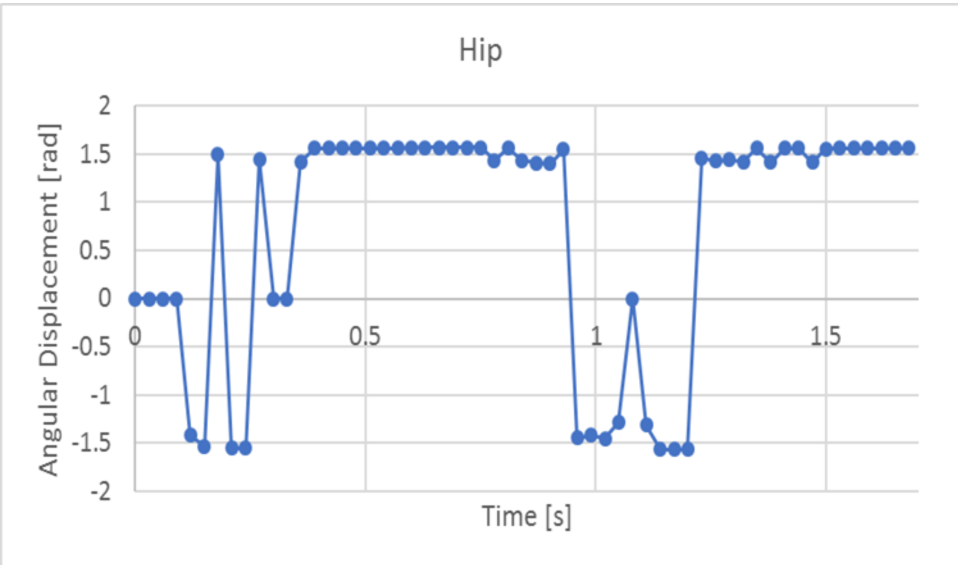

Figure 7.3 Joint angle of a hip during walking gait

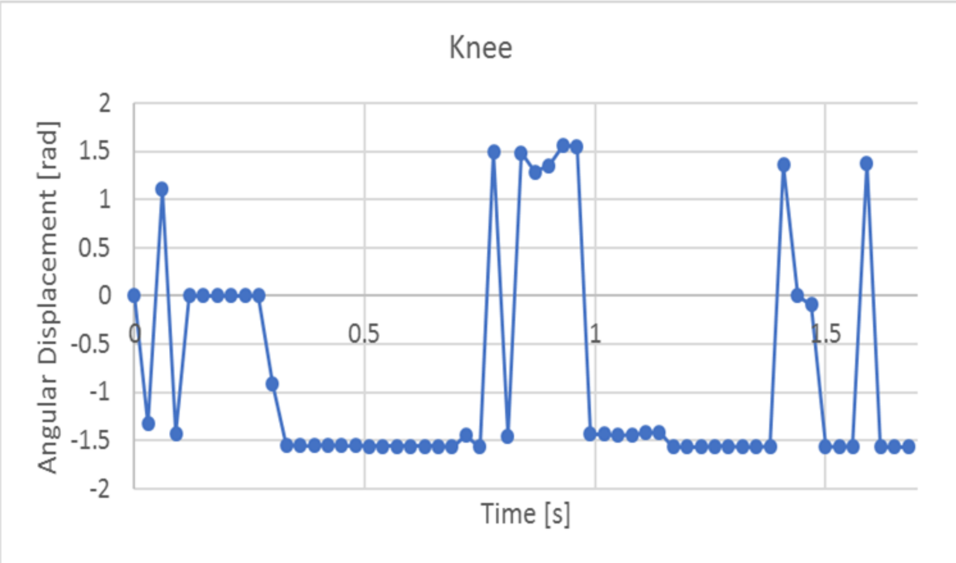

Figure 7.4 Joint angle of a knee during walking gait

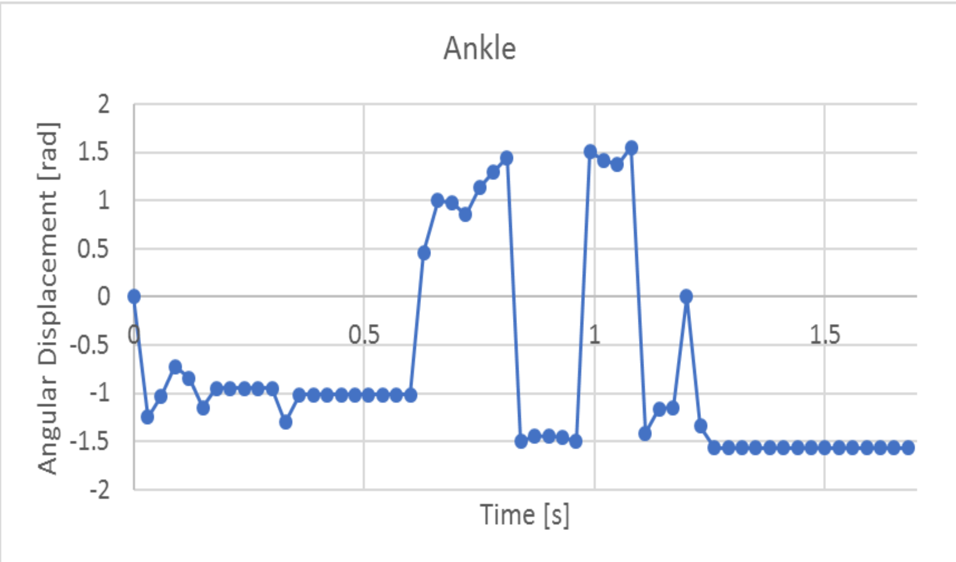

Figure 7.5 Joint angle of an ankle during walking gait

However, the simulation generated by the LS-DYNA software, the joint angle cannot be defined since the joint was created by combining the fixed node and moveable node and there is no specific parameter in the software to define the angle of stand-alone node. Therefore, in order to utilize the angle joint in the LS-DYNA software, the movement of the link that connected two joint has to be calculated. In this case, there are two link that connected the three joints. There are, hip to knee link and knee to ankle/feet link. The movement of the link can be defined in the LS-DYNA software and also can be calculated by measuring the joint angle between two joints simultaneously. The equation 7.2 was used to calculate the movement of the link.

$$\theta = tan^{-1}\left(\frac{x_a - x_b}{y_a - y_b}\right) \tag{7.1}$$

where x_a, x_b, y_a and y_b is an x coordinate for the first joint, an x coordinate for second joint, a y coordinate for first joint and a y coordinate for the second joint respectively.

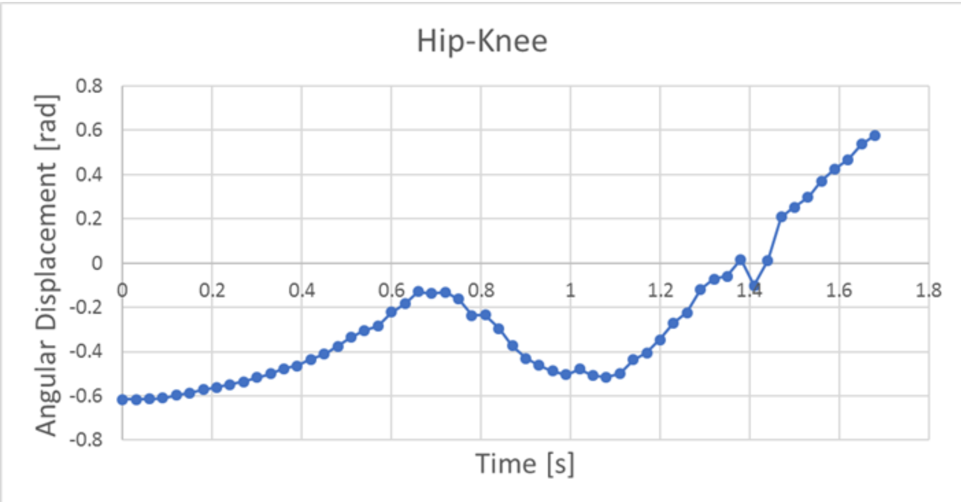

Figure 7.6 Angular displacement of the hip-knee link

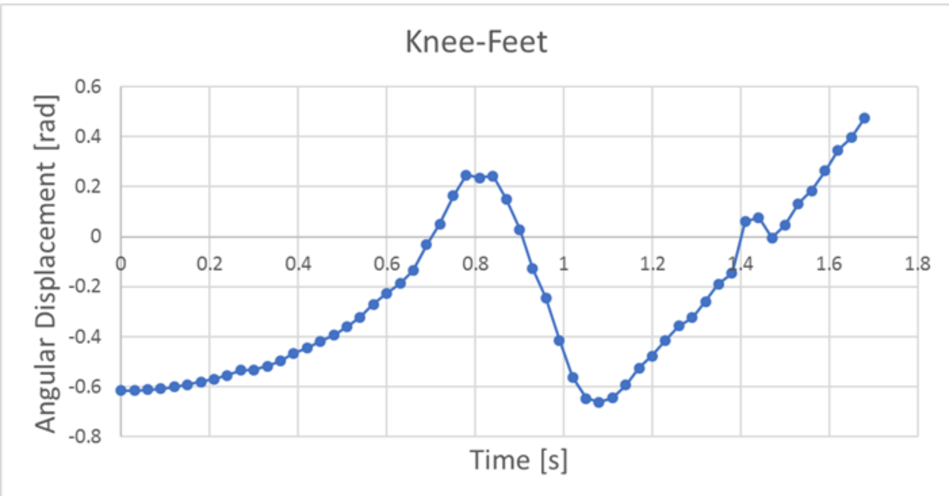

Figure 7.7 Angular displacement of the knee-feet link

Based on the calculated angular displacement, the simulation of gait will be conducted. The model use in the simulation will be explained in the next sub chapter of the proposal. By combining the video analysis method and gait simulation, the pressure distribution inside the socket during walking can be excess. Furthermore, the shear stress distribution can be observed. Ground force reaction for the prosthesis patient can be predict and the behaviour of the walking prosthetic can be observed. In the nutshell, simulation of gait gave huge amount of understanding to investigate the probability to improve the design of the socket and to evaluate the current socket design for the future references.

7.2.1.2 Gait Simulation Analysis through Finite Element Method

The residual limb with prosthesis was modelled as the structure with two revolute joints at hip and knee joint. The angle rotation at hip and knee joint around x-axis were defined on Figure 7.8. Magnetic resonance imaging (MRI) was used to obtain images of the residual limb with the socket prosthesis. The patient wore the socket prosthesis during the MRI. The residual limb with socket prosthesis was captured using 17 images with 10 mm separation perpendicular to the sagittal plane. Subsequently, the three-dimensional (3D) surfaces of bone and soft tissue were obtained. The MRI data were loaded as a 3D stack, contours were manually drawn in each slice, and lofted into a 3D body structure using a solid modelling software (PTC Creo Parametric). The model of the socket was offset from the surface of the residual limb within the socket. The model of the parts of the prosthesis were measured, and subsequently manufactured in real size dimensions using CAD software. After the modelling, all parts were imported to LS-Prepost Software for meshing.

The model consists of thirteen parts which are beam, bone, muscle tissue, fat tissue, socket, socket holder, knee joint, shank, frame, wood feet, outsole shoes and floor. Every part possessed different material specification and number of elements. The number of elements in this simulation was restricted to 30000 elements due to agreement in the licenses purchasing. Even though there is a limitation of element number in the simulation, the element was sufficient to complete the model design with high accuracy.

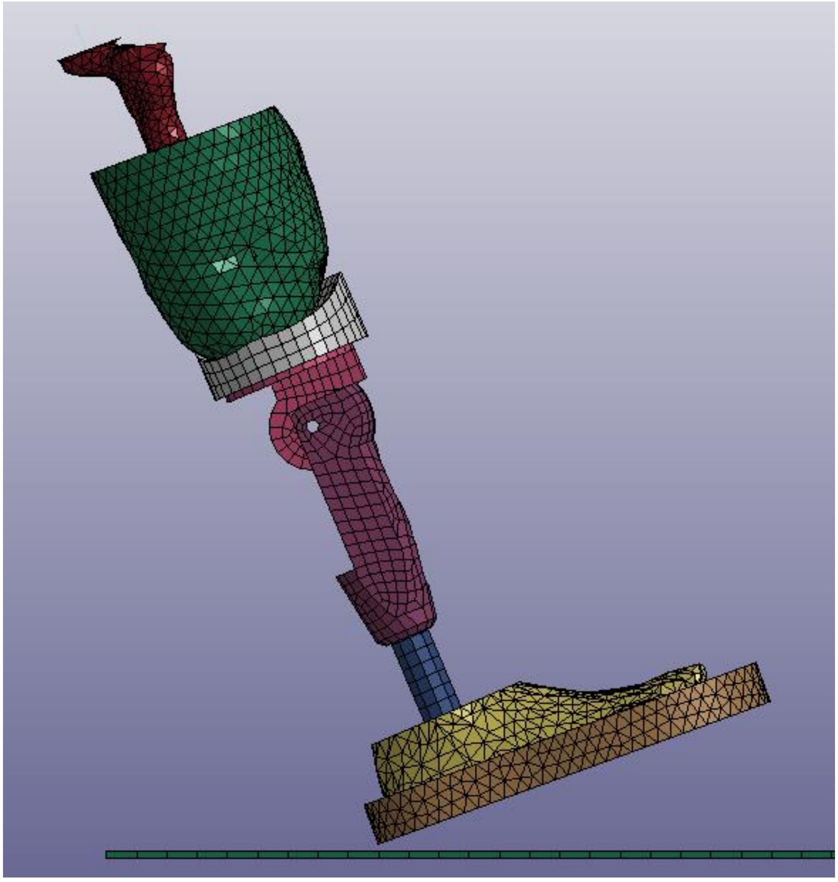

Figure 7.8 right amputee knee model for gait simulation in LS-Prepost environment.

In this proposal, the movement of the model is based on the movement from video analysis. The cooperation between video analysis and simulation has widely used in research field and the result was promising. Table 7.1 shows the material properties for entire model and table 7.2 shows the number of elements used in the simulation.

Table 7.1 Material properties

Name	Material	Density (Ton/mm^3)	Young Modulus (MPa)	Poisson ratio
Soft tissue	Soft tissue	1.00E-09	0.06	0.45
Socket	Acrylic	1.18E-09	1886	0.39
Wood circle	Wood	5.00E-10	1.00E+04	0.4
Knee circle	Steel	7.80E-09	2.10E+05	0.29
Bone	Bone	1.75E-09	17700	0.3
Wood feet	Wood	5.00E-10	1.00E+04	0.4
Feet	Polyurethane	1.20E-09	25	0.5
Frame	Steel	7.80E-09	2.10E+05	0.29

Shank	Aluminum	2.70E-09	7.00E+04	0.34

Table 7.2 Finite Element properties of the model

Name	Element	Number of nodes	Number of elements	Element
Fat Tissue	Elastic Solid	1632	6212	13
Muscle	Elastic Solid	1436	6312	13
Socket	Rigid Shell	598	1154	13
Wood circle	Rigid Solid	728	489	1
Knee	Rigid Solid	580	328	1
Bone	Rigid solid	121	271	13
Wood	Rigid solid	497	348	13
Feet	Elastic solid	941	2983	13
Frame	Rigid shell	460	388	16
Shank	Rigid shell	150	140	16
Outsole	Elastic Solid	1119	3291	13

In the simulation, an environment or also known as boundary condition need to be defined in order to realize the connection between the simulation and the experiment. One of the boundary conditions is a contact between parts. Two contact conditions were defined in the current FE model to perform nonlinear analyses. The first contact definition was a surface-to-surface contact between the feet and the floor. Generally, the stiffer and more rigid surface of the contact pair is defined as the master surface, while the deformable surface with softer material is selected as the slave surface. Hence, the outer surface of the feet was defined as the slave surface, and the sockets inner surface was defined as the master surface. The contact definition requires that the slave surface conforms to the master surface. Therefore, it is recommended that a finer mesh is applied over the slave surface and a coarser mesh over the master surface. A coefficient of friction equal to unity was assigned to model the interaction property for the contact surfaces and limit the relative sliding between the feet and the floor. The second contact definition applied a tie contact between the tissue and the socket. It provided a simple way to couple the tissue and the surface of the socket together permanently, which prevented nodes from separating or sliding relative to each other. The connection between the muscle and the bone was the set of the constrained extra nodes. The inner face of the muscle was constrained by the bone to limit all the degrees of motion between muscle and bone.

Finally, an equivalent load of 61 kg was applied on the hip joint. It is described as the human body weight. The analysis was carried out during one gait cycle that spanned a total time duration of 1.2 s. The starting time of the gait cycle is the time at which the heel strikes the floor, and the end-time is at the next heel strike. A finite element (FE) model was developed and solved using the nonlinear dynamic explicit method in LS-DYNA.

7.2.1.3 Expected Outcome

The complete simulation will gave the same movement in the walking video. The simulation will start from heels striking the floor and terminate when toe off out from the floor. By the gait simulation, the ground reaction force of the prosthetic leg can be predicted. The user has an ability to access the prediction easier. The simulation gave an opportunity for the prostheses to examine the socket or other prosthetic part in different condition such as, material differences, knee joint stiffness etc.

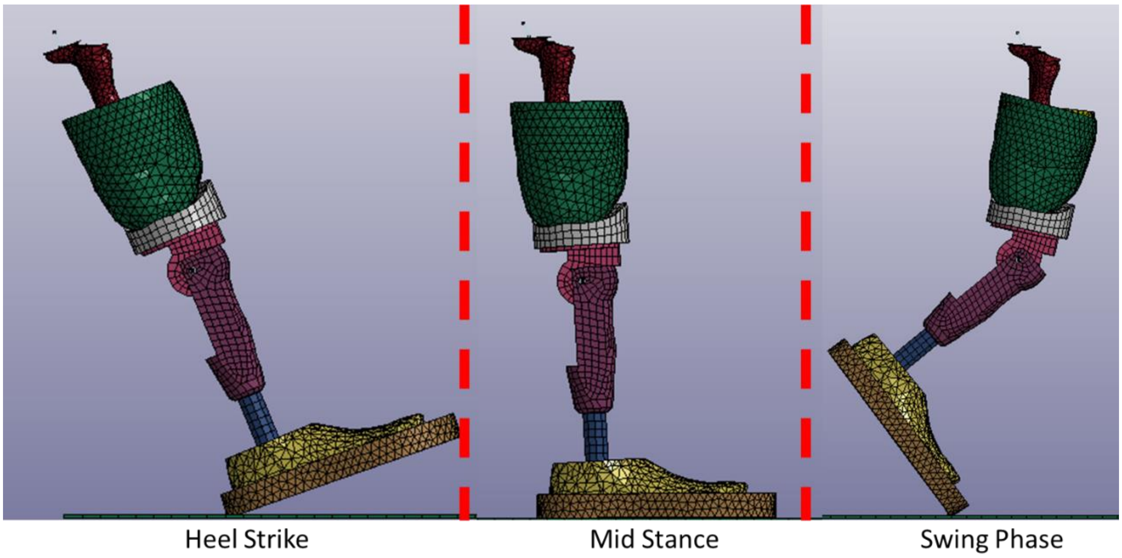

Figure 7.9 The complete simulation phase

Figure 7.10 shows the pressure distribution collected from the under heel in a outsole shoes surface. The pressure measurement taken from the entire shoes surface that contacted with the floor. Then the average pressure was calculated by divided it with the number of elements located in the surface.

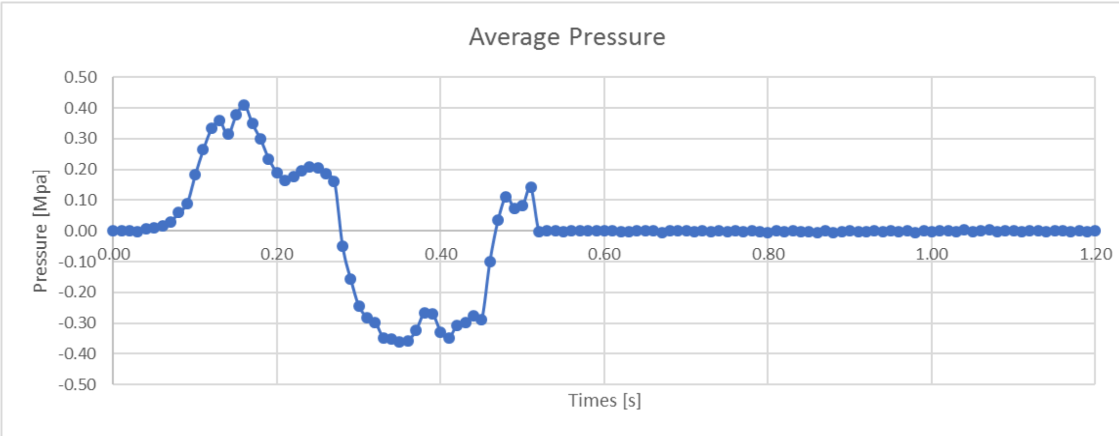

Figure 7.10 Average pressure distribution in an outsole surface during gait walking

Then the simulation also able to measure the force acting on the floor and the shoes. The measured force can be consider as a ground reaction force (GRF) of the prosthetic legs. GRF is a critical measurement used in the rehabilitation process. By measuring the GRF, the prostheses can able to adjust or improve the direction of the socket during attaching it to the socket holder. By determining the GRF, the rehabilitation for the walking posture can be done by investigating it with the simulation

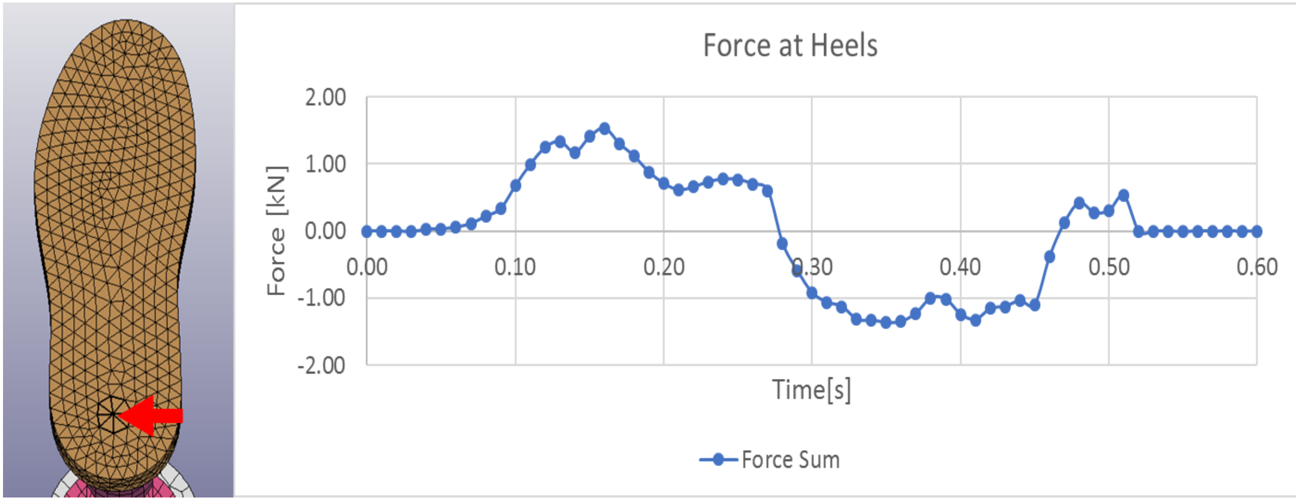

Figure 7.11 Sum of the force under the heel at the shoes surface

Finally, the proposed simulation can determine the pressure distribution inside the socket during walking gait. The pressure distribution inside the socket is an important measurement to validate the comfortability during wearing the socket and also an important parameter in selecting the liner used by the subject. Figure 7.12 onwards shows the pressure distribution measurement in eight location specifically in the socket.

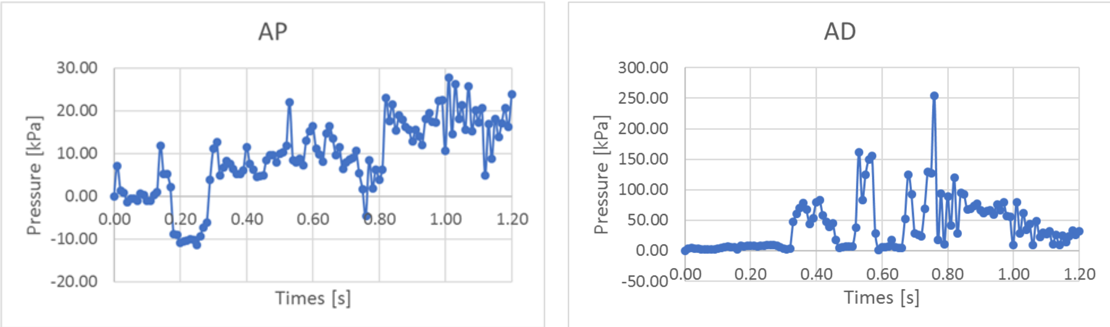

Figure 7.12 Pressure Distribution in anterior view

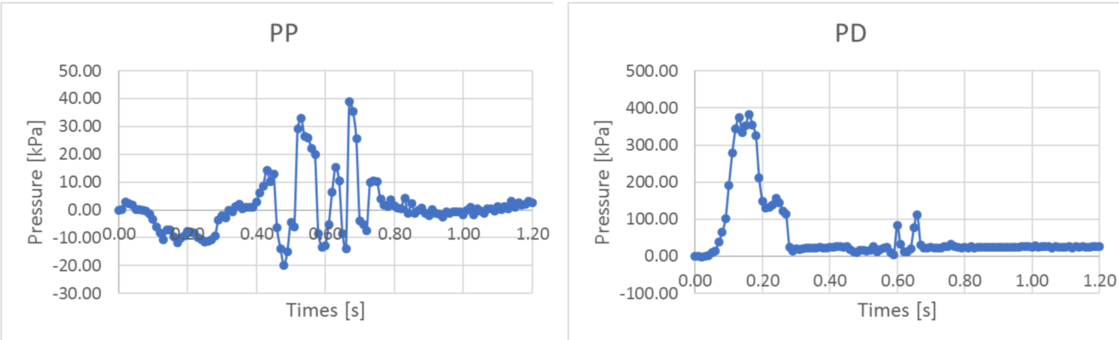

Figure 7.13 Pressure distribution in posterior view

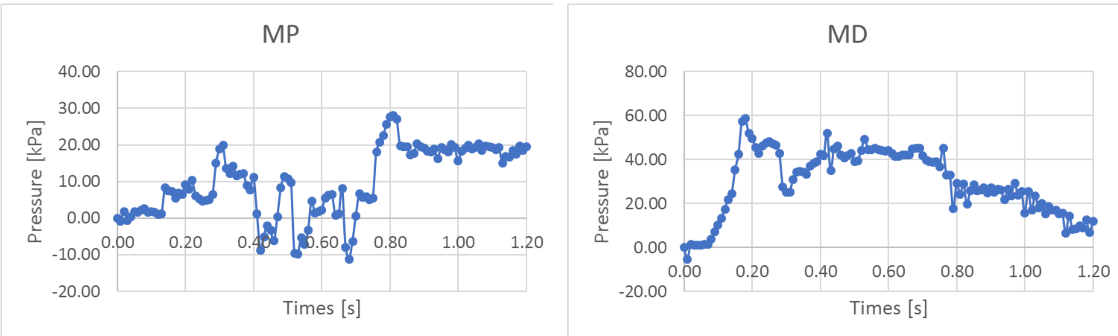

Figure 7.14 Pressure distribution in medial view

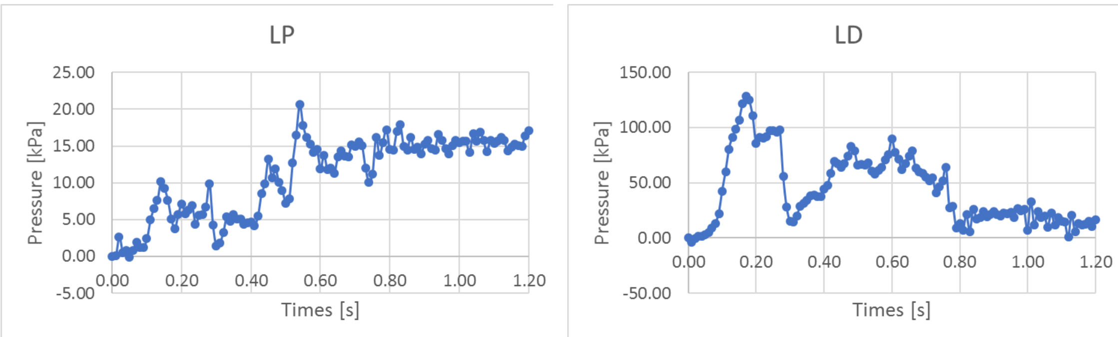

Figure 7.15 Pressure distribution in lateral view

As for the summary, the video analysis method is a reliable method to investigate the movement of walking for transfemoral prosthesis subject. The method can be used to calculate the necessary parameter required from the LS-DYNA software to generate the walking simulation. The simulation generated based on the motion analysis can be used to predict or measure the required outcome such as pressure distribution, GRF, shear stress, strain and resultant force occurred during the walking gait. As for the future work, the collected data will be compared with the experiment data to validate the accuracy of the measurement.

If the future work mentioned above are fully utilized, the desired result is obtained, the finite element analysis of evaluation function of the transfemoral prosthesis will be effective for many applications not only in bio-medical field. The prosthetist and designer will have a convenient and flexible tool for their work with the existence of the evaluation system. The patient will reduce the time for the comfort of the prosthesis and rehabilitation program.

7.3 Contribution of The Research

In the nutshell, the objective of the research has been accomplished. The research has proposed an evaluation system of transfemoral prosthetic socket by combining qualitative and quantitative analysis. The system was proposed to be use before the socket was fabricated. The contribution of the research can be seen in two main parts which are time and user friendly interface.

The evaluation system enables the entire time of producing the socket reduced. It is because, the implementation of the evaluation system before the socket fabricated help the engineer to bypass or reducing the fitting session time. The system gave a better understanding in creating the socket especially before it being fabricated. The system enables the socket being fabricated according the subject desire that based on the pressure analysis. The pressure analysis that been conducted in the research can be one of the measurements during pain assessment of the subject. The pressure analysis can be compared with the pain survey conducted to subject. With the comparison of the pain feeling and the pressure distribution, a relationship between them can be understand further.

Finally, the creation of 3D model based on the MRI data is a method that beneficial to prostheses and engineer. It is because it is a low-cost method with high accuracy. By using the MRI data only, prostheses able to create the 3D model mimicking the actual residuum. The model can be used to create a positive mould in the process of socket fabrication.

References

[1] A. Bennett Wilson Jr., B.S.M.E. `History of Amputation Surgery and Prosthetics`, Atlas of Limb Prosthetics: Surgical, Prosthetic, and Rehabilitation Principles, Chapter 1 http://www.oandplibrary.org/alp/chap01-01.asp

[2] Owings M, Kozak LJ, Hyattsville, Md;U.S. Dept. of Health and Human Services, Centers for Disease Control and Prevention, National Center for Health Statistics, 1998.

[3] Ephraim PL Travison TG Brookmeyer R Ziegler Graham K, MacKenzie EJ. Estimating the prevalence of limb loss in the united states: 2005 to 2050. Archives of Physical Medicine and Rehabilitation, 89(3):4229, 2008.

[4] https://www8.cao.go.jp/shougai/english/annualreport/2016/index-pdf.html

[5] Sawamura S,Tokyo: Ishiyaku Publisher, 2007; 116. [Japanese].

[6] Takechi H Nagashima H, Inoue H. Incidence and prognosis of dysvas- cular amputations in okayama prefecture [japanese]. Prosthet Orthot Int, 17:913, 1993.

[7] Kawamura J Hayashi Y, Mori Y. Epidemiological study on the lower limb amputees [japanese]. Jpn Soc Prothet Orthot, 15(1999):163170, 1999.

[8] Cabinet Office, Government of Japan. Available from www.esri.cao.go.jp (cited in May 2010).

[9] Kitakyusyu City Government, Available from www.city.kitakyushu.jp (cited in May 2010).

[10] World Health Organization. Guidelines for training personnel in developing countries for prosthetics and orthotics services. Geneva; 2005.

[11] Malaysia Statistics Department. Population clock. (cited 2017 February 12). Available from https://www.statistics.gov.my

[12] Mafauzy M. Diabetes mellitus in Malaysia. Med J Malaysia. 2006;61(4):397–398.

[13] Resnick HE, Valsania P, Phillips CL. Diabetes mellitus and nontraumatic lower extremity amputation in black and white Americans: the national health and nutrition examination survey epidemiologic follow-up study, 1971–1992. Arch Intern Med. 1999;159(20):2470–2475. https://doi.org/10.1001/archinte.159.20.2470

[14] Karel B, Ali F, William VH, Riley P. Time to act. The Netherlands: International Diabetes Federation and International Working Group of the Diabetic Foot; 2005.

[15] Arifin N, Hasbollah HR, Hanafi MH, Ibrahim AH, Wan Abdul Rahman WA, Che Aziz R. Provision of prosthetic services following lower limb amputation in Malaysia. Malays J Med Sci. 2017;24(5):106–111. https://doi.org/10.21315/mjms2017.24.5.12

[16] Boulton A. The diabetic foot: epidemiology, risk factors, and the status of care. Diabetes Voice, 50(SI):5–7, 2005.

[17] Omar Z: Orthotics & prosthetics: local technology and social service in Malaysia. ISPO An Asian Prosthetics and Orthotics Workshop Japan Final Report, 1998.

[18] National Amputee Statistical Database (NASDAB). Edinburgh: NASDAB, 2005. Available from URL: http://www.nasdab.co.uk.

[19] D. Beard and P. A. Gaines. Second edition. BJS 2002; 89: 249-249

[20] Radcliffe CW. Functional consideration in the fitting of above knee prostheses. In: Artificial Limbs. New York: Kringer; 1970: 35-60

[21] Gottschalk FA, Kourosh S, et. al. oes socket configuration influence the position of the femur in above-knee amputation? Journal Prosthetic Orthotic 1987; Vol. 2,94-102

[22] King C. Modern research and the forgotten prosthetic history of the Vietnam war. J Rehabil Res Dev. 2009; 46(9): xi-xxxvi.

[23] https://www.medicaldesignbriefs.com/component/content/article/mdb/features/articles/20250

[24] Van de Meent H Frlke JP. The endo-exo prosthesis for patients with a problematic amputation stump. Ned Tijdschr Geneeskd, 154(A2010), 2010.

[25] E.C. Martinez-Villalpando and H. Herr. Agonist-antagonist active knee prosthesis a preliminary study in level-ground walking. Journal of Rehabilitation Research and Development, 46(3):361374, 2009

[26] Klaus-Jurgen Bathe "Finite Element Procedures", Massachusetts Institute of Technology, Prentice Hall, Pearson Education Inc. 2nd edition ,2014.

[27] LS-DYNA Keyword User Manual, Vol.1, version 7.1, February 2013

[28] Ngon Dang Thien, Giang Nguyen Truong "An Approach to Design a Globoid CAM Using CREO Parametric 3.0" in 2016 3rd International Conference on Green Technology and Sustainable Development pp.200-205 (2016)

[29] Giorgio Colombo et al. "Automatic 3D Reconstruction of Transfemoral Residual Limb from MRI Images" in DHM/HCII 2013, Part II, LNCS 8026,2013, pp. 324–332

[30] Arun Dayal Udai, Amarendra Nath Sinha "Processing Magnetic Resonance Image for CAD Model development of Prosthetic Limbs Socket" in IEEE Region 10 Colloqium and the Third ICIIS, paper Id. No. 70, 2008,

[31] Damien Lacroix and Juan Fernaldo Ramirez Patino. Finite element analysis of donning procedure of a prosthetic transfemoral socket. Annals of Bioengineering, 39-12:2972-2983, December 2011.

[32] Roberts V C Zhang M, Makaft. Finite element modeling of a residual lower-limb in a prosthetic socket: A survey of the development in the first decade. Med Eng Phys, 20:360273,1998.

[33] Ming Zhang;Winson C. C. Lee. Quantifying the regional load-bearing ability of trans-tibial stumps. Prosthet Orthot Int, 30-1:25-34, April 2006.

[34] Ling Shen Feng Zheng Linlin Zhang, Ming Zhu. Finite element analysis of the contact interface between trans-femoral stump and prosthetic socket. Conf Proc IEEE Eng Med Biol Soc, 2013:1270-3, 2013.

[35] N. Shabshin, S. Portnoy, Z. Yizhar. Internal mechanical conditions in the soft tissues of a residual limb of a trans-tibial amputee. Journal of Biomechanics, 41(9):1897-1909, 2008.

[36] N. Shabshinc A. Kristalb Z. Yizhard A. Gefena S. Portnoy, I.Siev-Nerb. Patient-specific analyses of deep tissue loads post transtibial amputation in residual limbs of multiple prosthetic users. Journal of Biomechanics, 42(16):26862693, December 2009.

[37] S. Barbara and S. C. Dudley. Generic geometric finite element analysis of the transtibial residual limb and the prosthetic socket. Journal of rehabilitation research and development, 32:171–186, 1997.

[38] Boone D A Mak A FT, Zhang M. State-of-the-art research in lower-limb prosthetic biomechanics socket interface. J Rehabil Res Dev, 38:161174, 2001.

[39] Childress D S Silver-Thorn M B, Steege J W. A review of prosthetic interface stress investigations. J Rehabil. Res Dev, 33:253266, 1996.

[40] Sanders J E Zachariah S G. Interface mechanics in lower-limb external prosthetics: A review of finite element models. IEEE Trans Rehabil Eng., 4:288302, 1996.

[41] Roberts V C Zhang M, Makaft. Finite element modeling of a residual lower-limb in a prosthetic socket: A survey of the development in the first decade. Med Eng Phys, 20:360273, 1998.

[42] Sengeh, David M., et al. "Multi-material 3-D viscoelastic model of a transtibial residuum from in-vivo indentation and MRI data." Journal of the mechanical behaviour of biomedical materials 59 (2016): 379-392.

[43] Portnoy, S., et al. "Real-time patient-specific finite element analysis of internal stresses in the soft tissues of a residual limb: a new tool for prosthetic fitting." Annals of biomedical engineering 35.1 (2007): 120-135.

[44] Mehta B. V, Rajani S., Sinha G., “Comparison of image processing techniques (magnetic resonance imaging, computed tomography scan and

ultrasound) for 3D modeling and analysis of the human bones", Int.J. Digit Imaging, Vol. 10(3 Suppl 1), pp. 203-206, Aug. 1997.

[45] Chambers S, Cooney A, Caplan N, Dowen D, Kader D." The accuracy of magnetic resonance imaging (MRI) in detecting meniscal pathology" in J R Nav Med Serv. 2014;100(2):157-60.2014

[46] Creo, PTC Inc, www.ptc-jp.com/cad/creo

[47] Aziguli Wulamu, GOETTING Marc et al. "Approximation of NURBS Curves and Surfaces Using Adaptive Equidistant Parameterization" in Tsinghua Science and Technology, ISSN 1007-0214 07/21 Vol.10, No.3, pp 316-322, 2005.

[48] Roberts V C Zhang M, Makaft. Finite element modeling of a residual lower-limb in a prosthetic socket: A survey of the development in the first decade. Med Eng Phys, 20:360273,1998.

[49] Ming Zhang;Winson C. C. Lee. Quantifying the regional load-bearing ability of trans-tibial stumps. Prosthet Orthot Int, 30-1:25-34, April 2006.

[50] Damien Lacroix and Juan Fernaldo Ramirez Patino. Finite element analysis of donning procedure of a prosthetic transfemoral socket. Annals of Bioengineering, 39-12:2972?2983, December 2011.

[51] Ling Shen Feng Zheng Linlin Zhang, Ming Zhu. Finite element analysis of the contact interface between trans-femoral stump and prosthetic socket. Conf Proc IEEE Eng Med Biol Soc, 2013:1270-3, 2013.

[52] N. Shabshin, S. Portnoy, Z. Yizhar. Internal mechanical conditions in the soft tissues of a residual limb of a trans-tibial amputee. Journal of Biomechanics, 41(9):1897-1909, 2008.

[53] N. Shabshinc A. Kristalb Z. Yizhard A. Gefena S. Portnoy, I.Siev-Nerb. Patient-specific analyses of deep tissue loads post transtibial amputation in residual limbs of multiple prosthetic users. Journal of Biomechanics, 42(16):26862693, December 2009.

[54] L.V. Tuan et al.,Finite Element Analysis for Quantitative Evaluation of a Transfemoral Prosthesis Socket for Standing Posture, International Journal of Computer Applications (0975-8887), Vol. 170, No. 1, 2017

[55] M.S.Jamaludin, Akihiko Hanafusa "Accuracy Evaluation of 3D Reconstruction of Transfemoral Residual Limb Model Using Basic Spline Interpolation", IFMBE Proceedings, Vol. 68,No.2,pp 675-680,2017

[56] A. Ramos, J.A. Sim`oes "Tetrahedral versus hexahedral finite elements in numerical modelling of the proximal femur",Medical Engineering & Physics 28 (2006) 916?924,2006

[57] Roberts V C Zhang M, Makaft. Finite element modeling of a residual lower-limb in a prosthetic socket: A survey of the development in the first decade. Med Eng Phys, 20:360273,1998.

[58] C. C. Winson and M. Z. Lee. Design of monolimb using finite element modelling and statistics-based taguchi method. Clinical Biomechanics, 20:759?766, 2005.

[59] Fung YC. "Elasticity of soft tissue in simple elongation." Am J Physiol, 213:1532?1544.

[60] NETTA Corporation RETS Division Sensor Group. Capacitive three axis force sensor. PFS series. PD 3-32 User’s manual. NETTA Corporation, 2015.

[61] Mak M. Zhang and W. C. Lee. Regional differences in pain threshold and tolerance of the residual limb: including the effects of age and interface material. Archives of Physical Medicine Rehabilitation, 86:641–649, 2005.

[62] M. Zhang, M. Lord, A.R. Turner-Smith, V.C. Robert `Development of a non-linear finite element modelling of the below-knee prosthetic socket interface` Med. Eng. Phys. Vol.17, No. 8, pp. 559-566,1995

[63] A. Sugimoto. Characteristic of stump shape and stress during gait cycle for transfemoral prosthesis 345 socket. Master thesis, Shibaura Institute of Technology, 2013

[64] Boone D A Mak A FT, Zhang M. State-of-the-art research in lower-limb prosthetic biomechanics socket interface. J Rehabil Res Dev, 38:161174, 2001.

[65] Childress D S Silver-Thorn M B, Steege J W. A review of prosthetic interface stress investigations. J Rehabil. Res Dev, 33:253266, 1996.

[66] Sanders J E Zachariah S G. Interface mechanics in lower-limb external prosthetics: A review of finite element models. IEEE Trans Rehabil Eng., 4:288302, 1996.

[67] Roberts V C Zhang M, Makaft. Finite element modeling of a residual lower-limb in a prosthetic socket: A survey of the development in the first decade. Med Eng Phys, 20:360273, 1998.

[68] Sengeh, David M., et al. "Multi-material 3-D viscoelastic model of a transtibial residuum from in-vivo indentation and MRI data." Journal of the mechanical behaviour of biomedical materials 59 (2016): 379-392.

[69] Portnoy, S., et al. "Real-time patient-specific finite element analysis of internal stresses in the soft tissues of a residual limb: a new tool for prosthetic fitting." Annals of biomedical engineering 35.1 (2007): 120-135.

[70] C. Michael Schuch, `Report From: International Workshop on Above-Knee Fitting and Alignment Techniques`, Clinical Prosthetics and Orthotics, Vol. 12, No. 2, pp. 81-98, 1988

[71] M. S. Jamaludin; A. Hanafusa; S-I. Yamamoto; Y. Agarie; H. Otsuka; K. Onishi. Evaluation of the effect of the geometrical changes in prosthetic socket towards transfemoral residuum via finite element method. Proceeding of IEEE–EMBS Conference on Biomedical Engineering and Science (IECBES). 2018.

[72] Portnoy, S., Siev-Ner, I., Shabshin, N., Kristal, A., Yizhar, Z., Gefen, A., 2009. Patient-specific analyses of deep tissue loads post transtibial amputation in residual limbs of multiple prosthetic users. J. Biomech. 42 (16), 2686–2693.

[73] Silver-Thorn MB, Childress DS. Parametric analysis using the finite element method to investigate prosthetic interface stresses for persons with trans-tibial amputation. J Rehab Res Dev 1996; 33:227–38.

[74] Reynolds DP, Lord M. Interface load analysis for computer aided design of below-knee prosthetic sockets. Med Biol Eng Comput 1992; 30:419–26.

[75] Meulenbelt, H.E.J., Dijkstra, P.U., Jonkman, M.F., Geertzen, J.H.B., 2006. Skin problems in lower limb amputees: a systematic review. Disabil. Rehabil. 28 (10), 603–608

[76] J.A. Weiss. A constitutive model and finite element representation for transversely isotropic soft tissues - Ph.D. Dissertation. University of Utah, 1994.

[77] Jeff Crandall Bing Deng J. T. Wang Costin D. Untaroiu, Kurosh Darvish. Development and validation of a finite element model of the lower limb. ASME 2004 International Mechanical Engineering Congress and Exposition Transportation: Transportation and Environment, Anaheim, California, USA, November 13 19, 2004.

[78] Jeff Crandall Bing Deng J. T. Wang Costin D. Untaroiu, Kurosh Darvish. Characterization of the lower limb soft tissues in pedestrian finite element models. Paper Number 05- 0250, February 2005

[79] C. Untaroiu; K. Darvish; J. R. Crandall; B. Deng; J-T. R. Wang. Characterization of the lower limb soft tissues in pedestrian finite element models. 2005. Vol. 5, No. 250.

[80] A. B. David C. L. Winson, Z. Ming and C. Bill. Finite element analysis to determine effect of mono limb flexibility on structural strength and interaction. J Rehabil Res Dev, 41(6A):775–86, 2004

[81] Juan Fernando Ramrez and Jaime Andrs Vlez. Incidence of the boundary condition between bone and soft tissue in a finite element model of a transfemoral amputee. Prosthet Orthot Int, 36(4):405–14, December 2012

[82] PFS series. PD 3-32. User's manual. NETTA Corporation RETS Division Sensor Group.

[83] J. E. Sanders and S. Fatone. Residual limb volume change: systematic review of measurement and management. Journal of Rehabilitation Research Development. 2011. Vol. 48(8), pp. 949–986.

[84] A.Sugimoto. Charactheristic of stump shape and stress during gait cycle for transfemoral prosthesis socket. Master thesis, Shibaura Institute of Technology, 2013

[85] L. S. Feng; Z. L. Zhang; Ming Zhu. Finite element analysis of the contact interface between trans-femoral stump and prosthetic socket. Conference Proceedings of the IEEE Engineering in Medicine and Biology Society. 2013: Vol. 2013, pp. 1270–3.

[86] J. M. Zuniga. 3D printed antibacterial Prostheses, MDPI/Applied Science. 2018, Vol 8, pp. 1651–1661.

[87] K.-T. Nguyen; L. Benabou; S. Alfayad. Systematic review of prosthetic socket fabrication using 3D printing. Proceedings of the 4th International Conference on Mechatronic and Robotics Engineering. 2018. 137–141.

[88] D. Lacroix and J. F. R. Patino. Finite element analysis of donning procedure of a prosthetic transfemoral socket. Annals of Bioengineering. 2005. Vol. 39, No.12, pp. 2972–2983.

[89] G. Alotta; O. Barrera; A. Cocks; M. Di Paola. The finite element implementation of 3D fractional viscoelastic constitutive models. Journal of Finite Element in Analysis and Design. 2018. Vol. 146, pp. 28–41.

[90] L. Giovannelli; J.J. Rodenas a; J.M. Navarro-Jimenez a; M. Tura. Direct medical image-based finite element modelling for patient-specific simulation of future implants. Journal of finite elements in analysis and design. 2017. Vol.136, pp. 37–57.

[91] Sengeh, David M., et al. "Multi-material 3-D viscoelastic model of a transtibial residuum from in-vivo indentation and MRI data." Journal of the mechanical behavior of biomedical materials 59 (2016): 379-392.

[92] Lee, Winson CC, et al. "Finite element modeling of the contact interface between trans-tibial residual limb and prosthetic socket." Medical engineering & physics 26.8 (2004): 655-662.

[93] Portnoy, S., Siev-Ner, I., Shabshin, N., Gefen, A., 2011. Effects of sitting postures on risks for deep tissue injury in the residuum of a transtibial

prosthetic-user: a biomechanical case study. Comput. Methods Biomech. Biomed. Eng. 14 (11), 1009–1019

[94] B. V. Mehta; S. Rajani; G. Sinha, "Comparison of image processing techniques (magnetic resonance imaging, computed tomography scan and ultrasound) for 3D modeling and analysis of the human bones", Int.J. Digit Imaging. 2017. Vol. 10(3 Suppl 1), pp. 203–206.

[95] Udai, Arun Dayal, and Amarendra Nath Sinha. "Processing magnetic resonance images for CAD model development of prosthetic limbs socket." 2008 IEEE Region 10 and the Third international Conference on Industrial and Information Systems. IEEE, 2008.

[96] M. S. Jamaludin; A. Hanafusa; S-I. Yamamoto; Y. Agarie; H. Otsuka; K. Onishi. Evaluation of the effect of the geometrical changes in prosthetic socket towards transfemoral residuum via finite element method. Proceeding of IEEE–EMBS Conference on Biomedical Engineering and Science (IECBES). 2018

[97] M.S. Jamaludin and A. Hanafusa. Accuracy evaluation of 3D reconstruction of transfemoral residual limb model using basic spline interpolation, IFMBE Proceedings. 2017. Vol. 68, No.2, pp. 675–680.

[98] Portnoy, S., et al. "Real-time patient-specific finite element analysis of internal stresses in the soft tissues of a residual limb: a new tool for prosthetic fitting." Annals of biomedical engineering 35.1 (2007): 120–135.

[99] Le Van Tuan; S. Yamamoto; A. Hanafusa. "Finite element analysis for quantitative evaluation of a trans-femoral prosthesis socket for standing posture" in International Journal of Computer Applications (0975–8887). 2017. Vol. 170, No. 1, pp. 1–8.

[100] C. Untaroiu; K. Darvish; J. R. Crandall; B. Deng; J-T. R. Wang. Characterization of the lower limb soft tissues in pedestrian finite element models. In Proceedings of the 19th International technical conference on the Enhanced Safety of Vehicles, Washington, DC, USA, 6–9 June 2005 Vol.5, pp 124–131

[101] A. Mak; M. Zhang; W. C. Lee. Regional differences in pain threshold and tolerance of the residual limb: including the effects of age and interface

material. Archives of Physical Medicine Rehabilitation. 2005. Vol. 86, pp. 641–649.

[102] J. E. Sanders and S. Fatone. Residual limb volume change: systematic review of measurement and management. Journal of Rehabilitation Research Development. 2011. Vol. 48(8), pp. 949–986.

[103] S. G. Zachariah; R. Saxena; J. R. Fergason; J. E. Sanders. Shape and volume change in the transtibial residuum over the short term: Preliminary investigation of six subjects. Journal of Rehabilitation Research and Development (JRRD). 2004. Vol. 41, No. 5, pp. 683–694.

[104] Fong M. Seung H.S. Tedrake R., Zhang T.W. Actuating a simple 3d passive dynamic walker. Proceedings of the IEEE International Conference on Robotics and Automation (ICRA),New Orleans, Lousiana, 5:46564661, 2004.

[105] Smith D,, Michael J, W and Bowker J,H. American Academy of Orthopaedic Surgeons. 3rd Ed. USA. 2011.

List of Publication

1. M.S. Jamaludin and A. Hanafusa. Accuracy evaluation of 3D reconstruction of transfemoral residual limb model using basic spline interpolation, IFMBE Proceedings. 2017. Vol. 68, No.2, pp. 675–680.

2. Mohd Syahmi Jamaludin, Akihiko Hanafusa, Yamamoto Shin-Ichiroh, Yukio Agarie, Hiroshi Otsuka, ` Evaluation of Donning Simulation for Trans-Femoral Residuum with MCCT Socket Using Finite Element Analysis`, Asian Prosthetic and Orthotic Scientific Meeting (APOSM), 2018

3. M. S. Jamaludin, A. Hanafusa, S. Yamamoto, Y. Agarie, H. Otsuka and K. Onishi, "Evaluation of the Effects of Geometrical Changes in Prosthetic Socket Towards Transfemoral Residuum via Finite Element Method," 2018 IEEE-EMBS Conference on Biomedical Engineering and Sciences (IECBES), Sarawak, Malaysia, 2018, pp. 314-319.

   DOI: 10.1109/IECBES.2018.8626703

4. Mohd Syahmi Jamaludin, Akihiko Hanafusa, Shin-Ichirou Yamamoto, Yukio Agarie, Hiroshi Otsuka, Kengo Onishi, ` Finite Element Analysis of Muscle Distribution Effect in Geometrical Deformation of Stump During Interaction with Transfemoral Prosthetic Socket`, Japan Society of Medical Bio-Engineering (JSMBE) Conference, May 2019

5. Mohd Syahmi Jamaludin, Akihiko Hanafusa , Shinichiro Yamamoto , Yukio Agarie , Hiroshi Otsuka , Kengo Onishi ` Prediction of Transfemoral Stump Deformation During Donning Process in Bipedal Stances Using Finite Element Method`, International Symposium of Prosthetic and Orthotics (ISPO) 2019.

6. Mohd Syahmi Jamaludin, Akihiko Hanafusa , Yamamoto Shinichirou , Yukio Agarie ,Hiroshi Otsuka and Kengo Ohnishi, “Development of an Evaluation System for Magnetic Resonance Imaging Based Three-Dimensional Modeling of a Transfemoral Prosthetic Socket Using Finite

Elements", www.mdpi.com/journal/applsci, Appl. Sci. 2019, Vol. 9, 3662; doi:10.3390/app9183662

7. Mohd Syahmi Jamaludin, Akihiko Hanafusa , Yamamoto Shinichirou , Yukio Agarie ,Hiroshi Otsuka and Kengo Ohnishi, "Analysis of Pressure Distribution in Transfemoral Prosthetic Socket for Pre-Fabrication Evaluation Via Finite Element Method", https://www.mdpi.com/2306-5354/6/4/98. Bioengineering 2019, Vol.6, 98; doi:10.3390/bioengineering604009